MATHEMATICS OF COMPUTATION
Volume 00, Number 0, Pages 000–000
S 0025-5718(XX)0000-0

ROBUST ERROR ANALYSIS OF STABILIZED LINEAR EMAC-ESAV FINITE ELEMENT SCHEMES FOR THE INCOMPRESSIBLE NAVIER-STOKES EQUATIONS

RIHUI LAN, MENGYAO LIU, AND LILI JU

Abstract. In this paper, we propose and study first- and second-order (in time) stabilized linear finite element schemes for the incompressible Navier-Stokes (NS) equations. The EMAC formulation has emerged as a promising approach for conserving energy, momentum, and angular momentum of the NS equations, while the exponential scalar auxiliary variable (ESAV) has become a popular technique for designing linear energy-stable numerical schemes. Our method leverages the EMAC formulation and the Taylor-Hood element with grad-div stabilization for spatial discretization. We adopt the implicit-explicit BDF formulas coupled with a novel stabilized ESAV approach for time stepping. For the solution process, we develop an efficient decoupling technique for the resulting fully-discrete systems so that only one linear Stokes solve is needed at each time step, which is similar to the cost of classic implicit-explicit BDF schemes for the NS equations. Robust optimal error estimates are successfully derived for both velocity and pressure for the two proposed schemes, with Gronwall constants that are particularly independent of the viscosity. Furthermore, it is rigorously shown that the grad-div stabilization term can greatly alleviate the viscosity-dependence of the mesh size constraint, which is required for error estimation when such a term is not present in the schemes. Various numerical experiments are conducted to verify the theoretical results and demonstrate the effectiveness and efficiency of the grad-div and ESAV stabilization strategies and their combination in the proposed numerical schemes, especially for problems with high Reynolds numbers.

1. Introduction

In this paper, we consider the following non-stationary incompressible Navier-Stokes (NS) equations in the primitive variables:

$$\begin{cases} \boldsymbol{u}_t + (\boldsymbol{u}\cdot\nabla)\,\boldsymbol{u} - \nu\Delta\boldsymbol{u} + \nabla p = \boldsymbol{f}, & \text{in } (0,T]\times\Omega, \\ \nabla\cdot\boldsymbol{u} = 0, & \text{in } (0,T]\times\Omega, \end{cases} \tag{1}$$

subject to the Dirichlet boundary condition $\boldsymbol{u}(t,\boldsymbol{x}) = \boldsymbol{u}_D(\boldsymbol{x},t)$ on $(0,T]\times\partial\Omega$ and the initial condition $\boldsymbol{u}(0,\boldsymbol{x}) = \boldsymbol{u}_0(\boldsymbol{x})$ in Ω, where Ω denotes an open bounded and connected domain in $\mathbb{R}^d$ ($d = 2$ or 3), $T > 0$ is the terminal time, $\boldsymbol{u} = \boldsymbol{u}(t,\boldsymbol{x})$ is the fluid velocity, $p = p(t,\boldsymbol{x})$ is the fluid pressure, $\nu = \frac{1}{Re}$ is the viscosity with Re denoting the Reynolds number, and $\boldsymbol{f}$ is the external body force. It is highly demanding and challenging to design efficient, accurate and long-term stable numerical methods for solving the above incompressible NS equations (1) in scientific and engineering applications due to some well-known difficulties.

First, the incompressibility condition $\nabla\cdot\boldsymbol{u} = 0$ poses a significant challenge on designing stable numerical schemes. In [28], the authors investigated the divergence-free constraint and how it ruins and pollutes the numerical solutions. Usually, the inf-sup condition (also called as LBB condition) [7] has to be maintained at the discrete level and over the past decades many finite element methods have been developed to address this issue. Among them, the Taylor-Hood finite element [49] is the widely-used Stokes pair and easy to implement, but they cannot conserve the mass locally. Instead, the Scott-Vogelius element [45, 46] is another inf-sup stable pair and can conserve mass locally. However, the Scott-Vogelius element provides a stable Stokes pair only when the approximation order is higher than 3 or it requires a barycenter refinement, thus such

2000 *Mathematics Subject Classification.* Primary 65M60, 65M12, 35Q30.

Key words and phrases. Navier-Stokes equations, EMAC formulation, grad-div stabilization, stabilized exponential SAV, viscosity-independent Gronwall constant.

The first author's research was partially supported by Shandong Provincial Natural Science Fund for Excellent Young Scientists Fund Program (Overseas) under grant number 2023HWYQ-064 and National Natural Science Foundation of China under grant number 123015313. The third author's research was partially supported by U.S. National Science Foundation under grant numbers DMS-2109633 and DMS-2409634. Corresponding author (L. Ju).

©XXXX American Mathematical Society

divergence-free element is computationally expensive and not easy to implement in practice. In [15, 22] some other divergence-free elements were developed for general triangular meshes, which need either higher order polynomials or more effort on implementation. As a different approach, the projection method [12, 20] and the gauge method [52, 53] usually first relax the incompressibility constraint in solving the momentum equation and then take an extra projection step to recover the incompressibility. These methods often suffer from the splitting errors. For instance, the projection methods could incur the spurious oscillation due to the artificial boundary condition on the pressure. To overcome this issue, Quarteroni et al. [40] proposed the algebraic splitting (also known as Yosida method) to decouple the velocity and pressure unknowns based on the discretized linear system, where the boundary conditions are properly handled before splitting. Some related work and further developments can be found in [43, 42, 41].

Second, the convection term $(\boldsymbol{u}\cdot\nabla)\,\boldsymbol{u}$ is nonlinear which gives rise to a nonlinear system. While implicit schemes require a nonlinear solver at each time step, strong CFL conditions are needed in terms of numerical stability for explicit schemes which cause permissible time step sizes to be small. To alleviate this restriction, stabilization techniques are usually employed. [30] extrapolated the velocity at the convective term, and stabilized the scheme by adding $-\alpha h\Delta\boldsymbol{u}$, where α serves as a tuning parameter and h is the mesh size. On the other hand, the convection term is also skew-symmetry, which is crucial to maintain its energy and momentum conservation. There are several variants on the nonlinear term. The one presented in (1) is referred as the convective form, which could not inherently guarantee the skew-symmetry at the discrete level. Skew-symmetric and rotational forms were proposed to address this concern in [50, 18]. The energy, momentum, and angular momentum conserving (EMAC) formulation [10] has emerged as a promising alternative, designed to conserve energy, momentum, and angular momentum. The numerical schemes based on "enhanced-physics" principles usually offer nice accuracy and stability, particularly for long-term simulations, which is also why the EMAC formulation outperforms other variants of the nonlinear term. A linearized EMAC scheme was further proposed and studied In [11].

Third, large Reynolds number could change the laminar flow to the turbulent flow, where the mechanics of the latter one is still not fully studied. According to Kolmogorov's K41 theory [29], the mesh should be fine enough ($\approx Re^{-3/4}$ for each direction) to resolve the eddies. On the other hand, most of the numerical stability analysis applies the Gronwall's lemma [19, 6], leading to an exponential function with the Reynolds number (or the inverse of the viscosity) in the exponent since the Gronwall constant contains Re. An error estimate is said to be robust if the Gronwall constant does not depend on the viscosity. However, as pointed out in [16, Remark 4.9], robust error estimates of Taylor-Hood element for the NS equations could not be obtained if the EMAC formulation is not utilized for the nonlinear term. Later in [39], an EMAC scheme was proposed which is able to produce a viscosity-independent Gronwall constant so that long-term stability and accuracy could be achieved. It is also well-known that the addition of grad-div stabilization term [38, 9] into the weak formulation can further improve the local mass conservation and enhance the stability of numerical schemes, especially when the Reynolds number is large.

In recent years, the scalar auxiliary variable (SAV) [47, 48, 36] method and some of its variants have gained a lot of popularity in tackling time discretization of highly nonlinear terms and designing efficient linear energy-stable schemes for phase-field and multi-phase fluid models. This method introduces an extra scalar variable incorporating with the explicit nonlinear term and imposes an extra dynamics equation on the scalar variable to control the evolution of the system energy. The SAV approach was first applied to the NS equations in [35] to handle the nonlinear convection term, and later, a SAV-MAC scheme for the incompressible NS equations in the primitive variable form was proposed and analyzed with the projection method in [33, 34]. Among finite element methods combined with the SAV approach, [54] was the first work to provide an optimal a priori error estimate, but in which the skew-symmetric form of the convection term is considered and consequently the Gronwall constant depends on the Reynolds number. In [24], a robust error estimate for the H^1 divergence-free finite element (i.e., the Scott-Vogelius element) was obtained with a Gronwall constant independent of Reynolds number under a standard CFL condition (also referred as the mesh ratio condition [2]) $\tau = O(h^2)$ where τ is the time step size. A linear exponential SAV (ESAV) scheme based on the EMAC formulation was proposed in [23] for the NS equations, together with the Taylor-Hood element for spatial discretization. The authors also conducted an error estimate under two CFL conditions, i.e., $\tau\|\boldsymbol{u}\|^2_{L^\infty(0,T;L^\infty(\Omega))} \le h^2$ and $\tau h^{-d/2} \le 1$. However, the Gronwall constant still depends on the Reynolds number, failing to provide a robust viscosity-independent error estimate. Upon a closer examination of their proof, we further find that the condition $\tau h^{-d/2} \le 1$ could downgrade the convergent rate. In [23, Eq.

(4.31)], if $\tau h^{-d/2} \leq 1$ is enforced, the projection H^1 semi-norm approximation error is accumulated over time steps, suggesting the estimate [23, Eq. (4.5)] should be expressed as $\frac{h^{2k}}{\tau}$ instead of h^{2k}. Moreover, in deriving the L^∞ bound on the numerical solution, the mesh size h is also implicitly restricted by $O(e^{-ReT})$.

In this work, we develop first- and second-order (in time) linear numerical schemes for solving the incompressible NS equations. We take the EMAC formulation for the nonlinear term. For spatial discretization, we choose the Taylor-Hood element, which is easy to implement. To further improve mass conservation and stability, we also apply the grad-div stabilization technique into the weak form of the NS equations. For temporal discretization, we propose a novel stabilized ESAV approach and make use of the implicit-explicit backward differential formulas (BDFs). Our stabilized ESAV approach does not introduce any additional splitting error in time while effectively enhancing the stability and accuracy of the standard ESAV approach. In terms of the solution process, we develop an efficient decoupling technique for the resulting fully-discrete systems so that only one linear Stokes solve is needed at each time step. This ensures that the computational cost is similar to that of the classic implicit-explicit BDF schemes for the incompressible NS equations. As our main theoretical effort, we successfully establish robust optimal error estimates (i.e., the Gronwall constant is independent of viscosity) for the two proposed schemes. In order to overcome the difficulties encountered in [23], our error analysis takes a new approach partially motivated by the work of [32, 31, 2]. We also rigorously show that the grad-div stabilization term can greatly alleviate the viscosity-dependence of the mesh size constraint, which is required for error estimation when such a term is not present in the schemes. Furthermore, we numerically illustrate the significant effect on stability and accuracy brought by the grad-div and ESAV stabilization strategies and their combination.

The rest of paper is organized as follows. In Section 2, we will introduce the spatial discretization with the Taylor-Hood element and some preliminaries for error analysis. Following that, the first and second order stabilized linear EMAC finite element schemes together with their unconditional energy stability and decoupled solution strategy are presented in Section 3. Robust error estimates of the proposed schemes without and with the grad-div stabilization are derived in Section 4. Extensive numerical experiments are carried out in Section 5 to verify the theoretical results and demonstrate the effectiveness and efficiency of the proposed schemes, especially for problems with large Reynolds numbers. Finally, some concluding remarks are drawn in Section 6.

2. Preliminaries

Let us introduce some notations for simplicity of representation. Denote the inner product and the corresponding $L^2(\Omega)$ norm by $(\cdot,\cdot)$ and $\|\cdot\|_0$ respectively. Likewise, the $L^p(\Omega)$ $(1 \leq p \leq \infty)$ norm and the Sobolev space $W^{k,p}(\Omega)$ $(k \geq 0)$ norm are denoted by $\|\cdot\|_{L^p}$ and $\|\cdot\|_{W^{k,p}}$ respectively, and the $H^k(\Omega)$ norm and semi-norm for by $\|\cdot\|_k$ and $|\cdot|_k$ respectively. The space $H_0^1(\Omega)$ is the subspace of $H^1(\Omega)$ with vanishing trace on $\partial\Omega$. The norm of the dual space $H^{-1}(\Omega)$ of $H_0^1(\Omega)$ is denoted by $\|\cdot\|_{-1}$. For any function defined on $(0,T)\times\Omega$, we also have corresponding time-involving norms $\|\cdot\|_{L^\infty(0,T;W^{k,p}(\Omega))}$ and $\|\cdot\|_{L^m(0,T;W^{k,p}(\Omega))}$ $(1 \leq m \leq \infty)$ norms (will be abbreviated as $\|\cdot\|_{L^\infty(0,T;W^{k,p})}$ and $\|\cdot\|_{L^m(0,T;W^{k,p})}$ respectively). Without loss of generality, from now on we also assume the homogeneous Dirichlet boundary condition, i.e., $\boldsymbol{u}_D(\boldsymbol{x},t) = 0$ for any $(t,\boldsymbol{x}) \in (0,T]\times\partial\Omega$ except stated otherwise.

Let us define the Sobolev space pair $\boldsymbol{X} \times M$ as

$$\boldsymbol{X} = (H_0^1(\Omega))^d := \{\boldsymbol{v} \in (H^1(\Omega))^d \,|\, \boldsymbol{v}|_{\partial\Omega} = 0\}, \qquad M = L_0^2(\Omega) := \{q \in L^2(\Omega) \,|\, \textstyle\int_\Omega q = 0\}.$$

The standard weak form of the NS equations (1) is then given by: find $(\boldsymbol{u}(t), p(t)) \in \boldsymbol{X} \times M$ for $t \in (0,T]$ such that

$$\begin{cases} (\boldsymbol{u}_t, \boldsymbol{v}) + ((\boldsymbol{u}\cdot\nabla)\boldsymbol{u}, \boldsymbol{v}) + \nu(\nabla\boldsymbol{u}, \nabla\boldsymbol{v}) - (p, \nabla\cdot\boldsymbol{v}) = (\boldsymbol{f}, \boldsymbol{v}), & \forall\, \boldsymbol{v} \in \boldsymbol{X}, \\ (\nabla\cdot\boldsymbol{u}, q) = 0, & \forall\, q \in M. \end{cases} \tag{2}$$

Let $\mathcal{T}_h$ be a quasi-uniform triangulation of Ω with the mesh size $h = \max\{\mathrm{diam}(K) \,|\, K \in \mathcal{T}_h\}$. Then the Taylor-Hood mixed finite element pair $\boldsymbol{X}_h \times M_h$ [49] for spatial discretization is defined by

$$\boldsymbol{X}_h := \{\boldsymbol{v}_h \in \boldsymbol{X} \,|\, \boldsymbol{u}_h|_K \in (P^k(K))^d, \forall\, K \in \mathcal{T}_h\}, \quad M_h := \{q_h \in M \,|\, q_h|_K \in P^{k-1}(K), \forall\, K \in \mathcal{T}_h\},$$

where $P^k(K)$ is the set of polynomials with order up to k defined in the element K, and we will only consider the classic case of $k = 2$. The following approximation properties [8] hold:

$$\begin{aligned} &\inf_{\boldsymbol{v}\in\boldsymbol{X}_h} ||\boldsymbol{w}-\boldsymbol{v}||_k \le C_0^{(1)} h^{3-k}||\boldsymbol{w}||_3, \quad \forall\, \boldsymbol{w}\in (H^3(\Omega))^d,\ k=0,1,\\ &\inf_{q\in M_h} ||r-q||_0 \le C_0^{(2)} h^2||r||_2, \quad \forall\, r\in H^2(\Omega), \end{aligned} \tag{3}$$

where $C_0^{(1)} > 0$ and $C_0^{(2)} > 0$ are constants depending only on Ω. Let us set $C_0 = \max\{C_0^{(1)}, C_0^{(2)}\}$ for simplicity. It is well-known that the Taylor-Hood element satisfies the discrete inf-sup condition, i.e. there exists a constant $\gamma > 0$ such that

$$\inf_{q_h\in M_h}\sup_{\boldsymbol{v}_h\in\boldsymbol{X}_h} \frac{(q_h, \nabla\cdot\boldsymbol{v}_h)}{\|q_h\|_0\|\boldsymbol{v}_h\|_1} \ge \gamma. \tag{4}$$

Let us define $\boldsymbol{V}$ as the divergence-free subspace of $\boldsymbol{X}$ and $\boldsymbol{V}_h$ as the weakly divergence-free subspace of $\boldsymbol{X}_h$

$$\boldsymbol{V} := \{\boldsymbol{v}\in\boldsymbol{X} \,|\, \nabla\cdot\boldsymbol{v} = 0, \text{a.e. in } \Omega\}, \quad \boldsymbol{V}_h := \{\boldsymbol{v}_h\in\boldsymbol{X}_h \,\big|\, (q_h, \nabla\cdot\boldsymbol{v}_h) = 0, \forall\, q_h\in M_h\}.$$

It is noted that $\boldsymbol{V}_h \nsubseteq \boldsymbol{V}$. Then the Stokes projection $\mathrm{P}_{st} : \boldsymbol{V} \to \boldsymbol{V}_h$ [17, 51] is defined by

$$(\nabla \mathrm{P}_{st}\boldsymbol{w}, \nabla\boldsymbol{v}_h) = (\nabla\boldsymbol{w}, \nabla\boldsymbol{v}_h), \quad \forall\, \boldsymbol{w}\in\boldsymbol{V},\ \boldsymbol{v}_h\in\boldsymbol{V}_h. \tag{5}$$

Regarding the Stokes projection (5), a stability lemma was proved in [51], and an error estimate was shown in [13] in conjunction with the Aubin-Nitsche lift technique [4].

Lemma 2.1 (Stability of Stokes Projection [51])**.** *For any fixed $r\in[2,\infty]$, there exists a constant $C_1 > 0$ depending only on Ω such that*

$$\|\nabla \mathrm{P}_{st}\boldsymbol{w}\|_{L^r} \le C_1\|\nabla\boldsymbol{w}\|_{L^r}, \quad \forall\, \boldsymbol{w}\in\boldsymbol{V}.$$

Lemma 2.2 (Error estimate of Stokes Projection [13])**.** *There exists a constant $C_2 > 0$ depending only on Ω such that the following estimate holds:*

$$\|\boldsymbol{w} - \mathrm{P}_{st}\boldsymbol{w}\|_0 + h\|\boldsymbol{w} - \mathrm{P}_{st}\boldsymbol{w}\|_1 \le C_2 h^3\|\boldsymbol{w}\|_3, \quad \forall\, \boldsymbol{w}\in\boldsymbol{V}\cap(H^3(\Omega))^d.$$

Let us present some popular inverse inequalities as follows [8]:

Lemma 2.3. *For any fixed $0\le n\le m\le 1, 1\le q\le p\le\infty$, there exists a constant $\overline{C}_3 > 0$, depending only on Ω, such that*

$$\|\boldsymbol{w}_h\|_{W^{m,p}} \le \overline{C}_3 h^{n-m-d\left(\frac{1}{q}-\frac{1}{p}\right)}\|\boldsymbol{w}_h\|_{W^{n,q}}, \quad \forall\, \boldsymbol{w}_h\in\boldsymbol{X}_h.$$

In particular, we will use the following specific inverse estimates:

$$\|\boldsymbol{w}_h\|_{L^\infty} \le \overline{C}_3^{(1)} h^{-\frac{d}{2}}\|\boldsymbol{w}_h\|_{L^2}, \quad \|\boldsymbol{w}_h\|_{H^1} \le \overline{C}_3^{(2)} h^{-1}\|\boldsymbol{w}_h\|_{L^2}, \quad \|\boldsymbol{w}_h\|_{L^{\frac{2d}{d-1}}} \le \overline{C}_3^{(3)} h^{-\frac{1}{2}}\|\boldsymbol{w}_h\|_{L^2}, \tag{6}$$

thus we define the constant $C_3 = \max\{\overline{C}_3^{(1)}, \overline{C}_3^{(2)}, \overline{C}_3^{(3)}\}$ for simplicity.

Next let us also introduce some operators which are needed when estimating the pressure. Let us first define the linear operator $A_h : \boldsymbol{V}_h \to \boldsymbol{V}_h$ by

$$(A_h\boldsymbol{w}_h, \boldsymbol{v}_h) = (\nabla\boldsymbol{w}_h, \nabla\boldsymbol{v}_h), \quad \forall\, \boldsymbol{w}_h, \boldsymbol{v}_h\in\boldsymbol{V}_h,$$

and it holds that $\left\|A_h^{1/2}\boldsymbol{w}_h\right\|_0 = \|\nabla\boldsymbol{w}_h\|_0$ and $\left\|\nabla A_h^{-1/2}\boldsymbol{w}_h\right\|_0 = \|\boldsymbol{w}_h\|_0$. The linear operator $D_h : L^2(\Omega) \to \boldsymbol{V}_h$ is defined by

$$(D_h q, \boldsymbol{v}_h) = (\nabla\cdot\boldsymbol{v}_h, q), \quad \forall\, q\in L^2(\Omega),\ \boldsymbol{v}_h\in\boldsymbol{V}_h.$$

The discrete Leray projection $\Pi_h^{\mathrm{div}} : (L^2(\Omega))^d \to \boldsymbol{V}_h$ is defined by

$$\left(\Pi_h^{\mathrm{div}}\boldsymbol{w}, \boldsymbol{v}_h\right) = (\boldsymbol{w}, \boldsymbol{v}_h), \quad \forall\, \boldsymbol{w}\in(L^2(\Omega))^d,\ \boldsymbol{v}_h\in\boldsymbol{V}_h.$$

There also exist constants $C_4^{(1)} > 0$ and $C_4^{(2)} > 0$ depending only on Ω such that

$$\|\boldsymbol{w}\|_{-1} \le C_4^{(1)}\|\boldsymbol{w}\|_0, \quad \forall\, \boldsymbol{w}\in(L^2(\Omega))^d.$$

and the following inverse inequality holds [13]

$$\|\boldsymbol{w}_h\|_{-1} \le C_4^{(2)}\left(h\|\boldsymbol{w}_h\|_0 + \|A_h^{-1/2}\boldsymbol{w}_h\|_0\right), \quad \forall\, \boldsymbol{w}_h\in\boldsymbol{V}_h. \tag{7}$$

We set $C_4 = \max\{C_4^{(1)}, C_4^{(2)}\}$ for simplicity. By the Sobolev embedding theorems and Poincare's inequality [1], we know for any $\boldsymbol{w} \in X$,

$$\begin{cases} \|\boldsymbol{w}\|_{L^4} \le C_5^{(1)} \|\nabla \boldsymbol{w}\|_0, & \text{if } d = 2, \\ \|\boldsymbol{w}\|_{L^3} \le C_5^{(2)} \|\nabla \boldsymbol{w}\|_0, & \text{if } d = 3, \\ \|\boldsymbol{w}\|_{L^6} \le C_5^{(3)} \|\nabla \boldsymbol{w}\|_0, & \text{if } d = 3, \end{cases} \tag{8}$$

where the positive constants $C_5^{(i)}$'s depend only on Ω. We set $C_5 = \max\{C_5^{(1)}, C_5^{(2)}, C_5^{(3)}\}$ for simplicity.

For the temporal discretization, let us assume the uniform partition of the time interval $[0, T]$ with the time step size $\tau = \frac{T}{N}$ and set $t_n = n\tau$ for $n = 0, 1, ..., N$. For a generic variable φ, let φ^n denote its value at $t = t_n$, i.e, $\varphi^n = \varphi(t_n)$. The following consistency error formula will be utilized frequently for temporal error estimation.

Lemma 2.4 (Temporal consistency error [27]). *Assume $\boldsymbol{w}, \boldsymbol{w}_t$, and $\boldsymbol{w}_{tt} \in L^2(t_n, t_{n+1}; (L^2(\Omega))^d)$, then*

$$\left\| \boldsymbol{w}_t(t_n) - \frac{\boldsymbol{w}_{n+1} - \boldsymbol{w}_n}{\tau} \right\|_0^2 \le \tau \int_{t_n}^{t_{n+1}} \|\boldsymbol{w}_{tt}\|_0^2 \, dt = \tau \|\boldsymbol{w}_{tt}\|^2_{L^2(t_n, t_{n+1}; L^2)}. \tag{9}$$

We will also make use of the following discrete Gronwall's inequality in error analysis:

Lemma 2.5 (Discrete Gronwall Lemma [27]). *Let τ, H, and a_n, b_n, c_n, d_n (for integers $n \ge 0$) be finite non-negative numbers such that*

$$a_l + \tau \sum_{n=0}^{l} b_n \le \tau \sum_{n=0}^{l-1} d_n a_n + \tau \sum_{n=0}^{l} c_n + H, \quad \forall\, l \ge 1.$$

Then it holds

$$a_l + \tau \sum_{n=0}^{l} b_n \le \exp\left(\tau \sum_{n=0}^{l} d_n\right) \left(\tau \sum_{n=0}^{l} c_n + H\right), \quad \forall\, l \ge 1.$$

3. The stabilized linear EMAC-ESAV finite element schemes

Consider the following trilinear form $c(\cdot, \cdot, \cdot) : \boldsymbol{X} \times \boldsymbol{X} \times \boldsymbol{X} \to \mathbb{R}$,

$$c(\boldsymbol{u}, \boldsymbol{v}, \boldsymbol{w}) = 2(\boldsymbol{D}(\boldsymbol{u})\boldsymbol{v}, \boldsymbol{w}) + ((\nabla \cdot \boldsymbol{u})\boldsymbol{v}, \boldsymbol{w}) = (\mathcal{N}(\boldsymbol{u}, \boldsymbol{v}), \boldsymbol{w}), \tag{10}$$

where $\boldsymbol{D}(\boldsymbol{u}) = \frac{1}{2}(\nabla \boldsymbol{u} + (\nabla \boldsymbol{u})^T)$ is regarded as the symmetrization of $\nabla \boldsymbol{u}$ and $\mathcal{N}(\boldsymbol{u}, \boldsymbol{v}) = 2\boldsymbol{D}(\boldsymbol{u})\boldsymbol{v} + (\nabla \cdot \boldsymbol{u})\boldsymbol{v}$. This trilinear form $c(\cdot, \cdot, \cdot)$ is used to represent the nonlinear term in the EMAC formulation, and it holds $c(\boldsymbol{u}, \boldsymbol{u}, \boldsymbol{u}) = 0$. Notice that $(\boldsymbol{u} \cdot \nabla)\boldsymbol{u} = 2\boldsymbol{D}(\boldsymbol{u})\boldsymbol{u} - \frac{1}{2}\nabla|\boldsymbol{u}|^2$. By incorporating the term $-\frac{1}{2}\nabla|\boldsymbol{u}|^2$ into ∇p and modifing the pressure p to $P = p - \frac{1}{2}|\boldsymbol{u}|^2$, we obtain an equivalent EMAC weak formulation for the NS equations (1) as follows: find $(\boldsymbol{u}(t), P(t)) \in \boldsymbol{X} \times M$ for $t \in (0, T]$ such that

$$\begin{cases} (\boldsymbol{u}_t, \boldsymbol{v}) + c(\boldsymbol{u}, \boldsymbol{u}, \boldsymbol{v}) + \nu(\nabla \boldsymbol{u}, \nabla \boldsymbol{v}) - (P, \nabla \cdot \boldsymbol{v}) = (\boldsymbol{f}, \boldsymbol{v}), & \forall\, \boldsymbol{v} \in \boldsymbol{X}, \\ (\nabla \cdot \boldsymbol{u}, q) = 0, & \forall\, q \in M. \end{cases} \tag{11}$$

Next we define a SAV variable of exponential type as

$$Q(t) = \exp\left(-\tfrac{t}{T}\right), \quad \forall t \in (0, T].$$

By introducing an extra dynamics equation for $Q(t)$ into the PDE system (11) and adding an grad-div stabilization term into the momentum equation, we obtain the following transformed EMAC-ESAV formulation for the NS equations (1): Find $(\boldsymbol{u}(t), P(t)) \in \boldsymbol{X} \times M$ for $t \in (0, T]$, such that

$$\begin{cases} (\boldsymbol{u}_t, \boldsymbol{v}) + Q \exp\left(\tfrac{t}{T}\right) c(\boldsymbol{u}, \boldsymbol{u}, \boldsymbol{v}) - (P, \nabla \cdot \boldsymbol{v}) & \\ \qquad + \nu(\nabla \boldsymbol{u}, \nabla \boldsymbol{v}) + \mu(\nabla \cdot \boldsymbol{u}, \nabla \cdot \boldsymbol{v}) = (\boldsymbol{f}, \boldsymbol{v}), & \forall\, \boldsymbol{v} \in \boldsymbol{X}, \quad \text{(12a)} \\ (\nabla \cdot \boldsymbol{u}, q) = 0, & \forall\, q \in M, \quad \text{(12b)} \\ \frac{dQ}{dt} = -\frac{1}{T} Q + \frac{1}{\theta} \exp\left(\tfrac{t}{T}\right) c(\boldsymbol{u}, \boldsymbol{u}, \boldsymbol{u}), & \quad \text{(12c)} \end{cases}$$

where $\mu \geq 0$ is a stabilizing parameter associated with the grad-div term, and $0 < \theta \leq 1$ (i.e., $\frac{1}{\theta} \geq 1$) is a stabilizing parameter associated with the ESAV dynamics. It is noted that the EMAC-ESAV formulation (12) is equivalent to the original PDE system (11) since the terms $(\nabla \cdot \boldsymbol{u}, \nabla \cdot \boldsymbol{v}) = 0$ and $c(\boldsymbol{u}, \boldsymbol{u}, \boldsymbol{u}) = 0$ and consequently have no contributions to the system. We spatially discretize the weak form (12) via the finite element method with the Taylor-Hood element and apply the implicit-explicit BDF schemes (backward Euler and BDF2) for time stepping. Setting $\boldsymbol{u}_h^0 = \mathrm{P}_{st}\boldsymbol{u}_0$ and $Q^0 = Q(0) = 1$.

Then a fully-discrete first-order (in time) linear scheme for solving the EMAC-ESAV formulation (12) can be obtained as follows: for $n = 0, 1, \cdots, N-1$, find $(\boldsymbol{u}_h^{n+1}, P_h^{n+1}) \in \boldsymbol{X}_h \times M_h$ and $Q^{n+1} \in \mathbb{R}$ such that

$$
\begin{cases}
\left(\frac{\boldsymbol{u}_h^{n+1}-\boldsymbol{u}_h^n}{\tau}, \boldsymbol{v}_h\right) + Q^{n+1}\exp\left(\frac{t_{n+1}}{T}\right) c\left(\boldsymbol{u}_h^n, \boldsymbol{u}_h^n, \boldsymbol{v}_h\right) - \left(P_h^{n+1}, \nabla \cdot \boldsymbol{v}_h\right) & \\
\qquad + \nu\left(\nabla \boldsymbol{u}_h^{n+1}, \nabla \boldsymbol{v}_h\right) + \mu\left(\nabla \cdot \boldsymbol{u}_h^{n+1}, \nabla \cdot \boldsymbol{v}_h\right) = \left(\boldsymbol{f}^{n+1}, \boldsymbol{v}_h\right), & \forall\, \boldsymbol{v}_h \in \boldsymbol{X}_h, \quad \text{(13a)} \\
\left(\nabla \cdot \boldsymbol{u}_h^{n+1}, q_h\right) = 0, & \forall\, q_h \in M_h, \quad \text{(13b)} \\
\frac{Q^{n+1}-Q^n}{\tau} = -\frac{1}{T}Q^{n+1} + \frac{1}{\theta}\exp\left(\frac{t_{n+1}}{T}\right) c\left(\boldsymbol{u}_h^n, \boldsymbol{u}_h^n, \boldsymbol{u}_h^{n+1}\right). & \quad \text{(13c)}
\end{cases}
$$

We would refer the scheme (13) as the "sIMEX1-FEM" scheme. When the grad-div stabilizing parameter $\mu = 0$ and the ESAV stabilizing parameter $\theta = 1$, the scheme (13) reduces to the implicit-explicit ESAV scheme studied in [23]. It is easy to show that the first-order sIMEX1-FEM scheme (13) satisfies the following unconditional discrete energy stability:

Lemma 3.1. *(Discrete energy stability of sIMEX1-FEM) Assume $\boldsymbol{f} \in L^2\left(0, T; L^2(\Omega)\right)$, and given the initial approximation $\boldsymbol{u}_h^0$. Then, for any $\tau > 0$, there holds the following energy estimate on (13):*

$$
\begin{aligned}
&\tfrac{1}{2}\left\|\mathbf{u}_h^{l+1}\right\|_0^2 + \tfrac{\theta}{2}\left|Q^{l+1}\right|^2 + \tau\sum_{k=0}^{l}\left(\nu\left\|\nabla \mathbf{u}_h^{k+1}\right\|_0^2 + \mu\left\|\nabla \cdot \mathbf{u}_h^{k+1}\right\|_0^2\right) + \tfrac{\theta\tau}{T}\sum_{k=0}^{l}\left|Q^{k+1}\right|^2 \\
&\qquad \leq \exp(1)\left(\tfrac{1}{2}\left\|\mathbf{u}_h^0\right\|_0^2 + \tfrac{\theta}{2}\left|Q^0\right|^2 + \tfrac{\tau(\tau+T)}{2}\sum_{k=0}^{l}\left\|\boldsymbol{f}^{k+1}\right\|_0^2\right)
\end{aligned} \tag{14}
$$

for all $0 \leq l \leq N-1$.

Proof. Set $\boldsymbol{v}_h = \boldsymbol{u}_h^{n+1}$ in (13a) and multiply (13c) by θQ^{n+1}, then combining the two resulting equations leads to

$$
\begin{aligned}
&\tfrac{\|\boldsymbol{u}_h^{n+1}\|_0^2 - \|\boldsymbol{u}_h^n\|_0^2 + \|\boldsymbol{u}_h^{n+1}-\boldsymbol{u}_h^n\|_0^2}{2\tau} + \theta\tfrac{(Q^{n+1})^2 - (Q^n)^2 + (Q^{n+1}-Q^n)^2}{2\tau} + \nu\|\nabla \boldsymbol{u}_h^{n+1}\|_0^2 + \mu\|\nabla \cdot \boldsymbol{u}_h^{n+1}\|_0^2 + \tfrac{\theta}{T}(Q^{n+1})^2 \\
&\quad = \left(\boldsymbol{f}^{n+1}, \boldsymbol{u}_h^{n+1} - \boldsymbol{u}_h^n\right) + \left(\boldsymbol{f}^{n+1}, \boldsymbol{u}_h^n\right) \\
&\quad \leq \tfrac{\tau+T}{2}\|f^{n+1}\|_0^2 + \tfrac{\|\boldsymbol{u}_h^{n+1}-\boldsymbol{u}_h^n\|_0^2}{2\tau} + \tfrac{\|\boldsymbol{u}_h^n\|_0^2}{2T}.
\end{aligned}
$$

Summing over the above equation from $n = 0$ to $n = l$, and applying Lemma 2.5, we then obtain the above energy stability result (14). □

The corresponding second-order (in time) scheme for solving the EMAC-ESAV formulation (12) is given as follow: for $n = 1, 2, \cdots, N-1$, find $(\boldsymbol{u}_h^{n+1}, P_h^{n+1}) \in \boldsymbol{X}_h \times M_h$ and $Q^{n+1} \in \mathbb{R}$ such that

$$
\begin{cases}
\left(\frac{3\boldsymbol{u}_h^{n+1}-4\boldsymbol{u}_h^n+\boldsymbol{u}_h^{n-1}}{2\tau}, \boldsymbol{v}_h\right) + Q^{n+1}\exp\left(\frac{t_{n+1}}{T}\right) c\left(\widetilde{\boldsymbol{u}}_h^{n+1}, \widetilde{\boldsymbol{u}}_h^{n+1}, \boldsymbol{v}_h\right) & \\
\qquad - \left(P_h^{n+1}, \nabla \cdot \boldsymbol{v}_h\right) + \nu\left(\nabla \boldsymbol{u}_h^{n+1}, \nabla \boldsymbol{v}_h\right) + \mu\left(\nabla \cdot \boldsymbol{u}_h^{n+1}, \nabla \cdot \boldsymbol{v}_h\right) = \left(\boldsymbol{f}^{n+1}, \boldsymbol{v}_h\right), & \forall\, \boldsymbol{v}_h \in \boldsymbol{X}_h, \quad \text{(15a)} \\
\left(\nabla \cdot \boldsymbol{u}_h^{n+1}, q_h\right) = 0, & \forall\, q_h \in M_h, \quad \text{(15b)} \\
\frac{3Q^{n+1}-4Q^n+Q^{n-1}}{2\tau} = -\frac{1}{T}Q^{n+1} + \frac{1}{\theta}\exp\left(\frac{t_{n+1}}{T}\right) c\left(\widetilde{\boldsymbol{u}}_h^{n+1}, \widetilde{\boldsymbol{u}}_h^{n+1}, \boldsymbol{u}_h^{n+1}\right), & \quad \text{(15c)}
\end{cases}
$$

where $\widetilde{\boldsymbol{u}}_h^{n+1} = 2\boldsymbol{u}_h^n - \boldsymbol{u}_h^{n-1}$, and $Q^0 = 1$. We would refer the scheme (15) as the "sIMEX2-FEM" scheme. Note that we will take the sIMEX1-FEM scheme (13) to generate $(\boldsymbol{u}_h^1, P_h^1, Q^1)$ in order to start up the sIMEX2-FEM scheme (15). Some other schemes also surely can be used for the start-up such as the fully implicit Crank-Nicolson scheme [39]. For the energy stability of the second-order sIMEX2-FEM scheme (15), we have the following result.

Lemma 3.2. *(Discrete energy stability of sIMEX2-FEM) Assume* $\boldsymbol{f} \in L^2\left(0,T;L^2(\Omega)\right)$*, and given the initial approximation* $\boldsymbol{u}_h^0$*. Then, for any* $0<\tau\leq 1$*, there holds the following energy estimate on* (15)*:*

$$
\begin{aligned}
&\tfrac{1}{2}\|\boldsymbol{u}_h^{l+1}\|_0^2+\tfrac{1}{2}\|2\boldsymbol{u}_h^{l+1}-\boldsymbol{u}_h^{l}\|_0^2+\tfrac{\theta}{2}(Q^{l+1})^2+\tfrac{\theta}{2}(2Q^{l+1}-Q^{l})^2\\
&+2\tau\sum_{k=1}^{l}\left(\nu\|\nabla\boldsymbol{u}_h^{k+1}\|_0^2+\mu\|\nabla\cdot\boldsymbol{u}_h^{k+1}\|_0^2\right)+\tfrac{2\theta\tau}{T}\sum_{k=1}^{l}(Q^{k+1})^2\\
&\qquad\leq \exp(1)\left(\tfrac{1}{2}\|\boldsymbol{u}_h^{1}\|_0^2+\tfrac{1}{2}\|2\boldsymbol{u}_h^{1}-\boldsymbol{u}_h^{0}\|_0^2+\tfrac{\theta}{2}(Q^{1})^2+\tfrac{\theta}{2}(2Q^{1}-Q^{0})^2+2\tau(\tau+T)\sum_{k=1}^{l}\|\boldsymbol{f}^{k+1}\|_0^2\right)
\end{aligned}
\tag{16}
$$

for all $1\leq l\leq N-1$*.*

Proof. Set $\boldsymbol{v}_h=\boldsymbol{u}_h^{n+1}$ in (15a) and multiply (15c) by θQ^{n+1}, then combining the two produced equations leads to

$$
\begin{aligned}
&\tfrac{(\|\boldsymbol{u}_h^{n+1}\|_0^2+\|2\boldsymbol{u}_h^{n+1}-\boldsymbol{u}_h^{n}\|_0^2)-\left(\|\boldsymbol{u}_h^{n}\|_0^2+\|2\boldsymbol{u}_h^{n}-\boldsymbol{u}_h^{n-1}\|_0^2\right)+\|\boldsymbol{u}_h^{n+1}-2\boldsymbol{u}_h^{n}+\boldsymbol{u}_h^{n-1}\|_0^2}{4\tau}\\
&+\theta\tfrac{((Q^{n+1})^2+(2Q^{n+1}-Q^{n})^2)-\left((Q^{n})^2+(2Q^{n}-Q^{n-1})^2\right)+(Q^{n+1}-2Q^{n}+Q^{n-1})^2}{4\tau}\\
&+\nu\|\nabla\boldsymbol{u}_h^{n+1}\|_0^2+\mu\|\nabla\cdot\boldsymbol{u}_h^{n+1}\|_0^2+\tfrac{\theta}{T}(Q^{n+1})^2\\
&\quad=\left(\boldsymbol{f}^{n+1},\boldsymbol{u}_h^{n+1}-2\boldsymbol{u}_h^{n}+\boldsymbol{u}_h^{n-1}\right)+\left(\boldsymbol{f}^{n+1},2\boldsymbol{u}_h^{n}-\boldsymbol{u}_h^{n-1}\right)\\
&\quad\leq(\tau+T)\,\|f^{n+1}\|_0^2+\tfrac{\|\boldsymbol{u}_h^{n+1}-2\boldsymbol{u}_h^{n}+\boldsymbol{u}_h^{n-1}\|_0^2}{4\tau}+\tfrac{\|2\boldsymbol{u}_h^{n}-\boldsymbol{u}_h^{n-1}\|_0^2}{4T}.
\end{aligned}
$$

Summing over the above equation from $n=1$ to $n=l$, and applying Lemma 2.5, we then obtain the above energy stability result (16). □

System decoupling and solution process. Let us first consider the decoupling and solution strategy for the sIMEX1-FEM scheme (13). Starting from (13c), it holds

$$
Q^{n+1}=\tfrac{T}{T+\tau}Q^{n}+\tfrac{\tau T}{\theta(T+\tau)}\exp\left(\tfrac{t_{n+1}}{T}\right)c\left(\boldsymbol{u}_h^{n},\boldsymbol{u}_h^{n},\boldsymbol{u}_h^{n+1}\right).
\tag{17}
$$

Substituting (17) into (13a), we obtain the following new system:

$$
\begin{cases}
\left(\tfrac{\boldsymbol{u}_h^{n+1}-\boldsymbol{u}_h^{n}}{\tau},\boldsymbol{v}_h\right)+\tfrac{\tau T}{\theta(T+\tau)}\exp\left(\tfrac{2t_{n+1}}{T}\right)c\left(\boldsymbol{u}_h^{n},\boldsymbol{u}_h^{n},\boldsymbol{u}_h^{n+1}\right)c\left(\boldsymbol{u}_h^{n},\boldsymbol{u}_h^{n},\boldsymbol{v}_h\right)-\left(P_h^{n+1},\nabla\cdot\boldsymbol{v}_h\right)\\
\quad+\nu\left(\nabla\boldsymbol{u}_h^{n+1},\nabla\boldsymbol{v}_h\right)+\mu\left(\nabla\cdot\boldsymbol{u}_h^{n+1},\nabla\cdot\boldsymbol{v}_h\right)=\left(\boldsymbol{f}^{n+1},\boldsymbol{v}_h\right)-\tfrac{T}{T+\tau}Q^{n}\exp\left(\tfrac{t_{n+1}}{T}\right)c\left(\boldsymbol{u}_h^{n},\boldsymbol{u}_h^{n},\boldsymbol{v}_h\right), &\text{(18a)}\\
\left(\nabla\cdot\boldsymbol{u}_h^{n+1},q_h\right)=0, &\text{(18b)}
\end{cases}
$$

for any $\boldsymbol{v}_h\in\boldsymbol{X}_h$ and $q_h\in M_h$. When compared to the regular grad-div stabilized Stokes system, in the momentum equation (18a), we have an extra stabilization term

$$
\tfrac{\tau T}{\theta(T+\tau)}\exp\left(\tfrac{2t_{n+1}}{T}\right)c\left(\boldsymbol{u}_h^{n},\boldsymbol{u}_h^{n},\boldsymbol{u}_h^{n+1}\right)c\left(\boldsymbol{u}_h^{n},\boldsymbol{u}_h^{n},\boldsymbol{v}_h\right)
$$

produced from the ESAV dynamics equation. Clearly,

$$
c\left(\boldsymbol{u}_h^{n},\boldsymbol{u}_h^{n},\boldsymbol{u}_h^{n+1}\right)c\left(\boldsymbol{u}_h^{n},\boldsymbol{u}_h^{n},\boldsymbol{u}_h^{n+1}\right)\geq 0
$$

and the equality holds when $\boldsymbol{u}_h^{n+1}=\boldsymbol{u}_h^{n}$, thus the Stokes system (18) is well-posed due to the fact that the Taylor-Hood element is adopted (the discrete inf-sup condition holds). At each time step, we first solve $\boldsymbol{u}_h^{n+1}$ and P_h^{n+1} from (18), and then plug them into (17) to compute Q^{n+1}.

For the sIMEX2-FEM scheme (15), we correspondingly get

$$
Q^{n+1}=\tfrac{4T}{3T+2\tau}Q^{n}-\tfrac{T}{3T+2\tau}Q^{n-1}+\tfrac{2\tau T}{\theta(3T+2\tau)}\exp\left(\tfrac{t_{n+1}}{T}\right)c\left(\widetilde{\boldsymbol{u}}_h^{n+1},\widetilde{\boldsymbol{u}}_h^{n+1},\boldsymbol{u}_h^{n+1}\right).
\tag{19}
$$

Substituting (19) into (15a), we obtain the following new system:

$$
\begin{cases}
\left(\frac{3\boldsymbol{u}_h^{n+1}-4\boldsymbol{u}_h^n+\boldsymbol{u}_h^{n-1}}{2\tau},\boldsymbol{v}_h\right)+\frac{2\tau T}{\theta(3T+2\tau)}\exp\left(\frac{2t_{n+1}}{T}\right)c\left(\widetilde{\boldsymbol{u}}_h^{n+1},\widetilde{\boldsymbol{u}}_h^{n+1},\boldsymbol{u}_h^{n+1}\right)c\left(\widetilde{\boldsymbol{u}}_h^{n+1},\widetilde{\boldsymbol{u}}_h^{n+1},\boldsymbol{v}_h\right) \\
\quad -\left(P_h^{n+1},\nabla\cdot\boldsymbol{v}_h\right)+\nu\left(\nabla\boldsymbol{u}_h^{n+1},\nabla\boldsymbol{v}_h\right)+\mu\left(\nabla\cdot\boldsymbol{u}_h^{n+1},\nabla\cdot\boldsymbol{v}_h\right) \\
\quad =\left(\boldsymbol{f}^{n+1},\boldsymbol{v}_h\right)-\left(\frac{4T}{3T+2\tau}Q^n-\frac{T}{3T+2\tau}Q^{n-1}\right)\exp\left(\frac{t_{n+1}}{T}\right)c\left(\widetilde{\boldsymbol{u}}_h^{n+1},\widetilde{\boldsymbol{u}}_h^{n+1},\boldsymbol{v}_h\right), \qquad \text{(20a)} \\
\left(\nabla\cdot\boldsymbol{u}_h^{n+1},q_h\right)=0, \qquad \text{(20b)}
\end{cases}
$$

for any $\boldsymbol{v}_h\in\boldsymbol{X}_h$ and $q_h\in M_h$.

From (18) and (20), it is easy to see that the smaller θ, the stronger stabilization effect incurred by the extra ESAV term in the proposed schemes. We also note that some algebraic splitting techniques also can be further applied to solve the systems (18) and (20) as discussed in [40, 43, 42, 41].

Remark 3.3. *Traditionally, in the SAV-based schemes the velocity and pressure are often decoupled as* [34, 23]

$$\boldsymbol{u}_h^{n+1}=\boldsymbol{u}_{1,h}^{n+1}+G^{n+1}\boldsymbol{u}_{2,h}^{n+1},\quad P_h^{n+1}=P_{1,h}^{n+1}+G^{n+1}P_{2,h}^{n+1},$$

with $G^{n+1}=Q^{n+1}\exp\left(\frac{t_{n+1}}{T}\right)$, *which requires two linear Stokes solves, for* $\boldsymbol{u}_{1,h}^{n+1},P_{1,h}^{n+1}$ *and* $\boldsymbol{u}_{2,h}^{n+1},P_{2,h}^{n+1}$, *respectively at each time step and thus is less efficient.*

4. Robust fully-discrete error estimates

In this section, we will carefully analyze the convergences behavior in time and space of the proposed numerical schemes (13) and (15). For simplicity, we will assume the ESAV stabilizing parameter $\theta=1$ which corresponds to the classic choice for SAV methods.

4.1. Error estimate on the sIMEX1-FEM scheme.

We first consider the sIMEX1-FEM scheme (13). Let $(\boldsymbol{u},P)$ denote the solution to the system (11) (equivalently, $(\boldsymbol{u},P,Q)$ the solution of the system (12)) and $\{(\boldsymbol{u}_h^{n+1},P_h^{n+1},Q^{n+1})\}_{n=0}^{N-1}$ the numerical solution produced by the scheme (13). We assume that $(\boldsymbol{u},P)$ satisfies the following regularity requirement:

$$
\begin{cases}
\boldsymbol{u}\in L^\infty(0,T;(H_0^1(\Omega))^d\cap(H^3(\Omega))^d), \\
\boldsymbol{u}_t\in L^2(0,T;(H^3(\Omega))^d),\ \boldsymbol{u}_{tt}\in L^2(0,T;(H^1(\Omega))^d), \\
P\in L^\infty(0,T;H^2(\Omega)).
\end{cases} \qquad (21)
$$

Note that $\boldsymbol{u}\in L^\infty(0,T;(H^3(\Omega))^d)$ implies $\boldsymbol{u}\in L^\infty(0,T;(W^{1,\infty}(\Omega))^d)$. Since $Q(t)=\exp(-t/T)$ it holds $Q\in C^\infty[0,T]$.

In Sub-subsection 4.1.1, we first conduct error analysis with viscosity-independent (i.e., *Re*-independent) Gronwall constant for the scheme (13) with $\mu=0$, i.e., without grad-div stabilization. Our error estimates will essentially improve those obtained in [23] where the Gronwall constant is exponentially dependent of the inverse of the viscosity. In addition, we will identify an potential issue for the scheme with grad-div stabilization, that is, the spatial mesh size h must be restricted by $O(\nu^2)$ (thus very small when the Reynolds number is large). Later in Sub-subsection 4.1.2, the analysis results for the case of $\mu=0$ will be utilized to further derive the error estimates for the scheme (13) with $\mu>0$ and in this case the viscosity-dependence of the mesh size constraint can greatly be alleviated due to the existence of the grad-div stabilization term, which is practically very important when dealing with problems with large Reynolds number.

4.1.1. *The case of the grad-div stabilizing parameter* $\mu=0$. In this subsection, we consider the case of the grad-div stabilizing parameter $\mu=0$. Motivated by the work of [32, 31, 2], we will first derive a sub-optimal convergent result, based on which, we then bound the numerical solution and conduct optimal error estimation. Define $\eta(t)=\boldsymbol{u}(t)-\mathrm{P}_{st}\boldsymbol{u}(t)$ and $e_u^{n+1}=\mathrm{P}_{st}\boldsymbol{u}(t_{n+1})-\boldsymbol{u}_h^{n+1}$, then $\boldsymbol{u}(t_{n+1})-\boldsymbol{u}_h^{n+1}=\eta(t_{n+1})+e_u^{n+1}$. Define $e_Q^{n+1}=Q(t_{n+1})-Q^{n+1}$. Let us first focus on the error estimation of the velocity field $\boldsymbol{u}_h$.

Lemma 4.1. *Assume the grad-div stabilizing parameter* $\mu=0$. *There exists a viscosity-dependent positive constant* $0<h_0^{\{\nu\}}\le 1$ *such that if* $h\le h_0^{\{\nu\}}$ *and* $\tau\le h^2$, *then*

$$\left\|e_u^1\right\|_0^2+\nu\tau\left\|\nabla e_u^1\right\|_0^2+\left|e_Q^1\right|^2\le h^{-\frac{1}{2}}\left(h^4+\tau^2\right). \qquad (22)$$

Proof. Assume $\tau \le h^2 \le 1$. Letting $\boldsymbol{v} = \boldsymbol{v}_h$ in (12a) and $q = q_h$ in (12b), and subtracting (13a)-(13c) with $n = 1$ from the resulting equations with $t = t_1$, it yields

$$\begin{cases} \left(\frac{\partial \boldsymbol{u}}{\partial t}(t_1) - \frac{\boldsymbol{u}_h^1 - \boldsymbol{u}_h^0}{\tau}, \boldsymbol{v}_h\right) + Q(t_1)\exp\left(\frac{t_1}{T}\right) c\left(\boldsymbol{u}(t_1), \boldsymbol{u}(t_1), \boldsymbol{v}_h\right) - Q^1 \exp\left(\frac{t_1}{T}\right) c\left(\boldsymbol{u}_h^0, \boldsymbol{u}_h^0, \boldsymbol{v}_h\right) \\ \qquad\qquad - \left(P(t_1) - P_h^1, \nabla \cdot \boldsymbol{v}_h\right) + \nu\left(\nabla\left(\boldsymbol{u}(t_1) - \boldsymbol{u}_h^1\right), \nabla \boldsymbol{v}_h\right) = 0, \quad (23a) \\ \left(\nabla \cdot \left(\boldsymbol{u}(t_1) - \boldsymbol{u}_h^1\right), q_h\right) = 0, \quad (23b) \\ \frac{dQ}{dt}(t_1) - \frac{Q^1 - Q^0}{\tau} = -\frac{1}{T}\left(Q(t_1) - Q^1\right) \\ \qquad\qquad + \exp\left(\frac{t_1}{T}\right)\left[c\left(\boldsymbol{u}(t_1), \boldsymbol{u}(t_1), \boldsymbol{u}(t_1)\right) - c\left(\boldsymbol{u}_h^0, \boldsymbol{u}_h^0, \boldsymbol{u}_h^1\right)\right]. \quad (23c) \end{cases}$$

Choosing $\boldsymbol{v}_h = e_u^1$ in (23a), we then have the following error equation

$$\begin{aligned} &\left(\frac{e_u^1 - e_u^0}{\tau}, e_u^1\right) + \nu\left(\nabla e_u^1, \nabla e_u^1\right) \\ &= -\left(\boldsymbol{u}_t(t_1) - \frac{\boldsymbol{u}(t_1) - \boldsymbol{u}(t_0)}{\tau}, e_u^1\right) - \left(\frac{\eta(t_1) - \eta(t_0)}{\tau}, e_u^1\right) + \left(P(t_1) - \Pi_h P(t_1), \nabla \cdot e_u^1\right) \\ &\quad - Q(t_1)\exp\left(\frac{t_1}{T}\right) c\left(\boldsymbol{u}(t_1), \boldsymbol{u}(t_1), e_u^1\right) + Q^1 \exp\left(\frac{t_1}{T}\right) c\left(\boldsymbol{u}_h^0, \boldsymbol{u}_h^0, e_u^1\right) := \sum_{i=1}^5 \mathbb{I}_i, \end{aligned} \tag{24}$$

where $\Pi_h P(t_1)$ denotes the interpolation of $P(t_1)$ on M_h and the fact of $\left(P_h^1 - \Pi_h P(t_1), \nabla \cdot e_u^1\right) = 0$ has been used since $P_h^1 - \Pi_h P(t_1) \in M_h$ and (13b).

The left-hand side of (24) can be rewritten as

$$\left(\frac{e_u^1 - e_u^0}{\tau}, e_u^1\right) + \nu\left(\nabla e_u^1, \nabla e_u^1\right) = \frac{1}{2\tau}\left(\|e_u^1\|_0^2 - \|e_u^0\|_0^2 + \|e_u^1 - e_u^0\|_0^2\right) + \nu\left\|\nabla e_u^1\right\|_0^2. \tag{25}$$

For the first two terms on the right-hand side of (24), by Young's inequality we have the following estimates:

$$|\mathbb{I}_1| \le 32\tau \|\boldsymbol{u}_{tt}\|_{L^2(t_0,t_1;L^2)}^2 + \frac{\|e_u^1 - e_u^0\|_0^2}{64\tau} + \frac{\|e_u^0\|_0^2}{64}, \tag{26}$$

and

$$\begin{aligned} |\mathbb{I}_2| &\le \frac{32}{\tau}\|\eta_t\|_{L^2(t_0,t_1;L^2)}^2 + \frac{\|e_u^1 - e_u^0\|_0^2}{64\tau} + \frac{\|e_u^0\|_0^2}{64} \\ &\le \frac{32(C_2)^2}{\tau} h^6 \|\boldsymbol{u}_t\|_{L^2(t_0,t_1;H^3)}^2 + \frac{\|e_u^1 - e_u^0\|_0^2}{64\tau} + \frac{\|e_u^0\|_0^2}{64}, \end{aligned} \tag{27}$$

where Lemma 2.4 and $\tau \le 1$ are used. The third term on the right-hand side of (24) can be bounded as

$$|\mathbb{I}_3| \le \frac{\nu}{2}\|\nabla \cdot e_u^1\|_0^2 + \frac{1}{2\nu}\|P(t_1) - \Pi_h P(t_1)\|_0^2 \le \frac{\nu}{2}\|\nabla \cdot e_u^1\|_0^2 + \frac{C_0}{2\nu} h^4 \|P(t_1)\|_2^2. \tag{28}$$

Noticing $Q(t_1)\exp\left(\frac{t_1}{T}\right) = 1$, the fourth and fifth terms on the right-hand side of (24) can be reformulated as

$$\begin{aligned} \mathbb{I}_4 + \mathbb{I}_5 &= \left[-c\left(\boldsymbol{u}(t_1), \boldsymbol{u}(t_1), e_u^1\right) + c\left(\boldsymbol{u}(t_0), \boldsymbol{u}(t_0), e_u^1\right)\right] \\ &\quad + \left[-c\left(\boldsymbol{u}(t_0), \boldsymbol{u}(t_0), e_u^1\right) + c\left(\boldsymbol{u}_h^0, \boldsymbol{u}_n^0, e_u^1\right)\right] - e_Q^1 \exp\left(\frac{t_1}{T}\right) c\left(\boldsymbol{u}_h^0, \boldsymbol{u}_h^0, e_u^1\right). \end{aligned} \tag{29}$$

Note that

$$\begin{aligned} &\left|c\left(\boldsymbol{u}(t_1), \boldsymbol{u}(t_1), e_u^1\right) - c\left(\boldsymbol{u}(t_0), \boldsymbol{u}(t_0), e_u^1\right)\right| \\ &= \left|c\left(\boldsymbol{u}(t_1) - \boldsymbol{u}(t_0), \boldsymbol{u}(t_1), e_u^1\right) + c\left(\boldsymbol{u}(t_0), \boldsymbol{u}(t_1) - \boldsymbol{u}(t_0), e_u^1\right)\right| \\ &\le \frac{\|e_u^1 - e_u^0\|_0^2}{64\tau} + \frac{\|e_u^0\|_0^2}{64} + 96\tau(C_1)^2\left(\|\boldsymbol{u}(t_1)\|_{L^\infty}^2 + \|\nabla \boldsymbol{u}(t_0)\|_{L^\infty}^2\right)\|\boldsymbol{u}_t\|_{L^2(t_0,t_1;H^1)}^2. \end{aligned} \tag{30}$$

Since $\boldsymbol{u}(t_0) = \boldsymbol{u}_h^0 + \eta(t_0) + e_u^0$, we have

$$\begin{aligned} &c\left(\boldsymbol{u}(t_0), \boldsymbol{u}(t_0), e_u^1\right) - c\left(\boldsymbol{u}_h^0, \boldsymbol{u}_h^0, e_u^1\right) \\ &= c\left(\eta(t_0), \boldsymbol{u}(t_0), e_u^1\right) + c\left(e_u^0 + \boldsymbol{u}_h^0, \boldsymbol{u}(t_0), e_u^1\right) - c\left(\boldsymbol{u}_h^0, \boldsymbol{u}_h^0, e_u^1\right) \\ &= c\left(\eta(t_0), \boldsymbol{u}(t_0), e_u^1\right) + c\left(e_u^0 + \boldsymbol{u}_h^0, \boldsymbol{u}(t_0), e_u^1\right) - c\left(e_u^0 + \boldsymbol{u}_h^0, \boldsymbol{u}_h^0, e_u^1\right) + c\left(e_u^0, \boldsymbol{u}_n^0, e_u^1\right) \\ &= c\left(\eta(t_0), \boldsymbol{u}(t_0), e_u^1\right) + c\left(\mathrm{P}_{st}\boldsymbol{u}(t_0), \boldsymbol{u}(t_0) - \boldsymbol{u}_n^0, e_u^1\right) + c\left(e_u^0, \mathrm{P}_{st}\boldsymbol{u}(t_0), e_u^1\right) - c\left(e_u^0, e_u^0, e_u^1\right) \\ &= c\left(\eta(t_0), \boldsymbol{u}(t_0), e_u^1\right) + c\left(\mathrm{P}_{st}\boldsymbol{u}(t_0), \eta(t_0), e_u^1\right) + c\left(\mathrm{P}_{st}\boldsymbol{u}(t_0), e_u^0, e_u^1\right) \\ &\quad + c\left(e_u^0, \mathrm{P}_{st}\boldsymbol{u}(t_0), e_u^1\right) - c\left(e_u^0, e_u^0, e_u^1\right). \end{aligned} \tag{31}$$

By Holder's inequality, Sobolev embedding inequalities [1] and Lemma 2.1, for the first three terms on the right-hand side of (31) we have

$$
\begin{aligned}
\left|c\left(\eta(t_0),\boldsymbol{u}\left(t_0\right),e_u^1\right)\right| &\le \tfrac{\|e_u^1-e_u^0\|_0^2}{64\tau}+\tfrac{\|e_u^0\|_0^2}{64}+96(C_2)^2h^4\left\|\boldsymbol{u}\left(t_0\right)\right\|_{L^\infty}^2\left\|\boldsymbol{u}(t_0)\right\|_3^2,\\
\left|c\left(\mathrm{P}_{st}\boldsymbol{u}\left(t_0\right),\eta(t_0),e_u^1\right)\right| &\le \tfrac{\|e_u^1-e_u^0\|_0^2}{64\tau}+\tfrac{\|e_u^0\|_0^2}{64}+96(C_1C_2)^2h^6\left\|\nabla\boldsymbol{u}\left(t_0\right)\right\|_{L^\infty}^2\left\|\boldsymbol{u}(t_0)\right\|_3^2,\\
\left|c\left(\mathrm{P}_{st}\boldsymbol{u}\left(t_0\right),e_u^0,e_u^1\right)\right| &\le \tfrac{\|e_u^1-e_u^0\|_0^2}{64\tau}+\left(96(C_1)^2\left\|\nabla\boldsymbol{u}\left(t_0\right)\right\|_{L^\infty}^2+\tfrac{1}{64}\right)\left\|e_u^0\right\|_0^2.
\end{aligned}
\tag{32}
$$

For the last two terms on the right-hand side of (31), we have

$$
\begin{aligned}
\left|c\left(e_u^0,\mathrm{P}_{st}\boldsymbol{u}\left(t_0\right),e_u^1\right)\right| &= \left|c\left(e_u^0,\mathrm{P}_{st}\boldsymbol{u}\left(t_0\right),e_u^1-e_u^0\right)+c\left(e_u^0,\mathrm{P}_{st}\boldsymbol{u}\left(t_0\right),e_u^0\right)\right|\\
&= \left|c\left(e_u^0,\mathrm{P}_{st}\boldsymbol{u}\left(t_0\right),e_u^1-e_u^0\right)-\tfrac{1}{2}\left(\nabla\cdot\mathrm{P}_{st}\boldsymbol{u}\left(t_0\right)e_u^0,e_u^0\right)-\left((e_u^0\cdot\nabla)\mathrm{P}_{st}\boldsymbol{u}\left(t_0\right),e_u^0\right)\right|\\
&\le \tfrac{\|e_u^1-e_u^0\|_0^2}{64\tau}+50(C_1)^2\left(\tau h^{-2}(C_3)^2\left\|\boldsymbol{u}\left(t_0\right)\right\|_{L^\infty}^2+\left\|\nabla\boldsymbol{u}\left(t_0\right)\right\|_{L^\infty}^2\right)\left\|e_u^0\right\|_0^2,
\end{aligned}
\tag{33}
$$

where integration by parts is applied on the second equality, and

$$
\left|c\left(e_u^0,e_u^0,e_u^1\right)\right| = \left|c\left(e_u^0,e_u^0,e_u^1-e_u^0\right)\right| \le \tfrac{\|e_u^1-e_u^0\|_0^2}{64\tau}+48(C_3)^2\tau h^{-2}\left\|e_u^0\right\|_{L^\infty}^2\left\|e_u^0\right\|_0^2.
\tag{34}
$$

Combining all the above estimates for the terms of (24) and multiplying 2τ to both of its sides, we obtain based on the regularity assumption (21):

$$
\begin{aligned}
&\|e_u^1\|_0^2-\|e_u^0\|_0^2+\nu\tau\|\nabla e_u^1\|_0^2+\tfrac{3\|e_u^1-e_u^0\|_0^2}{4}\\
&\le 2\tau\Big(\tfrac{3}{32}+50\tau h^{-2}(C_1C_3)^2\left\|\boldsymbol{u}\left(t_0\right)\right\|_{L^\infty}^2+82(C_1)^2\left\|\nabla\boldsymbol{u}\left(t_0\right)\right\|_{L^\infty}^2+48(C_3)^2\tau h^{-2}\left\|e_u^0\right\|_{L^\infty}^2\Big)\|e_u^0\|_0^2\\
&\quad+128\tau^2\|\boldsymbol{u}_{tt}\|_{L^2(t_0,t_1;L^2)}^2+128(C_2)^2h^6\|\boldsymbol{u}_t\|_{L^2(t_0,t_1;H^3)}^2+\tau(C_0)^2\nu^{-1}h^4\|P\left(t_1\right)\|_2^2\\
&\quad+128\tau^2(C_1)^2\left(\|\boldsymbol{u}\left(t_1\right)\|_{L^\infty}^2+\|\nabla\boldsymbol{u}\left(t_0\right)\|_{L^\infty}^2\right)\|\boldsymbol{u}_t\|_{L^2(t_0,t_1;H^1)}^2\\
&\quad+128\tau h^4(C_2)^2\left(\left\|\boldsymbol{u}\left(t_0\right)\right\|_{L^\infty}^2+h^2(C_1)^2\left\|\nabla\boldsymbol{u}\left(t_0\right)\right\|_{L^\infty}^2\right)\|\boldsymbol{u}(t_0)\|_3^2\\
&\quad-2\tau e_Q^1\exp\left(\tfrac{t_1}{T}\right)c\left(\boldsymbol{u}_h^0,\boldsymbol{u}_h^0,e_u^1\right).
\end{aligned}
\tag{35}
$$

For the last term $2\tau e_Q^1\exp\left(\frac{t_1}{T}\right)c\left(\boldsymbol{u}_h^0,\boldsymbol{u}_h^0,e_u^1\right)$ on the right-hand side of (35), we temporarily leave it here and will come back with the analysis from the ESAV error equation.

To further simplify the representation, let us define $E_Q^1=e_Q^1\exp\left(\frac{t_1}{T}\right)$ and apply the fact $\exp(2)\le 8$ in our following derivations. Multiplying (23c) by e_Q^1, it yields

$$
\begin{aligned}
\tfrac{e_Q^1-e_Q^0}{\tau}e_Q^1+\tfrac{1}{T}\left(e_Q^1\right)^2 &= -\left(\tfrac{dQ}{dt}\left(t_1\right)-\tfrac{Q(t_1)-Q(t_0)}{\tau}\right)e_Q^1\\
&\quad+E_Q^1\left(c\left(\boldsymbol{u}\left(t_1\right),\boldsymbol{u}\left(t_1\right),\boldsymbol{u}\left(t_1\right)\right)-c\left(\boldsymbol{u}_h^0,\boldsymbol{u}_h^0,\boldsymbol{u}_h^1\right)\right).
\end{aligned}
\tag{36}
$$

The first term on the right-hand side of (36) can be estimated by

$$
\left|\left(\tfrac{dQ}{dt}\left(t_1\right)-\tfrac{Q(t_1)-Q(t_0)}{\tau}\right)e_Q^1\right| \le \tfrac{1}{8T}|e_Q^1|^2+2\tau T\int_{t_0}^{t_1}|Q_{tt}|^2dt.
\tag{37}
$$

For the second term on the right-hand side of (36), we use the fact

$$
c\left(\boldsymbol{u}\left(t_1\right),\boldsymbol{u}\left(t_1\right),\boldsymbol{u}\left(t_1\right)\right)=c\left(\boldsymbol{u}\left(t_0\right),\boldsymbol{u}\left(t_0\right),\boldsymbol{u}\left(t_0\right)\right)=0,
$$

and reformulate it into

$$
\begin{aligned}
&E_Q^1\left(c\left(\boldsymbol{u}\left(t_1\right),\boldsymbol{u}\left(t_1\right),\boldsymbol{u}\left(t_1\right)\right)-c\left(\boldsymbol{u}_h^0,\boldsymbol{u}_h^0,\boldsymbol{u}_h^1\right)\right)\\
&\quad=E_Q^1c\left(\boldsymbol{u}\left(t_0\right),\boldsymbol{u}\left(t_0\right),\boldsymbol{u}\left(t_0\right)-\boldsymbol{u}\left(t_1\right)\right)+E_Q^1c\left(\boldsymbol{u}\left(t_0\right)-\boldsymbol{u}_h^0,\boldsymbol{u}\left(t_0\right),\boldsymbol{u}\left(t_1\right)\right)\\
&\qquad+E_Q^1c\left(\boldsymbol{u}_h^0,\boldsymbol{u}\left(t_0\right)-\boldsymbol{u}_h^0,\boldsymbol{u}\left(t_1\right)\right)+E_Q^1c\left(\boldsymbol{u}_h^0,\boldsymbol{u}_h^0,\boldsymbol{u}\left(t_1\right)-\boldsymbol{u}_h^1\right)=:\textstyle\sum_{i=1}^4\mathbb{J}_i.
\end{aligned}
\tag{38}
$$

Note that for the first term on the right-hand side of (38), we have

$$
|\mathbb{J}_1| \le \frac{1}{8T}|e_Q^1|^2+48\tau T\left\|\boldsymbol{u}\left(t_0\right)\right\|_{L^\infty}^2\left\|\nabla\boldsymbol{u}\left(t_0\right)\right\|_0^2\left\|\boldsymbol{u}_t\right\|_{L^2(t_0,t_1;L^2)}^2.
\tag{39}
$$

The second term on the right-hand side of (38) can be estimated by integrating by parts

$$
\begin{aligned}
|\mathbb{J}_2| &= \left|E_Q^1 c\left(\eta(t_0)+e_u^0, \boldsymbol{u}\left(t_0\right), \boldsymbol{u}\left(t_1\right)\right)\right| \\
&\leq \frac{1}{8T}|e_Q^1|^2+48T(\|\nabla \boldsymbol{u}\left(t_0\right)\|_{L^\infty}^2\left\|\boldsymbol{u}\left(t_1\right)\right\|_0^2+\|\nabla \boldsymbol{u}\left(t_1\right)\|_{L^\infty}^2\left\|\boldsymbol{u}\left(t_0\right)\right\|_0^2)\left(\|\eta(t_0)\|_0^2+\left\|e_u^0\right\|_0^2\right).
\end{aligned} \tag{40}
$$

For the third term on the right-hand side of (38), we have

$$
\mathbb{J}_3 = E_Q^1\big(c\left(\mathrm{P}_{st}\boldsymbol{u}\left(t_0\right), \eta(t_0)+e_u^0, \boldsymbol{u}\left(t_1\right)\right)+c\left(e_u^0, \eta^n, \boldsymbol{u}\left(t_1\right)\right)+c\left(e_u^0, e_u^0, \boldsymbol{u}\left(t_1\right)\right)\big),
$$

where

$$
\begin{cases}
\left|E_Q^1 c\left(\mathrm{P}_{st}\boldsymbol{u}\left(t_0\right), \eta(t_0)+e_u^0, \boldsymbol{u}\left(t_1\right)\right)\right| \\
\qquad \leq \frac{1}{8T}|e_Q^1|^2+48T(C_1)^2\left\|\nabla \boldsymbol{u}\left(t_0\right)\right\|_{L^\infty}^2\left\|\boldsymbol{u}\left(t_1\right)\right\|_0^2\left(\|\eta(t_0)\|_0^2+\left\|e_u^0\right\|_0^2\right), \\
\left|E_Q^1 c\left(e_u^0, \eta(t_0), \boldsymbol{u}\left(t_1\right)\right)\right| \\
\qquad \leq \frac{1}{8T}|e_Q^1|^2+48T\left(\left\|\boldsymbol{u}\left(t_1\right)\right\|_{L^\infty}^2\|\nabla \eta(t_0)\|_0^2+\left\|\boldsymbol{u}\left(t_1\right)\right\|_{W^{1,\infty}}^2\|\eta(t_0)\|_0^2\right)\left\|e_u^0\right\|_0^2, \\
\left|E_Q^1 c\left(e_u^0, e_u^0, \boldsymbol{u}\left(t_1\right)\right)\right| \leq \frac{1}{8T}|e_Q^1|^2+48(C_3)^2Th^{-2}\left\|\boldsymbol{u}\left(t_1\right)\right\|_{L^\infty}^2\left\|e_u^0\right\|_0^4.
\end{cases} \tag{41}
$$

For the fourth term on the right-hand side of (38), we have

$$
\begin{aligned}
\mathbb{J}_4 &= E_Q^1 c\left(\boldsymbol{u}_h^0, \boldsymbol{u}_h^0, \eta^1\right)+E_Q^1 c\left(\boldsymbol{u}_h^0, \boldsymbol{u}_h^0, e_u^1\right) \\
&\leq \frac{|e_Q^1|^2}{4T}+24T(C_1)^4\|\nabla \boldsymbol{u}\left(t_0\right)\|_0^4\|\nabla \eta^1\|_0^2+E_Q^1 c\left(\boldsymbol{u}_h^0, \boldsymbol{u}_h^0, e_u^1\right) \\
&\leq \frac{|e_Q^1|^2}{4T}+24T(C_1)^4(C_2)^2h^4\|\nabla \boldsymbol{u}\left(t_0\right)\|_0^4\|\boldsymbol{u}\left(t_1\right)\|_3^2+E_Q^1 c\left(\boldsymbol{u}_h^0, \boldsymbol{u}_h^0, e_u^1\right).
\end{aligned} \tag{42}
$$

Combining all the above estimates for the terms of (38), we have the following estimate based on the regularity assumption (21) and the smoothness of Q:

$$
\begin{aligned}
|e_Q^1|^2-|e_Q^0|^2 \leq\ & 4\tau^2T\int_{t_0}^{t_1}|Q_{tt}|^2dt+96\tau^2T\left\|\boldsymbol{u}\left(t_0\right)\right\|_{L^\infty}^2\left\|\nabla \boldsymbol{u}\left(t_0\right)\right\|_0^2\left\|\boldsymbol{u}_t\right\|_{L^2(t_0,t_1;L^2)}^2 \\
&+96\tau h^6T(C_2)^2\left(\left((C_1)^2+1\right)\left\|\nabla \boldsymbol{u}\left(t_0\right)\right\|_{L^\infty}^2\left\|\boldsymbol{u}\left(t_1\right)\right\|_0^2+\left\|\nabla \boldsymbol{u}\left(t_1\right)\right\|_{L^\infty}^2\left\|\boldsymbol{u}\left(t_0\right)\right\|_0^2\right)\|\boldsymbol{u}(t_0)\|_3^2 \\
&+96\tau T\left(\left((C_1)^2+1\right)\left\|\nabla \boldsymbol{u}\left(t_0\right)\right\|_{L^\infty}^2\left\|\boldsymbol{u}\left(t_1\right)\right\|_0^2+\left\|\nabla \boldsymbol{u}\left(t_1\right)\right\|_{L^\infty}^2\left\|\boldsymbol{u}\left(t_0\right)\right\|_0^2\right)\left\|e_u^0\right\|_0^2 \\
&+96\tau h^4T(C_2)^2\left(\left\|\boldsymbol{u}\left(t_1\right)\right\|_{L^\infty}^2+h^2\left\|\boldsymbol{u}\left(t_1\right)\right\|_{W^{1,\infty}}^2\right)\|\boldsymbol{u}(t_0)\|_3^2\left\|e_u^0\right\|_0^2 \\
&+96\tau h^{-2}T(C_3)^2\left\|\boldsymbol{u}\left(t_1\right)\right\|_{L^\infty}^2\left\|e_u^0\right\|_0^4+48\tau h^4T(C_1)^4(C_2)^2\|\nabla \boldsymbol{u}\left(t_0\right)\|_0^4\|\boldsymbol{u}\left(t_1\right)\|_3^2 \\
&+2\tau E_Q^1 c\left(\boldsymbol{u}_h^0, \boldsymbol{u}_h^0, e_u^1\right).
\end{aligned} \tag{43}
$$

Applying $e_u^0=0$ and $e_Q^0=0$, we obtain from (35) and (43) that

$$
\begin{aligned}
&\|e_u^1\|_0^2+\nu\tau\|\nabla e_u^1\|_0^2+|e_Q^1|^2 \\
&\leq 128\tau^2\|\boldsymbol{u}_{tt}\|_{L^2(t_0,t_1;L^2)}^2+128(C_2)^2h^6\|\boldsymbol{u}_t\|_{L^2(t_0,t_1;H^3)}^2+\tau(C_0)^2\nu^{-1}h^4\|P\left(t_1\right)\|_2^2 \\
&\quad+128\tau^2(C_1)^2\left(\left\|\boldsymbol{u}\left(t_1\right)\right\|_{L^\infty}^2+\left\|\nabla \boldsymbol{u}\left(t_0\right)\right\|_{L^\infty}^2\right)\|\boldsymbol{u}_t\|_{L^2(t_0,t_1;H^1)}^2 \\
&\quad+128\tau h^4(C_2)^2\left(\left\|\boldsymbol{u}\left(t_0\right)\right\|_{L^\infty}^2+h^2(C_1)^2\left\|\nabla \boldsymbol{u}\left(t_0\right)\right\|_{L^\infty}^2\right)\|\boldsymbol{u}(t_0)\|_3^2 \\
&\quad+4\tau^2T\int_{t_0}^{t_1}|Q_{tt}|^2dt+96\tau^2T\left\|\boldsymbol{u}\left(t_0\right)\right\|_{L^\infty}^2\left\|\nabla \boldsymbol{u}\left(t_0\right)\right\|_0^2\left\|\boldsymbol{u}_t\right\|_{L^2(t_0,t_1;L^2)}^2 \\
&\quad+96\tau h^6T(C_2)^2\left(\left((C_1)^2+1\right)\left\|\nabla \boldsymbol{u}\left(t_0\right)\right\|_{L^\infty}^2\left\|\boldsymbol{u}\left(t_1\right)\right\|_0^2+\left\|\nabla \boldsymbol{u}\left(t_1\right)\right\|_{L^\infty}^2\left\|\boldsymbol{u}\left(t_0\right)\right\|_0^2\right)\|\boldsymbol{u}(t_0)\|_3^2 \\
&\quad+48\tau h^4T(C_1)^4(C_2)^2\|\nabla \boldsymbol{u}\left(t_0\right)\|_0^4\|\boldsymbol{u}\left(t_1\right)\|_3^2 \\
&\leq C_6^{\{T,\nu\}}(\tau^2+h^4),
\end{aligned} \tag{44}
$$

where the constant

$$C_6^{\{T,\nu\}} = 192(\widehat{C})^6\Big(\|\boldsymbol{u}_{tt}\|^2_{L^2(0,T;L^2)} + \|\boldsymbol{u}_t\|^2_{L^2(0,T;H^3)} + \nu^{-1}\|P\|^2_{L^\infty(0,T;H^2)} + \|\boldsymbol{u}\|^2_{L^\infty(0,T;H^3)}\|\boldsymbol{u}_t\|^2_{L^2(0,T;H^1)} + \|\boldsymbol{u}\|^4_{L^\infty(0,T;H^3)} + T\int_0^T |Q_{tt}|^2 dt + T\|\boldsymbol{u}\|^4_{L^\infty(0,T;H^3)}\|\boldsymbol{u}_t\|^2_{L^2(t_0,T;L^2)} + T\|\boldsymbol{u}\|^6_{L^\infty(0,T;H^3)} + T\|\boldsymbol{u}\|^4_{L^\infty(0,T;H^1)}\|\boldsymbol{u}\|^2_{L^\infty(0,T;H^3)}\Big),$$

with $\widehat{C} = \max\{C_0, C_1, C_2, C_3, 1\}$. Finally, the estimate (22) is obtained by setting

$$h_0^{\{\nu\}} = \min\{(C_6^{\{T,\nu\}})^{-2}, 1\}, \tag{45}$$

and the proof is completed. □

Remark 4.2. *First, we can see that Reynolds number dependency comes from (28). Second, although $e_u^0 = 0$ in (31), we still conduct the estimations accordingly in (32), (34) and (35) since the similar processes for e_u^1 and general case e_u^n will be needed in the later analysis.*

Thanks to Lemma 4.1, we have the estimate on e_u^1 under an upper bound $h_0^{\{\nu\}}$ for the mesh size. Next, we will turn to estimating e_u^2 to find a unified upper bound for the mesh size which is needed in the mathematical induction.

Lemma 4.3. *Assume the grad-div stabilizing parameter $\mu = 0$. There exists a viscosity-dependent positive constant $0 < h_*^{\{\nu\}} \le 1$ such that if $h \le h_*^{\{\nu\}}$ and $\tau \le h^2$, then*

$$\left\|e_u^2\right\|_0^2 + \nu\tau\sum_{i=0}^{1}\left\|\nabla e_u^{i+1}\right\|_0^2 + \left|e_Q^2\right|^2 \le h^{-\frac{1}{2}}\left(h^4 + \tau^2\right). \tag{46}$$

Proof. Assume $\tau \le h^2 \le 1$. Since $\tau \le h^2 \le h^{\frac{d+1}{2}}$, it yields

$$\left\|e_u^1\right\|_0^2 \le h^{-\frac{1}{2}}h^{d+1} = h^{d+\frac{1}{2}}. \tag{47}$$

Hence we have

$$h^{-2}\left\|e_u^1\right\|_0^2 \le h^{d-\frac{3}{2}}$$

and by the inverse inequality

$$\left\|e_u^1\right\|_{L^\infty}^2 \le (C_3)^2 h^{-d}\left\|e_u^1\right\|_0^2 \le (C_3)^2 h^{\frac{1}{2}}. \tag{48}$$

We then repeat the similar derivations for the following error equations done in the proof of Lemma 4.1 while changing the stepping from t_0 to t_1 to from t_1 to t_2:

$$\begin{aligned}&\left(\tfrac{e_u^2-e_u^1}{\tau}, e_u^2\right) + \nu\left(\nabla e_u^2, \nabla e_u^2\right)\\ &= -\left(\boldsymbol{u}_t(t_2) - \tfrac{\boldsymbol{u}(t_2)-\boldsymbol{u}(t_1)}{\tau}, e_u^2\right) - \left(\tfrac{\eta(t_2)-\eta(t_1)}{\tau}, e_u^2\right) + \left(P(t_2) - \Pi_h P(t_2), \nabla\cdot e_u^2\right)\\ &\quad - Q(t_2)\exp\left(\tfrac{t_2}{T}\right)c\left(\boldsymbol{u}(t_2), \boldsymbol{u}(t_2), e_u^2\right) + Q^2\exp\left(\tfrac{t_2}{T}\right)c\left(\boldsymbol{u}_h^1, \boldsymbol{u}_h^1, e_u^2\right),\end{aligned} \tag{49}$$

Due to the fact $e_u^1 \ne 0$, we need slightly modify (34), the third inequality of (41), and (42) respectively:

$$\begin{aligned}\left|c\left(e_u^1, e_u^1, e_u^2\right)\right| &\le \tfrac{\|e_u^2-e_u^1\|_0^2}{64\tau} + 48(C_3)^2\tau h^{-2}\left\|e_u^1\right\|_{L^\infty}^2\left\|e_u^1\right\|_0^2\\ &\le \tfrac{\|e_u^2-e_u^1\|_0^2}{64\tau} + 48(C_3)^4\tau h^{-\frac{3}{2}}\left\|e_u^1\right\|_0^2\\ &\le \tfrac{\|e_u^2-e_u^1\|_0^2}{64\tau} + 48(C_3)^4 h^{\frac{1}{2}}\left\|e_u^1\right\|_0^2,\end{aligned} \tag{50}$$

$$\begin{aligned}\left|E_Q^2 c\left(e_u^1, e_u^1, \boldsymbol{u}(t_2)\right)\right| &\le \tfrac{1}{8T}|e_Q^2|^2 + 48(C_3)^2 h^{-2}\left\|\boldsymbol{u}(t_2)\right\|_{L^\infty}^2\left\|e_u^1\right\|_0^4\\ &\le \tfrac{1}{8T}|e_Q^2|^2 + 48(C_3)^2 h^{d-\frac{3}{2}}\left\|\boldsymbol{u}(t_2)\right\|_{L^\infty}^2\left\|e_u^1\right\|_0^2,\end{aligned} \tag{51}$$

and

$$\begin{aligned}E_Q^2 c\left(\boldsymbol{u}_h^1, \boldsymbol{u}_h^1, \boldsymbol{u}(t_2) - \boldsymbol{u}_h^2\right) &= E_Q^2 c\left(\boldsymbol{u}_h^1, \boldsymbol{u}_h^1, \eta^2\right) + E_Q^1 c\left(\boldsymbol{u}_h^1, \boldsymbol{u}_h^1, e_u^2\right)\\ &\le \tfrac{|e_Q^2|^2}{4T} + 24T(C_5 C_7^{\{T\}})^4\|\nabla\eta^2\|_0^2 + E_Q^2 c\left(\boldsymbol{u}_h^1, \boldsymbol{u}_h^1, e_u^2\right)\\ &\le \tfrac{|e_Q^2|^2}{4T} + 24T(C_5 C_7^{\{T\}})^4(C_2)^2 h^4\|\boldsymbol{u}(t_2)\|_3^2 + E_Q^2 c\left(\boldsymbol{u}_h^1, \boldsymbol{u}_h^1, e_u^2\right),\end{aligned} \tag{52}$$

since

$$\begin{aligned}\|\nabla \boldsymbol{u}_h^1\|_0 &\le \|\nabla \boldsymbol{u}\,(t_1)\,\|_0 + \|\nabla \eta^1\|_0 + \|\nabla e_u^1\|_0\\ &\le \|\nabla \boldsymbol{u}\,(t_1)\,\|_0 + C_2 h^2 \|\boldsymbol{u}\,(t_1)\,\|_3 + C_3 h^{\frac{d}{2}-\frac{3}{4}} \le C_7^{\{T\}},\end{aligned}$$

with $C_7^{\{T\}} = (1+C_2)\|\boldsymbol{u}\|_{L^\infty(0,T;H^3)} + C_3 + 1$. Hence, we can analogously obtain that

$$\begin{aligned}&\|e_u^2\|_0^2 - \|e_u^1\|_0^2 + \nu\tau\|\nabla e_u^2\|_0^2 + |e_Q^2|^2 - |e_Q^1|^2\\ &\le 2\tau\left(\tfrac{3}{32} + 50(C_1)^2\,\|\boldsymbol{u}\,(t_1)\|_{L^\infty}^2 + 82(C_1)^2\,\|\nabla \boldsymbol{u}\,(t_1)\|_{L^\infty}^2 + 48(C_3)^4 h^{\frac{1}{2}}\right)\|e_u^1\|_0^2\\ &\quad + 128\tau^2\|\boldsymbol{u}_{tt}\|_{L^2(t_1,t_2;L^2)}^2 + 128(C_2)^2h^6\|\boldsymbol{u}_t\|_{L^2(t_1,t_2;H^3)}^2 + \tau(C_0)^2\nu^{-1}h^4\|P\,(t_2)\,\|_2^2\\ &\quad + 128\tau^2(C_1)^2\left(\|\boldsymbol{u}\,(t_2)\,\|_{L^\infty}^2 + \|\nabla \boldsymbol{u}\,(t_1)\,\|_{L^\infty}^2\right)\|\boldsymbol{u}_t\|_{L^2(t_1,t_2;H^1)}^2\\ &\quad + 128\tau h^4(C_2)^2\left(\|\boldsymbol{u}\,(t_1)\|_{L^\infty}^2 + h^2(C_1)^2\,\|\nabla \boldsymbol{u}\,(t_1)\|_{L^\infty}^2\right)\|\boldsymbol{u}(t_1)\|_3^2\\ &\quad + 4\tau^2 T\int_{t_1}^{t_2}|Q_{tt}|^2dt + 96\tau^2 T\,\|\boldsymbol{u}\,(t_1)\|_{L^\infty}^2\,\|\nabla \boldsymbol{u}\,(t_1)\|_0^2\,\|\boldsymbol{u}_t\|_{L^2(t_1,t_2;L^2)}^2\\ &\quad + 96\tau h^6T(C_2)^2\left(\left((C_1)^2+1\right)\|\nabla \boldsymbol{u}\,(t_1)\|_{L^\infty}^2\,\|\boldsymbol{u}\,(t_2)\|_0^2 + \|\nabla \boldsymbol{u}\,(t_2)\|_{L^\infty}^2\,\|\boldsymbol{u}\,(t_1)\|_0^2\right)\|\boldsymbol{u}(t_1)\|_3^2\\ &\quad + 96\tau T\left(\left((C_1)^2+1\right)\|\nabla \boldsymbol{u}\,(t_1)\|_{L^\infty}^2\,\|\boldsymbol{u}\,(t_2)\|_0^2 + \|\nabla \boldsymbol{u}\,(t_2)\|_{L^\infty}^2\,\|\boldsymbol{u}\,(t_1)\|_0^2\right)\|e_u^1\|_0^2\\ &\quad + 96\tau h^4T(C_2)^2\left(\|\boldsymbol{u}\,(t_2)\|_{L^\infty}^2 + h^2\,\|\boldsymbol{u}\,(t_2)\|_{W^{1,\infty}}^2\right)\|\boldsymbol{u}(t_1)\|_3^2\,\|e_u^1\|_0^2\\ &\quad + 96\tau h^{d-\frac{3}{2}}T(C_3)^2\,\|\boldsymbol{u}\,(t_2)\|_{L^\infty}^2\,\|e_u^1\|_0^2 + 48\tau h^4T(C_5C_7^{\{T\}})^4(C_2)^2\|\boldsymbol{u}\,(t_2)\,\|_3^2.\end{aligned}\tag{53}$$

Let us define

$$\begin{aligned}C_e(t_1,t_2) &:= 2\left(\tfrac{3}{32} + 50(C_1)^2\,\|\boldsymbol{u}\,(t_1)\|_{L^\infty}^2 + 82(C_1)^2\,\|\nabla \boldsymbol{u}\,(t_1)\|_{L^\infty}^2 + 48(C_3)^4\right)\\ &\quad + 96T\left(\left((C_1)^2+1\right)\|\nabla \boldsymbol{u}\,(t_1)\|_{L^\infty}^2\,\|\boldsymbol{u}\,(t_2)\|_0^2 + \|\nabla \boldsymbol{u}\,(t_2)\|_{L^\infty}^2\,\|\boldsymbol{u}\,(t_1)\|_0^2\right)\\ &\quad + 96T(C_2)^2\left(\|\boldsymbol{u}\,(t_2)\|_{L^\infty}^2 + \|\boldsymbol{u}\,(t_2)\|_{W^{1,\infty}}^2\right)\|\boldsymbol{u}(t_1)\|_3^2 + 96T(C_3)^2\,\|\boldsymbol{u}\,(t_2)\|_{L^\infty}^2,\end{aligned}$$

then we have $C_e(t_1,t_2) \le \mathcal{B}(T)$ with

$$\begin{aligned}\mathcal{B}(T) &= \tfrac{3}{16} + \left(264(C_1)^2 + 96T(C_3)^2\right)\|\boldsymbol{u}\|_{L^\infty(0,T;H^3)}^2 + 96(C_3)^4\\ &\quad + 96T\left((C_1)^2 + (C_2)^2 + 2\right)\|\boldsymbol{u}\|_{L^\infty(0,T;H^3)}^4.\end{aligned}\tag{54}$$

Note that $\mathcal{B}(T)$ is independent of the viscosity ν. Combining (53) with (44) and applying $\tau \le h^2 \le 1$, it leads to

$$\|e_u^2\|_0^2 + \nu\tau\sum_{i=0}^{1}\|\nabla e_u^{i+1}\|_0^2 + |e_Q^2|^2 \le \tau\sum_{i=0}^{1}C_e(t_i,t_{i+1})\|e_u^i\|_0^2 + \mathcal{G}(T,\nu)(\tau^2+h^4),\tag{55}$$

where

$$\begin{aligned}\mathcal{G}(T,\nu) &= 128\|\boldsymbol{u}_{tt}\|_{L^2(0,t_2;L^2)}^2 + 128(C_2)^2\|\boldsymbol{u}_t\|_{L^2(0,T;H^3)}^2 + (C_0)^2\nu^{-1}T\|P\|_{L^\infty(0,T;H^2)}^2\\ &\quad + 128(C_1)^2\|\boldsymbol{u}\|_{L^\infty(0,T;H^3)}^2\|\boldsymbol{u}_t\|_{L^2(0,T;H^1)}^2 + 128(C_2\widehat{C})^2T\|\boldsymbol{u}\|_{L^\infty(0,T;H^3)}^4\\ &\quad + 4T\int_0^T|Q_{tt}|^2dt + 96T\|\boldsymbol{u}\|_{L^\infty(0,T;H^3)}^4\|\boldsymbol{u}_t\|_{L^2(0,t_2;L^2)}^2 + 96T^2(C_2)^2\left((C_1)^2+1\right)\|\boldsymbol{u}\|_{L^\infty(0,T;H^3)}^6\\ &\quad + 48T(C_5C_7^{\{T\}})^4(C_2)^2\left(\|\boldsymbol{u}\|_{L^\infty(0,T;H^1)}^4 + 1\right)\|\boldsymbol{u}\|_{L^\infty(0,T;H^3)}^2.\end{aligned}$$

Applying the Gronwall's inequality in Lemma 2.5 with $l=2$, we have

$$\begin{aligned}\|e_u^2\|_0^2 + \nu\tau\sum_{i=0}^{1}\|\nabla e_u^{i+1}\|_0^2 + |e_Q^2|^2 &\le \exp\left(\tau\sum_{i=0}^{1}C_e(t_i,t_{i+1})\right)\mathcal{G}(T,\nu)(h^4+\tau^2)\\ &\le \exp\left(T\mathcal{B}(T)\right)\mathcal{G}(T,\nu)(h^4+\tau^2).\end{aligned}\tag{56}$$

Finally, the estimate (46) is obtained by setting

$$h_*^{\{\nu\}} = \min\{h_0^{\{\nu\}}, h_1^{\{\nu\}}\}\tag{57}$$

with

$$h_1^{\{\nu\}} = \exp\left(-2T\mathcal{B}(T)\right)\left(\mathcal{G}(T,\nu)\right)^{-2}, \tag{58}$$

and the proof is completed. □

It is noted that in the above we pick $h_*^{\{\nu\}}$ only related to the terminal time T and the viscosity ν, thus such choice can be potentially applied to all remaining time steps $n = 2, 3, \cdots, N-1$. Based on Lemmas 4.1 and 4.3, we next show the following error estimate for the fully-discrete scheme (13) in the case of $\mu = 0$.

Theorem 4.4 (Error Estimates of the Velocity for the sIMEX1-FEM Scheme with $\mu = 0$)**.** *Assume the grad-div stabilizing parameter $\mu = 0$. If $h \le h_*^{\{\nu\}}$ with $h_*^{\{\nu\}}$ defined in (57) and $\tau \le h^2$, then the following error estimate for the velocity holds*

$$\left\|e_u^{n+1}\right\|_0^2 + \nu\tau\sum_{i=0}^{n}\left\|\nabla e_u^{i+1}\right\|_0^2 + \left|e_Q^{n+1}\right|^2 \le \exp\left(T\mathcal{B}(T)\right)\mathcal{G}(T,\nu)(h^4+\tau^2) \tag{59}$$

for all $0 \le n \le N-1$.

Proof. We first use mathematical induction to prove

$$\left\|e_u^{n+1}\right\|_0^2 + \nu\tau\sum_{i=0}^{n}\left\|\nabla e_u^{i+1}\right\|_0^2 + \left|e_Q^{n+1}\right|^2 \le h^{-\frac{1}{2}}\left(h^4+\tau^2\right), \quad \forall\, n = 0, \ldots, N-1. \tag{60}$$

Thanks to Lemmas 4.1 and 4.3,, we first know that (60) holds for $n = 0$ and $n = 1$. Next, let us assume the estimate (60) holds for $n = m-1$ ($m \le N-1$). Thus it holds that $\|e_u^m\|_0^2 \le h^{-\frac{1}{2}}h^{d+1} = h^{d+\frac{1}{2}}$ and $\|e_u^m\|_{L^\infty}^2 \le (C_3)^2 h^{-d}\|e_u^n\|_0^2 \le (C_3)^2 h^{\frac{1}{2}}$. Following the same arguments in the proof of Lemma 4.3 with the following error equation

$$\begin{aligned}
&\left(\tfrac{e_u^{m+1}-e_u^m}{\tau}, e_u^{m+1}\right) + \nu\left(\nabla e_u^{m+1}, \nabla e_u^{m+1}\right) = \\
&-\left(\boldsymbol{u}_t\left(t_{m+1}\right) - \tfrac{\boldsymbol{u}(t_{m+1})-\boldsymbol{u}(t_m)}{\tau}, e_u^{m+1}\right) - \left(\tfrac{\eta(t_{m+1})-\eta(t_m)}{\tau}, e_u^{m+1}\right) \\
&+\left(P\left(t_{m+1}\right) - \Pi_h P\left(t_{m+1}\right), \nabla\cdot e_u^{m+1}\right) - Q(t_{m+1})\exp\left(\tfrac{t_{m+1}}{T}\right)c\left(\boldsymbol{u}\left(t_{m+1}\right), \boldsymbol{u}\left(t_{m+1}\right), e_u^{m+1}\right) \\
&+Q^{m+1}\exp\left(\tfrac{t_{m+1}}{T}\right)c\left(\boldsymbol{u}_h^m, \boldsymbol{u}_h^m, e_u^{m+1}\right),
\end{aligned} \tag{61}$$

we can similarly show

$$\begin{aligned}
\left\|e_u^{m+1}\right\|_0^2 + \nu\tau\sum_{i=0}^{m}\left\|\nabla e_u^{i+1}\right\|_0^2 + \left|e_Q^{m+1}\right|^2 &\le \exp\left(T\mathcal{B}(T)\right)\mathcal{G}(T,\nu)(h^4+\tau^2) \\
&\le h^{-\frac{1}{2}}\left(h^4+\tau^2\right),
\end{aligned} \tag{62}$$

which means that the estimate (60) is also true for $n = m$. Then by the definition of $h_*^{\{\nu\}}$, the estimate (59) naturally holds as the by-product of the first inequality in (62) and the definition of $h_*^{\{\nu\}}$. The proof is completed. □

Remark 4.5. *Based on the definition of $h_*^{\{\nu\}}$ in (57), one can see that the mesh size h theoretically must to be restricted by $O(\nu^2)$ in Theorem 4.4. Moreover, the error estimate (59) has a viscosity-independent Gronwall constant $\exp\left(-2T\mathcal{B}(T)\right)$. These give essential improvements over the error estimation results obtained in [24], in which the Gronwall constant contains a term of $\exp(T/\nu)$ and the mesh size is restricted by $O(\exp(-T/\nu))$.*

Next we turn to estimate the pressure P_h via the negative-norm arguments as in [13].

Theorem 4.6 (Error Estimates of the Pressure for the sIMEX1-FEM Scheme with $\mu = 0$)**.** *Assume the grad-div stabilizing parameter $\mu = 0$. If $h \le h_*^{\{\nu\}}$ with $h_*^{\{\nu\}}$ defined in (57) and $\tau \le h^2$, then the following error estimate for the pressure holds*

$$\tau\sum_{i=0}^{n}\left\|P\left(t_{i+1}\right) - P_h^{i+1}\right\|_0^2 \le \mathcal{K}(T,\nu)(h^4+\tau^2) \tag{63}$$

for all $0 \le n \le N-1$, *where* $\mathcal{K}(T,\nu) > 0$ *is a constant depending on* T *and* ν.

Proof. We can easily obtain the following error equation at $t = t_{i+1}$ $(0 \le i \le N-1)$:

$$
\begin{aligned}
&\left(\tfrac{e_u^{i+1}-e_u^i}{\tau}, \boldsymbol{v}_h\right) + \nu\left(\nabla e_u^{i+1}, \nabla \boldsymbol{v}_h\right) \\
&= -\left(\boldsymbol{u}_t\left(t_{i+1}\right) - \tfrac{\boldsymbol{u}(t_{i+1})-\boldsymbol{u}(t_i)}{\tau}, \boldsymbol{v}_h\right) - \left(\tfrac{\eta^{i+1}-\eta^i}{\tau}, \boldsymbol{v}_h\right) - c\left(\boldsymbol{u}\left(t_{i+1}\right), \boldsymbol{u}\left(t_{i+1}\right), \boldsymbol{v}_h\right) \\
&\quad + Q^{i+1}\exp\left(\tfrac{t_{i+1}}{T}\right) c\left(\boldsymbol{u}_h^i, \boldsymbol{u}_h^i, \boldsymbol{v}_h\right) + \left(P\left(t_{i+1}\right) - P_h^{i+1}, \nabla\cdot \boldsymbol{v}_h\right).
\end{aligned} \tag{64}
$$

Projecting the above equation onto $\boldsymbol{V}_h$ by picking $\boldsymbol{v}_h \in \boldsymbol{V}_h$, we then have

$$
\begin{aligned}
\tfrac{e_u^{i+1}-e_u^i}{\tau} =& -\nu A_h e_u^{i+1} - \Pi_h^{\mathrm{div}}\left(\mathcal{N}(\boldsymbol{u}(t_{i+1}), \boldsymbol{u}(t_{i+1})) - Q^{i+1}\exp\left(\tfrac{t_{i+1}}{T}\right)\mathcal{N}(\boldsymbol{u}_h^i, \boldsymbol{u}_h^i)\right) \\
&- D_h(P(t_{i+1}) - \Pi_h P(t_{i+1})) - \Pi_h^{\mathrm{div}}\left(\boldsymbol{u}_t(t_{i+1}) - \tfrac{\boldsymbol{u}(t_{i+1})-\boldsymbol{u}(t_i)}{\tau}\right) - \Pi_h^{\mathrm{div}}\left(\tfrac{\eta^{i+1}-\eta^i}{\tau}\right).
\end{aligned} \tag{65}
$$

By using the discrete inf-sup condition (4), it holds

$$
\begin{aligned}
\gamma\|\Pi_h P\left(t_{i+1}\right) - P_h^{i+1}\|_0 &\le \sup_{\boldsymbol{v}_h\in\boldsymbol{X}_h} \tfrac{(\Pi_h P(t_{i+1}) - P_h^{i+1}, \nabla\cdot\boldsymbol{v}_h)}{\|\boldsymbol{v}_h\|_1} \\
&\le \left\|\boldsymbol{u}_t\left(t_{i+1}\right) - \tfrac{\boldsymbol{u}(t_{i+1})-\boldsymbol{u}(t_i)}{\tau}\right\|_{-1} + \left\|\tfrac{\eta^{i+1}-\eta^i}{\tau}\right\|_{-1} + \left\|\tfrac{e_u^{i+1}-e_u^i}{\tau}\right\|_{-1} \\
&\quad + \nu\|\nabla e_u^{i+1}\|_0 + \left\|\mathcal{N}(\boldsymbol{u}(t_{i+1}), \boldsymbol{u}(t_{i+1})) - Q^{i+1}\exp\left(\tfrac{t_{i+1}}{T}\right)\mathcal{N}(\boldsymbol{u}_h^i, \boldsymbol{u}_h^i)\right\|_{-1} \\
&\quad + C_0 h^2 \|P\left(t_{i+1}\right)\|_2 =: \textstyle\sum_{i=1}^6 \mathbb{K}_i.
\end{aligned} \tag{66}
$$

For the first two terms on the right-hand side of (66), we have

$$
\mathbb{K}_1 \le C_4\left\|\boldsymbol{u}_t\left(t_{i+1}\right) - \tfrac{\boldsymbol{u}(t_{i+1})-\boldsymbol{u}(t_i)}{\tau}\right\|_0 \le C_4\tau^{\frac{1}{2}}\|\boldsymbol{u}_{tt}\|_{L^2(t_i,t_{i+1};L^2)}, \tag{67}
$$

and

$$
\mathbb{K}_2 \le \tfrac{C_2C_4}{\tau^{\frac{1}{2}}} h^3 \|\boldsymbol{u}_t\|_{L^2(t_i,t_{i+1};H^3)}. \tag{68}
$$

For the fifth term on the right-hand side of (66), we have

$$
\begin{aligned}
\mathbb{K}_5 &= \sup_{\|\phi\|_1=1} \left|c\left(\boldsymbol{u}\left(t_{i+1}\right), \boldsymbol{u}\left(t_{i+1}\right), \phi\right) - Q^{i+1}\exp\left(\tfrac{t_{i+1}}{T}\right) c\left(\boldsymbol{u}_h^i, \boldsymbol{u}_h^i, \phi\right)\right| \\
&\le \sup_{\|\phi\|_1=1} \Big(\left|c\left(\boldsymbol{u}\left(t_{i+1}\right), \boldsymbol{u}\left(t_{i+1}\right), \phi\right) - c\left(\boldsymbol{u}\left(t_i\right), \boldsymbol{u}\left(t_i\right), \phi\right)\right| \\
&\quad + \left|c\left(\boldsymbol{u}\left(t_i\right), \boldsymbol{u}\left(t_i\right), \phi\right) - c\left(\boldsymbol{u}_h^i, \boldsymbol{u}_h^i, \phi\right)\right| + \left|e_Q^{i+1}\exp\left(\tfrac{t_{i+1}}{T}\right) c\left(\boldsymbol{u}_h^i, \boldsymbol{u}_h^i, \phi\right)\right| \Big)
\end{aligned} \tag{69}
$$

For the first term on the right-hand side of (69), we have

$$
\begin{aligned}
&\left|c\left(\boldsymbol{u}\left(t_{i+1}\right), \boldsymbol{u}\left(t_{i+1}\right), \phi\right) - c\left(\boldsymbol{u}\left(t_i\right), \boldsymbol{u}\left(t_i\right), \phi\right)\right| \\
&\quad \le \left|c\left(\boldsymbol{u}\left(t_{i+1}\right) - \boldsymbol{u}\left(t_i\right), \boldsymbol{u}\left(t_{i+1}\right), \phi\right)\right| + \left|c\left(\boldsymbol{u}\left(t_i\right), \boldsymbol{u}\left(t_{i+1}\right) - \boldsymbol{u}\left(t_i\right), \phi\right)\right| \\
&\quad \le 6\tau^{\frac{1}{2}}\|\boldsymbol{u}_t\|_{L^2(t_i,t_{i+1};L^2)}\|\boldsymbol{u}\left(t_{i+1}\right)\|_{W^{1,\infty}}\|\phi\|_1,
\end{aligned} \tag{70}
$$

where the integration by parts is applied on $c\left(\boldsymbol{u}\left(t_{i+1}\right) - \boldsymbol{u}\left(t_i\right), \boldsymbol{u}\left(t_{i+1}\right), \phi\right)$. For the second term on the right-hand side of (69), it holds

$$
\begin{aligned}
&c\left(\boldsymbol{u}\left(t_i\right), \boldsymbol{u}\left(t_i\right), \phi\right) - c\left(\boldsymbol{u}_h^i, \boldsymbol{u}_h^i, \phi\right) \\
&\quad = c\left(\boldsymbol{u}\left(t_i\right) - \boldsymbol{u}_h^i, \boldsymbol{u}\left(t_i\right), \phi\right) + c\left(\mathrm{P}_{st}\boldsymbol{u}\left(t_i\right), \boldsymbol{u}\left(t_i\right) - \boldsymbol{u}_h^i, \phi\right) + c\left(e_u^i, \boldsymbol{u}\left(t_i\right) - \boldsymbol{u}_h^i, \phi\right).
\end{aligned}
$$

With integration by parts, we have

$$
\begin{aligned}
&\left|c\left(\boldsymbol{u}\left(t_i\right) - \boldsymbol{u}_h^i, \boldsymbol{u}\left(t_i\right), \phi\right)\right| \\
&= \left|\left(\boldsymbol{u}\left(t_i\right)\cdot\nabla(\boldsymbol{u}\left(t_i\right) - \boldsymbol{u}_h^i), \phi\right) + \left((\nabla(\boldsymbol{u}\left(t_i\right) - \boldsymbol{u}_h^i))^T\boldsymbol{u}\left(t_i\right), \phi\right) + \left(\nabla\cdot(\boldsymbol{u}\left(t_i\right) - \boldsymbol{u}_h^i)\boldsymbol{u}\left(t_i\right), \phi\right)\right| \\
&= \Big|-\left(\boldsymbol{u}\left(t_i\right)\cdot\nabla\phi, \boldsymbol{u}\left(t_i\right) - \boldsymbol{u}_h^i\right) - \left(\nabla\cdot\boldsymbol{u}\left(t_i\right)(\boldsymbol{u}\left(t_i\right) - \boldsymbol{u}_h^i), \phi\right) - \left(\phi\cdot\nabla\boldsymbol{u}\left(t_i\right), \boldsymbol{u}\left(t_i\right) - \boldsymbol{u}_h^i\right) \\
&\quad - \left(\nabla\cdot\phi(\boldsymbol{u}\left(t_i\right) - \boldsymbol{u}_h^i), \boldsymbol{u}\left(t_i\right)\right) - \left((\boldsymbol{u}\left(t_i\right) - \boldsymbol{u}_h^i)\cdot\nabla\boldsymbol{u}\left(t_i\right), \phi\right) - \left((\boldsymbol{u}\left(t_i\right) - \boldsymbol{u}_h^i)\cdot\nabla\phi, \boldsymbol{u}\left(t_i\right)\right)\Big| \\
&\le 6\|\boldsymbol{u}\left(t_i\right)\|_{W^{1,\infty}}\|\boldsymbol{u}\left(t_i\right) - \boldsymbol{u}_h^i\|_0\|\phi\|_1,
\end{aligned} \tag{71}
$$

By Lemma 2.1, we have

$$c\left(\mathrm{P}_{st}\boldsymbol{u}\left(t_i\right),\boldsymbol{u}\left(t_i\right)-\boldsymbol{u}_h^i,\phi\right)\leq C_1\|\boldsymbol{u}\left(t_i\right)\|_{W^{1,\infty}}\|\boldsymbol{u}\left(t_i\right)-\boldsymbol{u}_h^i\|_0\|\phi\|_1. \tag{72}$$

By Sobolev embedding inequalities (8) and Lemma 4.1, it holds

$$\begin{aligned}
&\left|c\left(e_u^i,\boldsymbol{u}\left(t_i\right)-\boldsymbol{u}_h^i,\phi\right)\right| \\
&\quad=\left|\left(\left(\boldsymbol{u}\left(t_i\right)-\boldsymbol{u}_h^i\right)\cdot\nabla e_u^i,\phi\right)+\left(\left(\nabla e_u^i\right)^T\left(\boldsymbol{u}\left(t_i\right)-\boldsymbol{u}_h^i\right),\phi\right)+\left(\nabla\cdot e_u^i(\boldsymbol{u}\left(t_i\right)-\boldsymbol{u}_h^i),\phi\right)\right| \\
&\quad\leq 3\|\boldsymbol{u}\left(t_i\right)-\boldsymbol{u}_h^i\|_0\|\nabla e_u^i\|_{L^{\frac{2d}{d-1}}}\|\phi\|_{L^{2d}}\leq 3C_3C_5\|\boldsymbol{u}\left(t_i\right)-\boldsymbol{u}_h^i\|_0h^{-\frac{1}{2}}\|\nabla e_u^i\|_0\|\phi\|_1 \\
&\quad\leq 3(C_3)^2C_5\|\boldsymbol{u}\left(t_i\right)-\boldsymbol{u}_h^i\|_0h^{-\frac{3}{2}}\|e_u^i\|_0\|\phi\|_1\leq 3(C_3)^2C_5h^{\frac{1}{4}}\|\boldsymbol{u}\left(t_i\right)-\boldsymbol{u}_h^i\|_0\|\phi\|_1.
\end{aligned} \tag{73}$$

Lastly, with integration by parts, we also have

$$\begin{aligned}
&\left|e_Q^{i+1}\exp\left(\tfrac{t_{i+1}}{T}\right)c\left(\boldsymbol{u}_h^i,\boldsymbol{u}_h^i,\phi\right)\right| \\
&\quad=\left|e_Q^{i+1}\exp\left(\tfrac{t_{i+1}}{T}\right)\left(\left(\boldsymbol{u}_h^i\cdot\nabla\boldsymbol{u}_h^i,\phi\right)+\left(\left(\nabla\boldsymbol{u}_h^i\right)^T\boldsymbol{u}_h^i,\phi\right)+\left(\nabla\cdot\boldsymbol{u}_h^i\boldsymbol{u}_h^i,\phi\right)\right)\right| \\
&\quad=\left|e_Q^{i+1}\exp\left(\tfrac{t_{i+1}}{T}\right)\left(-\left(\boldsymbol{u}_h^i\cdot\nabla\phi,\boldsymbol{u}_h^i\right)-\tfrac{1}{2}\left(\nabla\cdot\phi\boldsymbol{u}_h^i,\boldsymbol{u}_h^i\right)\right)\right| \\
&\quad\leq\ 6(C_5)^2\left|e_Q^{i+1}\right|\|\nabla\boldsymbol{u}_h^i\|_0^2\|\phi\|_1\leq\ 6(C_5C_7^{\{T\}})^2\left|e_Q^{i+1}\right|\|\phi\|_1.
\end{aligned} \tag{74}$$

Thus we get from (69)-(74)

$$\begin{aligned}
\mathbb{K}_5\leq 6&\left(\tau^{\frac{1}{2}}\|\boldsymbol{u}_t\|_{L^2(t_i,t_{i+1};L^2)}\|\boldsymbol{u}\left(t_{i+1}\right)\|_{W^{1,\infty}}+(C_5)^2\left|e_Q^{i+1}\right|\|\boldsymbol{u}(t_i)\|_3^2\right) \\
&+\left((6+C_1)\|\boldsymbol{u}\left(t_i\right)\|_{W^{1,\infty}}+3(C_3)^2C_5h^{\frac{1}{4}}\right)\|\boldsymbol{u}\left(t_i\right)-\boldsymbol{u}_h^i\|_0.
\end{aligned} \tag{75}$$

Now, we are turning to analyze the third term on the right-hand side of (66). According to [13], we have by (7)

$$\mathbb{K}_3\leq C_4(C_3+1)\left\|A_h^{-\frac{1}{2}}\tfrac{e_u^{i+1}-e_u^i}{\tau}\right\|_0, \tag{76}$$

and by (65)

$$\begin{aligned}
\left\|A_h^{-\frac{1}{2}}\tfrac{e_u^{i+1}-e_u^i}{\tau}\right\|_0\leq\ &\nu\|\nabla e_u^{i+1}\|_0+\left\|\mathcal{N}(\boldsymbol{u}(t_{i+1}),\boldsymbol{u}(t_{i+1}))-Q^{i+1}\exp\left(\tfrac{t_{i+1}}{T}\right)\mathcal{N}(\boldsymbol{u}_h^i,\boldsymbol{u}_h^i)\right\|_{-1} \\
&+C_0h^2\|P\left(t_{i+1}\right)\|_2+\left\|\boldsymbol{u}_t(t_{i+1})-\tfrac{\boldsymbol{u}(t_{i+1})-\boldsymbol{u}(t_i)}{\tau}\right\|_{-1}+\left\|\tfrac{\eta^{i+1}-\eta^i}{\tau}\right\|_{-1}.
\end{aligned} \tag{77}$$

Combination of all the above estimates gives us

$$\begin{aligned}
&\gamma\|P\left(t_{i+1}\right)-P_h^{i+1}\|_0 \\
&\quad\leq(C_4(C_3+1)+1)\left(\nu\|\nabla e_u^{i+1}\|_0+C_4\tau^{\frac{1}{2}}\|\boldsymbol{u}_{tt}\|_{L^2(t_i,t_{i+1};L^2)}+\tfrac{C_2C_4}{\tau^{\frac{1}{2}}}h^3\|\boldsymbol{u}_t\|_{L^2(t_i,t_{i+1};H^3)}\right. \\
&\qquad+6\left(\tau^{\frac{1}{2}}\|\boldsymbol{u}_t\|_{L^2(t_i,t_{i+1};L^2)}\|\boldsymbol{u}\left(t_{i+1}\right)\|_{W^{1,\infty}}+(C_5C_7^{\{T\}})^2\left|e_Q^{i+1}\right|\right) \\
&\qquad\left.+\left((6+C_1)\|\boldsymbol{u}\left(t_i\right)\|_{W^{1,\infty}}+3(C_3)^2C_5h^{\frac{1}{4}}\right)\|\boldsymbol{u}\left(t_i\right)-\boldsymbol{u}_h^i\|_0+C_0h^2\|P\left(t_{i+1}\right)\|_2\right).
\end{aligned}$$

Taking square on the both sizes, multiplying by τ, summing up from $i=0$ to n, and applying the Cauchy-Schwarz inequality and Theorem 4.4, we finally obtain

$$\begin{aligned}
&\tau\sum_{i=0}^{n}\|P\left(t_{i+1}\right)-P_h^{i+1}\|_0^2 \\
&\leq\tfrac{8(C_4(C_3+1)+1)^2}{\gamma^2}\left(C_8^{\{T\}}\exp\left(T\mathcal{B}(T)\right)\mathcal{G}(T,\nu)(h^4+\tau^2)\right. \\
&\quad+(C_4)^2\tau^2\|\boldsymbol{u}_{tt}\|_{L^2(t_0,T;L^2)}^2+(C_2C_4)^2h^6\|\boldsymbol{u}_t\|_{L^2(t_0,T;H^3)}^2+36\tau^2\|\boldsymbol{u}\|_{L^\infty(t_0,T;H^3)}^2\|\boldsymbol{u}_t\|_{L^2(t_0,T;L^2)}^2 \\
&\quad\left.+4((6+C_1)^2\|\boldsymbol{u}\|_{L^\infty(t_0,T;H_3)}^2+9(C_3)^4(C_5)^2)C_2T\|\boldsymbol{u}\|_{L^\infty(t_0,T;H^3)}^2h^4\right) \\
&\leq\mathcal{K}(T,\nu)(h^4+\tau^2),
\end{aligned}$$

where $C_8^{\{T\}} = (C_0)^2 + 1 + 36(C_5 C_7^{\{T\}})^4 + 4((6+C_1)^2\|\boldsymbol{u}\|^2_{L^\infty(t_0,T;H_3)} + 9(C_3)^4(C_5)^2)T$ and

$$\begin{aligned}\mathcal{K}(T,\nu) =& \tfrac{8(C_4(C_3+1)+1)^2}{\gamma^2}\Big(C_8^{\{T\}}\exp\left(T\mathcal{B}(T)\right)\mathcal{G}(T,\nu) + (C_4)^2\|\boldsymbol{u}_{tt}\|^2_{L^2(t_0,T;L^2)}\\ &+ (C_2C_4)^2\|\boldsymbol{u}_t\|^2_{L^2(t_0,T;H^3)} + 36\|\boldsymbol{u}\|^2_{L^\infty(t_0,T;H^3)}\|\boldsymbol{u}_t\|^2_{L^2(t_0,T;L^2)}\\ &4((6+C_1)^2\|\boldsymbol{u}\|^2_{L^\infty(t_0,T;H^3)} + 9(C_3)^4(C_5)^2)C_2T\|\boldsymbol{u}\|^2_{L^\infty(t_0,T;H^3)}\Big),\end{aligned}$$

which completes the proof. □

Remark 4.7. *The CFL condition $\tau \le h^2$ is needed in Theorems 4.4 and 4.6 due to the estimation with the viscosity-independent Gronwall constant. If we would like to disregard the viscosity-independent requirement, then the CFL condition can be easily relaxed to $\tau \le h^{\frac{d}{2}+\epsilon_0}$ for any $\epsilon_0 \in (0, \frac{4-d}{3})$ if $h \le \widehat{h}^{\{\nu,\epsilon_0\}}$ where $\widehat{h}^{\{\nu,\epsilon_0\}} > 0$ is a constant depending on ν and ϵ_0.*

4.1.2. *The case of the grad-div stabilizing parameter $\mu > 0$.* In the previous subsection, we have conducted error estimates for the scheme (13) with $\mu = 0$. Although the Gronwall constant is independent of the viscosity ν, the mesh size h theoretically must be restricted by $O(\nu^2)$. This still could cause potential issues in practice when dealing with problems with large Reynolds number . In this subsection, we consider the case of the grad-div stabilizing parameter $\mu > 0$ and show this viscosity dependence of the mesh size constraint can be alleviated by adding the grad-div stabilization term.

Lemma 4.8. *Assume the grad-div stabilizing parameter $\mu > 0$. There exists a viscosity-independent positive constant $\widehat{h}_* > 0$ such that if $h < \widehat{h}_*$, and $\tau \le h^2$, then there holds the following estimate:*

$$\left\|e_u^{n+1}\right\|_0^2 + \nu\tau\sum_{i=0}^{n}\left\|\nabla e_u^{i+1}\right\|_0^2 + \mu\tau\sum_{i=0}^{n}\|\nabla\cdot e_u^{n+1}\|_0^2 + \left|e_Q^{n+1}\right|^2 \le h^{-\frac{1}{2}}\left(h^4+\tau^2\right) \tag{78}$$

for all $0 \le n \le N-1$,

Proof. The proof mainly follows the same arguments used in Lemmas 4.1 and 4.3 and Theorem 4.4. Note that the updated error equation with $\mu > 0$ at $t = t_{m+1}$ $(0 \le m \le N-1)$ is almost the same as (61) except its left-hand side now has one more term from the grad-div stabilization and can be written as

$$\frac{1}{2\tau}\left(\|e_u^{m+1}\|_0^2 - \|e_u^m\|_0^2 + \|e_u^{m+1}-e_u^m\|_0^2\right) + \nu\left\|\nabla e_u^{m+1}\right\|_0^2 + \mu\|\nabla\cdot e_u^{m+1}\|_0^2. \tag{79}$$

For the pressure term in the left-hand side of the error equation, instead of (28), it now can be estimated as

$$\begin{aligned}\left(P\left(t_{m+1}\right) - \Pi_h P\left(t_{m+1}\right), \nabla\cdot e_u^{m+1}\right) &\le \tfrac{\mu}{2}\|\nabla\cdot e_u^{m+1}\|_0^2 + \tfrac{1}{2\mu}\|P\left(t_{m+1}\right) - \Pi_h P\left(t_{m+1}\right)\|_0^2\\ &\le \tfrac{\mu}{2}\|\nabla\cdot e_u^{m+1}\|_0^2 + \tfrac{C_0}{2\mu}h^4\|P\left(t_{m+1}\right)\|_2^2.\end{aligned}$$

Consequently, $C_6^{\{T,\nu\}}$ in (44) is changed to $C_6^{\{T,\mu\}}$, and in stead of (45), we set

$$\widehat{h}_0 = \min\{(C_6^{\{T,\mu\}})^{-2}, 1\}.$$

Similarly, $\mathcal{G}(T,\nu)$ in (55) is changed to $\mathcal{G}(T,\mu)$, and in stead of (57), we pick

$$\widehat{h}_1 = \exp\left(-2T\mathcal{B}(T)\right)\left(\mathcal{G}(T,\mu)\right)^{-2}.$$

Note that both $\widehat{h}_0$ and $\widehat{h}_1$ are viscosity-independent. Then the estimate (78) can be similarly obtained via the mathematical induction with $\widehat{h}_* = \min\{\widehat{h}_0, \widehat{h}_1\}$. □

The followingl error estimates are immediately obtained as in Theorems 4.4 and 4.6.

Theorem 4.9 (Error Estimates for the sIMEX1-FEM Scheme with $\mu > 0$)**.** *Assume the grad-div stabilizing parameter $\mu > 0$. If $h \le \widehat{h}_*$ and $\tau \le h^2$, then the following error estimates hold:*

$$\left\|e_u^{n+1}\right\|_0^2 + \nu\tau\sum_{i=0}^{n}\left\|\nabla e_u^{i+1}\right\|_0^2 + \mu\tau\sum_{i=0}^{n}\|\nabla\cdot e_u^{n+1}\|_0^2 + \left|e_Q^{n+1}\right|^2 \le \exp\left(T\mathcal{B}(T)\right)\mathcal{G}(T,\mu)\left(h^4+\tau^2\right), \tag{80}$$

and

$$\tau\sum_{i=0}^{n}\left\|P\left(t_{i+1}\right) - P_h^{i+1}\right\|_0^2 \le \mathcal{K}(T,\mu)(h^4+\tau^2). \tag{81}$$

for all $0 \le n \le N-1$.

4.2. **Error estimate on the sIMEX2-FEM scheme.** In this subsection, we turn to analyze the convergent behavior in time and space of the proposed sIMEX2-FEM scheme (15). Many techniques used in the error analysis of the sIMEX1-FEM scheme (13) could be directly applied. With $\{(\boldsymbol{u}_h^1, P_h^1, Q^1)$ generated from the first-order scheme (13) (to start up of the second-order scheme (15)), let $\{(\boldsymbol{u}_h^{n+1}, P_h^{n+1}, Q^{n+1})\}_{n=1}^{N-1}$ denote the numerical solution produced by the scheme (15). We assume that the exact solution $(\boldsymbol{u}, P)$ satisfies the following regularity requirement:

$$\begin{cases} \boldsymbol{u} \in L^\infty(0,T;(H_0^1(\Omega))^d \cap (H^3(\Omega))^d), \boldsymbol{u}_t \in L^\infty(0,T;(H^3(\Omega))^d), \\ \boldsymbol{u}_{tt} \in L^\infty(0,T;(L^2(\Omega))^d),\ \boldsymbol{u}_{ttt} \in L^2(0,T;(H^1(\Omega))^d), \\ P \in L^\infty(0,T;H^2(\Omega)). \end{cases} \tag{82}$$

Define

$$\begin{aligned} \widetilde{\mathcal{B}}(T,\mu) = 192(\widehat{C})^6 \Big(& \|\boldsymbol{u}_{tt}\|^2_{L^\infty(0,T;L^2)} + \|\boldsymbol{u}_t\|^2_{L^2(0,T;H^3)} + \mu^{-1}\|P\|^2_{L^\infty(0,T;H^2)} + \|\boldsymbol{u}\|^2_{L^\infty(0,T;H^3)}\|\boldsymbol{u}_t\|^2_{L^\infty(0,T;H^1)} \\ & + \|\boldsymbol{u}\|^4_{L^\infty(0,T;H^3)} + \tfrac{1}{T} + T\|\boldsymbol{u}\|^4_{L^\infty(0,T;H^3)}\|\boldsymbol{u}_t\|^2_{L^\infty(t_0,T;L^2)} + T\|\boldsymbol{u}\|^6_{L^\infty(0,T;H^3)} \\ & + T\|\boldsymbol{u}\|^4_{L^\infty(0,T;H^1)}\|\boldsymbol{u}\|^2_{L^\infty(0,T;H^3)} \Big), \end{aligned}$$

then we have the following result.

Lemma 4.10. *Assume the grad-div stabilizing parameter* $\mu > 0$. *If* $\tau < h^2$, *there holds*

$$\left\|e_u^1\right\|_0^2 + \nu\tau\left\|\nabla e_u^1\right\|_0^2 + \mu\tau\|\nabla\cdot e_u^1\|_0^2 + \left|e_Q^1\right|^2 \le \widetilde{\mathcal{B}}(T,\mu)(\tau^4 + h^4). \tag{83}$$

Furthermore, there exists a viscosity-independent positive constant $0 < \widetilde{h}_0 \le 1$ *such that if* $h \le \widetilde{h}_0$, *then*

$$\left\|e_u^1\right\|_0^2 + \nu\tau\left\|\nabla e_u^1\right\|_0^2 + \mu\tau\|\nabla\cdot e_u^1\|_0^2 + \left|e_Q^1\right|^2 \le h^{-\frac{1}{2}}\left(h^4 + \tau^4\right). \tag{84}$$

Proof. By picking $\widetilde{h}_0 = \min\left\{(\widetilde{\mathcal{B}}(T,\mu))^{-2}, 1\right\}$, the estimate (84) comes directly from (83). Hence, it suffices to show the estimate (83), which can be accomplished via modifying the proof of Lemma 4.1. Specifically, we will update the estimates (26), (30), (37), and (39). The estimation (26) is replaced by

$$|\mathbb{I}_1| \le 32\tau^2\|\boldsymbol{u}_{tt}\|^2_{L^2(t_0,t_1;L^2)} + \tfrac{\|e_u^1 - e_u^0\|_0^2 + \|e_u^0\|_0^2}{64\tau} \le 32\tau^3\|\boldsymbol{u}_{tt}\|^2_{L^\infty(t_0,T;L^2)} + \tfrac{\|e_u^1 - e_u^0\|_0^2 + \|e_u^0\|_0^2}{64\tau},$$

where $\|\boldsymbol{u}_{tt}\|^2_{L^\infty(t_0,t_1;L^2)} \le \|\boldsymbol{u}_{tt}\|^2_{L^\infty(t_0,T;L^2)}$ is applied. The estimation (30) is replaced by

$$\begin{aligned} & \left|c\left(\boldsymbol{u}\left(t_1\right),\boldsymbol{u}\left(t_1\right),e_u^1\right) - c\left(\boldsymbol{u}\left(t_0\right),\boldsymbol{u}\left(t_0\right),e_u^1\right)\right| \\ & \le \tfrac{\|e_u^1 - e_u^0\|_0^2 + \|e_u^0\|_0^2}{64\tau} + 96\tau^2(C_1)^2\left(\|\boldsymbol{u}\left(t_1\right)\|_{L^\infty}^2 + \|\nabla\boldsymbol{u}\left(t_0\right)\|_{L^\infty}^2\right)\|\boldsymbol{u}_t\|^2_{L^2(t_0,t_1;H^1)} \\ & \le \tfrac{\|e_u^1 - e_u^0\|_0^2 + \|e_u^0\|_0^2}{64\tau} + 96\tau^3(C_1)^2\left(\|\boldsymbol{u}\left(t_1\right)\|_{L^\infty}^2 + \|\nabla\boldsymbol{u}\left(t_0\right)\|_{L^\infty}^2\right)\|\boldsymbol{u}_t\|^2_{L^\infty(t_0,T;H^1)}. \end{aligned}$$

The estimation (37) is replaced by

$$\left|\left(\tfrac{dQ}{dt}\left(t_1\right) - \tfrac{Q(t_1)-Q(t_0)}{\tau}\right)e_Q^1\right| \le \tfrac{|e_Q^1|^2}{8\tau T} + 2\tau^2 T\int_{t_0}^{t_1}|Q_{tt}|^2 dt \le \tfrac{|e_Q^1|^2}{8\tau T} + \tfrac{2\tau^3}{T}.$$

Lastly, the estimation (39) is replaced by

$$\begin{aligned} |\mathbb{J}_1| & \le \tfrac{|e_Q^1|^2}{8\tau T} + 48\tau^2 T\left\|\boldsymbol{u}\left(t_0\right)\right\|_{L^\infty}^2\left\|\nabla\boldsymbol{u}\left(t_0\right)\right\|_0^2\|\boldsymbol{u}_t\|^2_{L^2(t_0,t_1;L^2)} \\ & \le \tfrac{|e_Q^1|^2}{8\tau T} + 48\tau^3 T\left\|\boldsymbol{u}\left(t_0\right)\right\|_{L^\infty}^2\left\|\nabla\boldsymbol{u}\left(t_0\right)\right\|_0^2\|\boldsymbol{u}_t\|^2_{L^\infty(t_0,T;L^2)}. \end{aligned}$$

Then, following the argument proving Lemma 4.1, we have

$$
\begin{aligned}
&\|e_u^1\|_0^2+\nu\tau\|\nabla e_u^1\|_0^2+\mu\tau\|\nabla\cdot e_u^1\|_0^2+|e_Q^1|^2\\
&\quad\le 128\tau^4\|\boldsymbol{u}_{tt}\|^2_{L^\infty(t_0,T;L^2)}+128(C_2)^2h^6\|\boldsymbol{u}_t\|^2_{L^2(t_0,t_1;H^3)}+\tau(C_0)^2\mu^{-1}h^4\|P(t_1)\|_2^2\\
&\qquad+128\tau^4(C_1)^2\left(\|\boldsymbol{u}(t_1)\|^2_{L^\infty}+\|\nabla\boldsymbol{u}(t_0)\|^2_{L^\infty}\right)\|\boldsymbol{u}_t\|^2_{L^\infty(t_0,T;H^1)}\\
&\qquad+128\tau h^4(C_2)^2\left(\|\boldsymbol{u}(t_0)\|^2_{L^\infty}+h^2(C_1)^2\|\nabla\boldsymbol{u}(t_0)\|^2_{L^\infty}\right)\|\boldsymbol{u}(t_0)\|_3^2\\
&\qquad+\tfrac{4\tau^4}{T}+96\tau^4T\|\boldsymbol{u}(t_0)\|^2_{L^\infty}\|\nabla\boldsymbol{u}(t_0)\|_0^2\|\boldsymbol{u}_t\|^2_{L^\infty(t_0,T;L^2)}\\
&\qquad+96\tau h^6T(C_2)^2\left(((C_1)^2+1)\|\nabla\boldsymbol{u}(t_0)\|^2_{L^\infty}\|\boldsymbol{u}(t_1)\|_0^2+\|\nabla\boldsymbol{u}(t_1)\|^2_{L^\infty}\|\boldsymbol{u}(t_0)\|_0^2\right)\|\boldsymbol{u}(t_0)\|_3^2\\
&\qquad+48\tau h^4T(C_1)^4(C_2)^2\|\nabla\boldsymbol{u}(t_0)\|_0^4\|\boldsymbol{u}(t_1)\|_3^2\\
&\quad\le\widetilde{\mathcal{B}}(T,\mu)(\tau^4+h^4),
\end{aligned}
$$

which completes the proof. □

Next, we will adopt the mathematical induction again to prove the robust error estimates.

Lemma 4.11. *There exists a viscosity-independent positive constant $0<\widetilde{h}_*\le 1$ such that if $h\le\widetilde{h}_*$, and $\tau\le h^2$, then*

$$
\left\|e_u^2\right\|_0^2+(e_Q^2)^2+4\tau\nu\sum_{i=1}^{1}\left\|\nabla e_u^{i+1}\right\|_0^2+2\tau\mu\sum_{i=1}^{1}\left\|\nabla\cdot e_u^{i+1}\right\|_0^2\le h^{-\frac{1}{2}}\left(h^4+\tau^4\right).
$$

Proof. Assume $\tau\le h^2\le 1$. Since $\tau\le h^2\le h^{\frac{d+1}{2}}$, it yields

$$
\left\|e_u^1\right\|_0^2\le h^{-\frac{1}{2}}h^{d+1}=h^{d+\frac{1}{2}}.
$$

Hence we have

$$
h^{-2}\left\|e_u^1\right\|_0^2\le h^{d-\frac{3}{2}}
$$

and by the inverse inequality

$$
\left\|e_u^1\right\|^2_{L^\infty}\le(C_3)^2h^{-d}\left\|e_u^1\right\|_0^2\le(C_3)^2h^{\frac{1}{2}}. \tag{85}
$$

At $t=t_2$, we have the following error equation

$$
\begin{cases}
\left(\frac{\partial\boldsymbol{u}}{\partial t}(t_2)-\frac{3\boldsymbol{u}_h^2-4\boldsymbol{u}_h^1+\boldsymbol{u}_h^0}{2\tau},\boldsymbol{v}_h\right)+c\left(\boldsymbol{u}(t_2),\boldsymbol{u}(t_2),\boldsymbol{v}_h\right)-Q^2\exp\left(\frac{t_2}{T}\right)c\left(\widetilde{\boldsymbol{u}}_h^2,\widetilde{\boldsymbol{u}}_h^2,\boldsymbol{v}_h\right)\\
-\left(P(t_2)-P_h^2,\nabla\cdot\boldsymbol{v}_h\right)+\nu\left(\nabla(\boldsymbol{u}(t_2)-\boldsymbol{u}_h^2),\nabla\boldsymbol{v}_h\right)+\mu\left(\nabla\cdot(\boldsymbol{u}(t_2)-\boldsymbol{u}_h^2),\nabla\cdot\boldsymbol{v}_h\right)=0, &\text{(86a)}\\
\left(\nabla\cdot(\boldsymbol{u}(t_2)-\boldsymbol{u}_h^2),q_h\right)=0, &\text{(86b)}\\
\frac{dQ}{dt}(t_2)-\frac{3Q^2-4Q^1+Q^0}{2\tau}=-\frac{1}{T}(Q(t_2)-Q^2)\\
\qquad\qquad+\exp\left(\frac{t_2}{T}\right)\left[c\left(\boldsymbol{u}(t_2),\boldsymbol{u}(t_2),\boldsymbol{u}(t_2)\right)-c\left(\widetilde{\boldsymbol{u}}_h^2,\widetilde{\boldsymbol{u}}_h^2,\boldsymbol{u}_h^2\right)\right]. &\text{(86c)}
\end{cases}
$$

Let $\tilde{e}_u^2=2e_u^1-e_u^0$ and $\boldsymbol{v}_h=e_u^2$ in (86a), then we have

$$
\begin{aligned}
&\tfrac{\left\|e_u^2\right\|_0^2-\left\|e_u^1\right\|_0^2+\left\|2e_u^2-e_u^1\right\|^2-\left\|2e_u^1-e_u^0\right\|^2}{4\tau}+\tfrac{\left\|e_u^2-\tilde{e}_u^2\right\|_0^2}{4\tau}+\nu\left\|\nabla e_u^2\right\|_0^2+\mu\left\|\nabla\cdot e_u^2\right\|_0^2\\
&=-\left(\tfrac{\partial\boldsymbol{u}}{\partial t}\big|_{t=t_2},e_u^2\right)+\left(\tfrac{3\boldsymbol{u}(t_2)-4\boldsymbol{u}(t_1)+\boldsymbol{u}(t_0)}{2\tau},e_u^2\right)-\left(\tfrac{3\eta(t_2)-4\eta(t_1)+\eta(t_0)}{2\tau},e_u^2\right)\\
&\quad-c\left(\boldsymbol{u}(t_2),\boldsymbol{u}(t_2),e_u^2\right)+Q^2\exp\left(\tfrac{t_2}{T}\right)c\left(\widetilde{\boldsymbol{u}}_h^2,\widetilde{\boldsymbol{u}}_h^2,e_u^2\right)-\left(P(t_2)-\Pi_hP(t_2),\nabla\cdot e_u^2\right):=\sum_{i=1}^{6}\widetilde{\mathbb{I}}_i,
\end{aligned} \tag{87}
$$

where

$$\begin{aligned}
\widetilde{\mathbb{I}}_1+\widetilde{\mathbb{I}}_2 &\le \left\| \tfrac{\partial \boldsymbol{u}}{\partial t}\big|_{t=t_2} - \tfrac{3\boldsymbol{u}(t_2)-4\boldsymbol{u}(t_1)+\boldsymbol{u}(t_0)}{2\tau}\right\|_0 \left(\left\|e_u^2-\tilde{e}_u^2\right\|_0+\left\|\tilde{e}_u^2\right\|_0\right)\\
&\le \tfrac{\tau^3}{4}(1+16\tau)\left\|\boldsymbol{u}_{ttt}\right\|^2_{L^2(t_0,t_2;L^2)} + \tfrac{\left\|e_u^2-\tilde{e}_u^2\right\|_0^2}{64\tau} + \tfrac{4\left\|e_u^1\right\|_0^2+\left\|e_u^0\right\|_0^2}{2},\\
\widetilde{\mathbb{I}}_3 &\le \left\| \tfrac{3\eta(t_2)-4\eta(t_1)+\eta(t_0)}{2\tau}\right\|_0 \left(\left\|e_u^2-\tilde{e}_u^2\right\|_0+\left\|\tilde{e}_u^2\right\|_0\right)\\
&\le \tfrac{17(C_2)^2\tau h^6}{6}(1+16\tau)\left\|\boldsymbol{u}_t\right\|^2_{L^2(t_0,t_2;H^3)} + \tfrac{\left\|e_u^2-\tilde{e}_u^2\right\|_0^2}{64\tau} + \tfrac{4\left\|e_u^1\right\|_0^2+\left\|e_u^0\right\|_0^2}{2},\\
\widetilde{\mathbb{I}}_6 &\le \tfrac{\mu}{2}\|\nabla\cdot e_u^2\|_0^2 + \tfrac{1}{2\mu}\|P(t_2)-\Pi_h P(t_2)\|_0^2 \le \tfrac{\mu}{2}\|\nabla\cdot e_u^2\|_0^2 + \tfrac{C_0}{2\mu}h^4\|P(t_2)\|_2^2.
\end{aligned}$$

In addition,

$$\begin{aligned}
-\widetilde{\mathbb{I}}_4+\widetilde{\mathbb{I}}_5 &= c\left(\boldsymbol{u}(t_2)-\widetilde{\boldsymbol{u}}(t_2),\boldsymbol{u}(t_2),e_u^2\right)+c\left(\widetilde{\boldsymbol{u}}(t_2),\boldsymbol{u}(t_2)-\widetilde{\boldsymbol{u}}(t_2),e_u^2\right)\\
&\quad + c\left(\widetilde{\boldsymbol{u}}(t_2),\widetilde{\boldsymbol{u}}(t_2),e_u^2\right) - c\left(\widetilde{\boldsymbol{u}}_h^2,\widetilde{\boldsymbol{u}}_h^2,e_u^2\right)+e_Q^2\exp\left(\tfrac{t_2}{T}\right)c\left(\widetilde{\boldsymbol{u}}_h^2,\widetilde{\boldsymbol{u}}_h^2,e_u^2\right) := \sum_{i=1}^{5}\widetilde{\mathbb{J}}_i,
\end{aligned}$$

where $\widetilde{\mathbb{J}}_5$ will be canceled out by the ESAV dynamics equation part. It holds that

$$\begin{aligned}
\widetilde{\mathbb{J}}_1 &\le 3\|\boldsymbol{u}(t_2)\|_{L^\infty}\|\boldsymbol{u}(t_2)-\widetilde{\boldsymbol{u}}(t_2)\|_1\left(\left\|e_u^2-\tilde{e}_u^2\right\|_0+\left\|\tilde{e}_u^2\right\|_0\right)\\
&\le \tfrac{4\left\|e_u^1\right\|_0^2+\left\|e_u^0\right\|_0^2}{2}+\tfrac{\left\|e_u^2-\tilde{e}_u^2\right\|_0^2}{64\tau}+9(1+16\tau)\|\boldsymbol{u}(t_2)\|_{L^\infty}^2\|\boldsymbol{u}(t_2)-\widetilde{\boldsymbol{u}}(t_2)\|_1^2\\
&\le \tfrac{4\left\|e_u^1\right\|_0^2+\left\|e_u^0\right\|_0^2}{2}+\tfrac{\left\|e_u^2-\tilde{e}_u^2\right\|_0^2}{64\tau}+72(1+16\tau)\tau^3\|\boldsymbol{u}(t)\|_{L^\infty(0,T;L^\infty)}^2\|\boldsymbol{u}(t)\|_{H^2(t_0,t_2;H^1)}^2,
\end{aligned}$$

and

$$\begin{aligned}
\widetilde{\mathbb{J}}_2 &\le \tfrac{4\left\|e_u^1\right\|_0^2+\left\|e_u^0\right\|_0^2}{2}+\tfrac{\left\|e_u^2-\tilde{e}_u^2\right\|_0^2}{64\tau}+72(1+16\tau)\tau^3\|\widetilde{\boldsymbol{u}}(t_2)\|_{L^\infty}^2\|\boldsymbol{u}(t)\|_{H^2(t_0,t_2;L^2)}^2\\
&\le \tfrac{4\left\|e_u^1\right\|_0^2+\left\|e_u^0\right\|_0^2}{2}+\tfrac{\left\|e_u^2-\tilde{e}_u^2\right\|_0^2}{64\tau}+576(2+32\tau)\tau^3\|\boldsymbol{u}(t)\|_{L^\infty(0,T;L^\infty)}^2\|\boldsymbol{u}(t)\|_{H^2(t_0,t_2;L^2)}^2.
\end{aligned}$$

Similar to analysis (31) and (50), we can obtain

$$\begin{aligned}
\widetilde{\mathbb{J}}_3+\widetilde{\mathbb{J}}_4 &= c\left(\tilde{\eta}(t_2),\widetilde{\boldsymbol{u}}(t_2),e_u^2\right)+c\left(\mathrm{P}_{st}\widetilde{\boldsymbol{u}}(t_2),\tilde{\eta}(t_2),e_u^2\right)+c\left(\mathrm{P}_{st}\widetilde{\boldsymbol{u}}(t_2),\tilde{e}_u^2,e_u^2\right)\\
&\quad + c\left(\tilde{e}_u^2,\mathrm{P}_{st}\widetilde{\boldsymbol{u}}(t_2),e_u^2\right)-c\left(\tilde{e}_u^2,\tilde{e}_u^2,e_u^2-\tilde{e}_u^2\right).
\end{aligned}\tag{88}$$

By Holder's inequality, Sobolev embedding inequalities [1], and Lemma 2.1, we have

$$\begin{aligned}
c\left(\tilde{\eta}(t_2),\widetilde{\boldsymbol{u}}(t_2),e_u^2\right) &\le \tfrac{\left\|e_u^2-\tilde{e}_u^2\right\|_0^2}{64\tau}+\tfrac{4\left\|e_u^1\right\|_0^2+\left\|e_u^0\right\|_0^2}{32}+96(C_2)^2h^4\left\|\widetilde{\boldsymbol{u}}(t_2)\right\|_{L^\infty}^2\left\|\widetilde{\boldsymbol{u}}(t_2)\right\|_3^2\\
&\le \tfrac{\left\|e_u^2-\tilde{e}_u^2\right\|_0^2}{64\tau}+\tfrac{4\left\|e_u^1\right\|_0^2+\left\|e_u^0\right\|_0^2}{32}+9600(C_2)^2h^4\left\|\boldsymbol{u}(t)\right\|_{L^\infty(0,T;H^3)}^4.
\end{aligned}$$

Similarly, there holds

$$c\left(\mathrm{P}_{st}\widetilde{\boldsymbol{u}}(t_2),\tilde{\eta}(t_2),e_u^2\right)\le \tfrac{\left\|e_u^2-\tilde{e}_u^2\right\|_0^2}{64\tau}+\tfrac{4\left\|e_u^1\right\|_0^2+\left\|e_u^0\right\|_0^2}{32}+9600(C_1C_2)^2h^6\left\|\boldsymbol{u}(t)\right\|_{L^\infty(0,T;H^3)}^4,$$

and

$$c\left(\mathrm{P}_{st}\widetilde{\boldsymbol{u}}(t_2),\tilde{e}_u^2,e_u^2\right)\le \tfrac{\left\|e_u^2-\tilde{e}_u^2\right\|_0^2}{64\tau}+(18C_1\left\|\boldsymbol{u}(t)\right\|_{L^\infty(0,T;H^3)}+144C_1^2\tau)(4\left\|e_u^1\right\|_0^2+\left\|e_u^0\right\|_0^2).$$

The fourth term of the right-hand side of (88) can be estimated as

$$\begin{aligned}
c\left(\tilde{e}_u^2,\mathrm{P}_{st}\widetilde{\boldsymbol{u}}(t_2),e_u^2\right) &= c\left(\tilde{e}_u^2,\mathrm{P}_{st}\widetilde{\boldsymbol{u}}(t_2),e_u^2-\tilde{e}_u^2\right)+c\left(\tilde{e}_u^2,\mathrm{P}_{st}\widetilde{\boldsymbol{u}}(t_2),\tilde{e}_u^2\right)\\
&= c\left(\tilde{e}_u^2,\mathrm{P}_{st}\widetilde{\boldsymbol{u}}(t_2),e_u^2-\tilde{e}_u^2\right)-\frac{1}{2}\left(\nabla\cdot\mathrm{P}_{st}\widetilde{\boldsymbol{u}}(t_2)\tilde{e}_u^2,\tilde{e}_u^2\right)-\left((\tilde{e}_u^2\cdot\nabla)\mathrm{P}_{st}\widetilde{\boldsymbol{u}}(t_2),\tilde{e}_u^2\right)\\
&\le \tfrac{\left\|e_u^2-\tilde{e}_u^2\right\|_0^2}{64\tau}+50(C_1)^2\left(\tau h^{-2}(C_3)^2\left\|\widetilde{\boldsymbol{u}}(t_2)\right\|_{L^\infty}^2+\left\|\nabla\widetilde{\boldsymbol{u}}(t_2)\right\|_{L^\infty}^2\right)\left\|\tilde{e}_u^2\right\|_0^2,
\end{aligned}\tag{89}$$

where integration-by-part is applied on the second equality. Using (85), it gives us

$$c\left(\tilde{e}_u^2,\tilde{e}_u^2,e_u^2-\tilde{e}_u^2\right)\le\frac{\|e_u^2-\tilde{e}_u^2\|_0^2}{64\tau}+144(C_3)^2\tau h^{-\frac{3}{2}}\|\tilde{e}_u^2\|_0^2\le\frac{\|e_u^2-\tilde{e}_u^2\|_0^2}{64\tau}+288(C_3)^2(4\|e_u^1\|_0^2+\|e_u^0\|_0^2),\tag{90}$$

where $h \le 1$ and $\tau \le h^2$ are applied. Hence,

$$\widetilde{\mathbb{J}}_3 + \widetilde{\mathbb{J}}_4 \le \tfrac{5\|e_u^2 - \tilde{e}_u^2\|_0^2}{64\tau} + \left(\tfrac{1}{16} + (18C_1 + 100C_1^2(C_3^2+1))\,\|\boldsymbol{u}(t)\|_{L^\infty(0,T;H^3)} + 144C_1^2\tau + 288(C_3)^2\right)(4\|e_u^1\|_0^2 + \|e_u^0\|_0^2).$$

Next, multiplying e_Q^2 on (86c), it turns to

$$\tfrac{(e_Q^2)^2-(e_Q^1)^2+(2e_Q^2-e_Q^1)^2-(2e_Q^1-e_Q^0)^2+(e_Q^2-2e_Q^1+e_Q^0)^2}{4\tau} + \tfrac{1}{T}(e_Q^2)^2 = \left(-\tfrac{dQ}{dt}(t_2) + \tfrac{3Q(t_2)-4Q(t_1)+Q(t_0)}{2\tau}\right)e_Q^2 + e_Q^2\exp\left(\tfrac{t_2}{T}\right)\left[c\left(\boldsymbol{u}(t_2),\boldsymbol{u}(t_2),\boldsymbol{u}(t_2)\right) - c\left(\widetilde{\boldsymbol{u}}_h^2,\widetilde{\boldsymbol{u}}_h^2,\boldsymbol{u}_h^2\right)\right],$$

where

$$\left(-\tfrac{dQ}{dt}(t_2) + \tfrac{3Q(t_2)-4Q(t_1)+Q(t_0)}{2\tau}\right)e_Q^2 \le \tfrac{\tau^3}{4}(1+16\tau)\int_{t_0}^{t_2}|Q_{ttt}|^2dt + \tfrac{|e_Q^2-e_Q^1|^2}{64\tau} + 2(e_Q^1)^2,$$

and

$$\begin{aligned}
&e_Q^2\exp\left(\tfrac{t_2}{T}\right)\left[c\left(\boldsymbol{u}(t_2),\boldsymbol{u}(t_2),\boldsymbol{u}(t_2)\right) - c\left(\widetilde{\boldsymbol{u}}_h^2,\widetilde{\boldsymbol{u}}_h^2,\boldsymbol{u}_h^2\right)\right]\\
=\;& e_Q^2\exp\left(\tfrac{t_2}{T}\right)\left[c\left(\widetilde{\boldsymbol{u}}(t_2),\widetilde{\boldsymbol{u}}(t_2),\widetilde{\boldsymbol{u}}(t_2)\right) - c\left(\widetilde{\boldsymbol{u}}_h^2,\widetilde{\boldsymbol{u}}_h^2,\boldsymbol{u}_h^2\right)\right]\\
=\;& e_Q^2\exp\left(\tfrac{t_2}{T}\right)\left[c\left(\tilde{\eta}(t_2)+\tilde{e}_u^2,\widetilde{\boldsymbol{u}}(t_2),\widetilde{\boldsymbol{u}}(t_2)\right) + c\left(\widetilde{\boldsymbol{u}}_h^2,\tilde{\eta}(t_2)+\tilde{e}_u^2,\widetilde{\boldsymbol{u}}(t_2)\right) + c\left(\widetilde{\boldsymbol{u}}_h^2,\widetilde{\boldsymbol{u}}_h^2,\widetilde{\boldsymbol{u}}(t_2)-\boldsymbol{u}(t_2)\right)\right.\\
&\left. + c\left(\widetilde{\boldsymbol{u}}_h^2,\widetilde{\boldsymbol{u}}_h^2,\eta(t_2)\right) + c\left(\widetilde{\boldsymbol{u}}_h^2,\widetilde{\boldsymbol{u}}_h^2,e_u^2\right)\right].
\end{aligned}$$

First of all, we have

$$\begin{aligned}
\|\nabla\widetilde{\boldsymbol{u}}_h^2\|_0 &\le \|\nabla\widetilde{\boldsymbol{u}}(t_2)\|_0 + \|\nabla\tilde{\eta}^2\|_0 + \|\nabla\tilde{e}_u^2\|_0\\
&\le 2\|\nabla\boldsymbol{u}(t_1)\|_0 + \|\nabla\boldsymbol{u}(t_0)\|_0 + C_2h^2(2\|\boldsymbol{u}(t_1)\|_3 + \|\boldsymbol{u}(t_0)\|_3) + 3C_3h^{\frac{d}{2}-\frac{3}{4}} \le 3C_7^{\{T\}}.
\end{aligned}$$

Applying $\exp(1) < 3$, we can have the following estimate

$$\begin{aligned}
&e_Q^2\exp\left(\tfrac{t_2}{T}\right)\left[c\left(\boldsymbol{u}(t_2),\boldsymbol{u}(t_2),\boldsymbol{u}(t_2)\right) - c\left(\widetilde{\boldsymbol{u}}_h^2,\widetilde{\boldsymbol{u}}_h^2,\boldsymbol{u}_h^2\right)\right]\\
\le\;& e_Q^2\exp\left(\tfrac{t_2}{T}\right)c\left(\widetilde{\boldsymbol{u}}_h^2,\widetilde{\boldsymbol{u}}_h^2,e_u^2\right) + 9C_2h^2|e_Q^2|\|\widetilde{\boldsymbol{u}}(t_2)\|_3\|\widetilde{\boldsymbol{u}}(t_2)\|_0^2 + 18|e_Q^2|\|\widetilde{\boldsymbol{u}}(t_2)\|_{L^\infty}\|\nabla\widetilde{\boldsymbol{u}}(t_2)\|_0\|\tilde{e}_u^2\|_0\\
&+ 9C_2C_7^{\{T\}}h^3|e_Q^2|\|\widetilde{\boldsymbol{u}}(t_2)\|_{L^\infty}\|\widetilde{\boldsymbol{u}}(t_2)\|_3 + 9C_7^{\{T\}}|e_Q^2|\|\widetilde{\boldsymbol{u}}(t_2)\|_{L^\infty}\|\tilde{e}_u^2\|_0\\
&+ 9\sqrt{8}(C_7^{\{T\}})^2\tau^{\frac{3}{2}}|e_Q^2|\|\nabla\boldsymbol{u}(t)\|_{H^2(t_0,t_2;L^2)} + 9C_2(C_5C_7^{\{T\}})^2h^2|e_Q^2|\|\boldsymbol{u}(t_2)\|_3\\
\le\;& e_Q^2\exp\left(\tfrac{t_2}{T}\right)c\left(\widetilde{\boldsymbol{u}}_h^2,\widetilde{\boldsymbol{u}}_h^2,e_u^2\right) + \tfrac{1}{2T}|e_Q^2|^2 + \tfrac{7\cdot90^2}{2}T(C_2)^2h^4\|\boldsymbol{u}\|_{L^\infty(0,T;H^3)}^4\\
&+ 7\cdot90^2T((C_2)^2 + (C_7^{\{T\}})^2)\|\boldsymbol{u}\|_{L^\infty(0,T;H^3)}^2(4\|e_u^1\|_0^2 + \|e_u^0\|_0^2)\\
&+ \tfrac{7\cdot90^2}{2}T(C_2C_7^{\{T\}})^2h^6\|\boldsymbol{u}\|_{L^\infty(0,T;H^3)}^4 + \tfrac{56\cdot9^2}{2}T(C_7^{\{T\}})^4\tau^3\|\boldsymbol{u}_{tt}\|_{L^2(t_0,t_2;H^3)}^2\\
&+ \tfrac{7\cdot9^2}{2}T(C_2)^2(C_5C_7^{\{T\}})^4h^4\|\boldsymbol{u}\|_{L^\infty(0,T;H^3)}^2.
\end{aligned}$$

Finally, we have

$$\begin{aligned}
&\tfrac{\|e_u^2\|_0^2-\|e_u^1\|_0^2+\|2e_u^2-e_u^1\|^2-\|2e_u^1-e_u^0\|^2}{4\tau} + \tfrac{(e_Q^2)^2-(e_Q^1)^2+(2e_Q^2-e_Q^1)^2-(2e_Q^1-e_Q^0)^2}{4\tau} + \nu\left\|\nabla e_u^2\right\|_0^2 + \tfrac{\mu}{2}\left\|\nabla\cdot e_u^2\right\|_0^2 + \tfrac{1}{2T}(e_Q^2)^2\\
\le\;& \left(\tfrac{33}{16} + (18C_1 + 100C_1^2(C_3^2+1))\,\|\boldsymbol{u}(t)\|_{L^\infty(0,T;H^3)} + 144C_1^2\tau + 288(C_3)^2\right)(4\|e_u^1\|_0^2 + \|e_u^0\|_0^2)\\
&+ 9600(C_2)^2h^4(1+(C_1)^2h^2)\,\|\boldsymbol{u}(t)\|_{L^\infty(0,T;H^3)}^4 + 7\cdot90^2T((C_2)^2 + (C_7^{\{T\}})^2)\|\boldsymbol{u}\|_{L^\infty(0,T;H^3)}^2(4\|e_u^1\|_0^2 + \|e_u^0\|_0^2)\\
&+ 2(e_Q^1)^2 + \tfrac{\tau^3}{4}(1+16\tau)\,\|\boldsymbol{u}_{ttt}\|_{L^2(t_0,t_2;L^2)}^2 + \tfrac{17(C_2)^2\tau h^6}{6}(1+16\tau)\,\|\boldsymbol{u}_t\|_{L^2(t_0,t_2;H^3)}^2 + \tfrac{C_0}{2\mu}h^4\|P(t_2)\|_2^2\\
&+ 72(1+16\tau)\tau^3\|\boldsymbol{u}(t)\|_{L^\infty(0,T;L^\infty)}^2\|\boldsymbol{u}(t)\|_{H^2(t_0,t_2;H^1)}^2 + 576(2+32\tau)\tau^3\|\boldsymbol{u}(t)\|_{L^\infty(0,T;H^3)}^2\|\boldsymbol{u}(t)\|_{H^2(t_0,t_2;L^2)}^2\\
&+ \tfrac{\tau^3}{4}(1+16\tau)\int_{t_0}^{t_2}|Q_{ttt}|^2dt + \tfrac{7\cdot90^2}{2}T(C_2)^2h^4\|\boldsymbol{u}\|_{L^\infty(0,T;H^3)}^4 + \tfrac{7\cdot90^2}{2}T(C_2C_7^{\{T\}})^2h^6\|\boldsymbol{u}\|_{L^\infty(0,T;H^3)}^4\\
&+ \tfrac{56\cdot9^2}{2}T(C_7^{\{T\}})^4\tau^3\|\boldsymbol{u}_{tt}\|_{L^2(t_0,t_2;H^3)}^2 + \tfrac{7\cdot9^2}{2}T(C_2)^2(C_5C_7^{\{T\}})^4h^4\|\boldsymbol{u}\|_{L^\infty(0,T;H^3)}^2.
\end{aligned}$$

Define

$$\begin{aligned}
C_9^{\{T\}} =& 20\left(\tfrac{33}{16} + (18C_1 + 100C_1^2(C_3^2+1))\,\|\boldsymbol{u}(t)\|_{L^\infty(0,T;H^3)} + 144C_1^2\tau + 288(C_3)^2\right.\\
&\left. + 7\cdot90^2T((C_2)^2 + (C_7^{\{T\}})^2)\|\boldsymbol{u}\|_{L^\infty(0,T;H^3)}^2\right),
\end{aligned}$$

then applying $e_u^0 = 0$ and $e_Q^0 = 0$, we have

$$\begin{aligned}
&\left\|e_u^2\right\|_0^2 + \left\|2e_u^2 - e_u^1\right\|^2 + (e_Q^2)^2 + (2e_Q^2 - e_Q^1)^2 + 4\tau\nu \sum_{i=1}^{1} \left\|\nabla e_u^{i+1}\right\|_0^2 + 2\tau\mu \sum_{i=1}^{1} \left\|\nabla \cdot e_u^{i+1}\right\|_0^2 + \tfrac{2\tau}{T} \sum_{i=1}^{1} (e_Q^{i+1})^2 \\
&\quad \le 5\left\|e_u^1\right\|_0^2 + 5(e_Q^1)^2 + \tau \sum_{i=1}^{1} C_9^{\{T\}} (\|e_u^i\|_0^2 + (e_Q^i)^2) + 2\widetilde{\mathcal{G}}(T,\mu)(\tau^4 + h^4),
\end{aligned}$$

where

$$\begin{aligned}
\widetilde{\mathcal{G}}(T,\mu) = {} & 17\left\|\boldsymbol{u}_{ttt}\right\|^2_{L^2(t_0,T;L^2)} + \tfrac{34(C_2)^2}{3}(1+16\tau)\left\|\boldsymbol{u}_t\right\|^2_{L^2(t_0,T;H^3)} + \tfrac{2C_0}{\mu}T\|P\left(t_2\right)\|^2_{L^\infty(t_0,T;H^2)} \\
& + 4896\|\boldsymbol{u}\left(t\right)\|^2_{L^\infty(0,T;L^\infty)}\|\boldsymbol{u}(t)\|^2_{H^2(t_0,T;H^1)} + 78366\|\boldsymbol{u}\left(t\right)\|^2_{L^\infty(0,T;H^3)}\|\boldsymbol{u}(t)\|^2_{H^2(t_0,T;L^2)} \\
& + 17\int_{t_0}^{T}|Q_{ttt}|^2dt + 14\cdot 90^2T^2(C_2)^2\|\boldsymbol{u}\|^4_{L^\infty(0,T;H^3)} + 14\cdot 90^2T^2(C_2C_7^{\{T\}})^2\|\boldsymbol{u}\|^4_{L^\infty(0,T;H^3)} \\
& + 9600(C_2)^2(1+(C_1)^2)\|\boldsymbol{u}\|^4_{L^\infty(0,T;H^3)} + 112\cdot 9^2T(C_7^{\{T\}})^4\|\boldsymbol{u}_{tt}\|^2_{L^2(t_0,T;H^3)} \\
& + 14\cdot 9^2T^2(C_2)^2(C_5C_7^{\{T\}})^4\|\boldsymbol{u}\|^2_{L^\infty(0,T;H^3)}.
\end{aligned}$$

Applying Lemma 2.5 and 4.10, we have

$$\begin{aligned}
&\left\|e_u^2\right\|_0^2 + \left\|2e_u^2 - e_u^1\right\|_0^2 + (e_Q^2)^2 + (2e_Q^2 - e_Q^1)^2 + 4\tau\nu \sum_{i=1}^{1} \left\|\nabla e_u^{i+1}\right\|_0^2 + 2\tau\mu \sum_{i=1}^{1} \left\|\nabla \cdot e_u^{i+1}\right\|_0^2 + \tfrac{2\tau}{T} \sum_{i=1}^{1} (e_Q^{i+1})^2 \\
&\quad \le \exp(\tau \sum_{i=1}^{1} C_9^{\{T\}}) \left(5\widetilde{\mathcal{B}}(T,\mu) + 2\widetilde{\mathcal{G}}(T,\mu)\right)(\tau^4 + h^4).
\end{aligned}$$

Picking $\widetilde{h}_* = \min\left\{\widetilde{h}_0, 1, \exp(-2TC_9^{\{T\}})\left(5\widetilde{\mathcal{B}}(T,\mu) + 2\widetilde{\mathcal{G}}(T,\mu)\right)^{-2}\right\}$ completes the proof. □

The following error estimates are immediately obtained via the mathematical induction.

Theorem 4.12 (Error Estimates of the sIMEX2-FEM Scheme with $\mu > 0$)**.** *Assume the grad-div stabilizing parameter $\mu > 0$. If $h \le \widetilde{h}_*$ and $\tau \le h^2$, then the following error estimates hold:*

$$\left\|e_u^{n+1}\right\|_0^2 + (e_Q^{n+1})^2 + 4\tau\nu \sum_{i=1}^{n} \left\|\nabla e_u^{i+1}\right\|_0^2 + 2\tau\mu \sum_{i=1}^{n} \left\|\nabla \cdot e_u^{i+1}\right\|_0^2 \le \exp(TC_9^{\{T\}})\left(5\widetilde{\mathcal{B}}(T,\mu) + 2\widetilde{\mathcal{G}}(T,\mu)\right)(\tau^4 + h^4)$$

and

$$\tau \sum_{i=1}^{n} \left\|P\left(t_{i+1}\right) - P_h^{i+1}\right\|_0^2 \le \widetilde{\mathcal{K}}(T,\mu)(h^4 + \tau^4). \tag{91}$$

for all $1 \le n \le N-1$, where $\widetilde{\mathcal{K}}(T,\mu) > 0$ is a constant depending on T and μ.

Proof. We will show the estimate on pressure. Similar to (65), we have

$$\begin{aligned}
\tfrac{3e_u^{i+1} - 4e_u^i + e_u^{i-1}}{2\tau} = {} & -\nu A_h e_u^{i+1} - \Pi_h^{\mathrm{div}}\left(\mathcal{N}(\boldsymbol{u}(t_{i+1}), \boldsymbol{u}(t_{i+1})) - Q^{i+1}\exp\left(\tfrac{t_{i+1}}{T}\right)\mathcal{N}(\widetilde{\boldsymbol{u}}_h^{i+1}, \widetilde{\boldsymbol{u}}_h^{i+1})\right) \\
& - D_h(P(t_{i+1}) - \Pi_h P(t_{i+1})) - \Pi_h^{\mathrm{div}}\left(\boldsymbol{u}_t(t_{i+1}) - \tfrac{3\boldsymbol{u}(t_{i+1}) - 4\boldsymbol{u}(t_i) + \boldsymbol{u}(t_{i-1})}{2\tau}\right) \\
& - \Pi_h^{\mathrm{div}}\left(\tfrac{3\eta^{i+1} - 4\eta^i + \eta^{i-1}}{2\tau}\right).
\end{aligned} \tag{92}$$

By using the discrete inf-sup condition (4), it holds

$$\begin{aligned}
\gamma\|\Pi_h P\left(t_{i+1}\right) - P_h^{i+1}\|_0 &\le \sup_{\boldsymbol{v}_h \in \boldsymbol{X}_h} \tfrac{(\Pi_h P(t_{i+1}) - P_h^{i+1}, \nabla\cdot\boldsymbol{v}_h)}{\|\boldsymbol{v}_h\|_1} \\
&\le \left\|\boldsymbol{u}_t\left(t_{i+1}\right) - \tfrac{3\boldsymbol{u}(t_{i+1}) - 4\boldsymbol{u}(t_i) + \boldsymbol{u}(t_{i-1})}{2\tau}\right\|_{-1} + \left\|\tfrac{3\eta^{i+1} - 4\eta^i + \eta^{i-1}}{2\tau}\right\|_{-1} \\
&\quad + \left\|\tfrac{3e_u^{i+1} - 4e_u^i + e_u^{i-1}}{2\tau}\right\|_{-1} + \nu\|\nabla\cdot e_u^{i+1}\|_0 + C_0h^2\|P\left(t_{i+1}\right)\|_2 \\
&\quad + \left\|\mathcal{N}(\boldsymbol{u}(t_{i+1}), \boldsymbol{u}(t_{i+1})) - Q^{i+1}\exp\left(\tfrac{t_{i+1}}{T}\right)\mathcal{N}(\widetilde{\boldsymbol{u}}_h^{i+1}, \widetilde{\boldsymbol{u}}_h^{i+1})\right\|_{-1} =: \textstyle\sum_{i=1}^{6} \widetilde{\mathbb{K}}_i.
\end{aligned} \tag{93}$$

For the first two terms on the right-hand side of (93), we have

$$\widetilde{\mathbb{K}}_1 \le C_4\left\|\boldsymbol{u}_t\left(t_{i+1}\right) - \tfrac{3\boldsymbol{u}(t_{i+1}) - 4\boldsymbol{u}(t_i) + \boldsymbol{u}(t_{i-1})}{2\tau}\right\|_0 \le \tfrac{\tau^{\frac{3}{2}}C_4}{2}\left\|\boldsymbol{u}_{ttt}\right\|_{L^2(t_{i-1},t_{i+1};L^2)}, \tag{94}$$

and

$$\widetilde{\mathbb{K}}_2 \leq \frac{\sqrt{102}C_2C_4\tau^{\frac{1}{2}}h^3}{6}\left\|\boldsymbol{u}_t\right\|_{L^2(t_{i-1},t_{i+1};H^3)}.$$

For the sixth term on the right-hand side of (93), we have

$$\begin{aligned}\widetilde{\mathbb{K}}_6 =& \sup_{\|\phi\|_1=1}\left|c\left(\boldsymbol{u}\left(t_{i+1}\right),\boldsymbol{u}\left(t_{i+1}\right),\phi\right)-Q^{i+1}\exp\left(\tfrac{t_{i+1}}{T}\right)c\left(\widetilde{\boldsymbol{u}}_h^{i+1},\widetilde{\boldsymbol{u}}_h^{i+1},\phi\right)\right| \\ \leq& \sup_{\|\phi\|_1=1}\Big(\left|c\left(\boldsymbol{u}\left(t_{i+1}\right),\boldsymbol{u}\left(t_{i+1}\right),\phi\right)-c\left(\widetilde{\boldsymbol{u}}\left(t_{i+1}\right),\widetilde{\boldsymbol{u}}\left(t_{i+1}\right),\phi\right)\right| \\ &+\left|c\left(\widetilde{\boldsymbol{u}}\left(t_{i+1}\right),\widetilde{\boldsymbol{u}}\left(t_{i+1}\right),\phi\right)-c\left(\widetilde{\boldsymbol{u}}_h^{i+1},\widetilde{\boldsymbol{u}}_h^{i+1},\phi\right)\right|+\left|e_Q^{i+1}\exp\left(\tfrac{t_{i+1}}{T}\right)c\left(\widetilde{\boldsymbol{u}}_h^{i+1},\widetilde{\boldsymbol{u}}_h^{i+1},\phi\right)\right|\Big)\end{aligned} \tag{95}$$

For the first term on the right-hand side of (95), we have

$$\begin{aligned}&\left|c\left(\boldsymbol{u}\left(t_{i+1}\right),\boldsymbol{u}\left(t_{i+1}\right),\phi\right)-c\left(\widetilde{\boldsymbol{u}}\left(t_{i+1}\right),\widetilde{\boldsymbol{u}}\left(t_{i+1}\right),\phi\right)\right| \\ &\quad\leq\left|c\left(\boldsymbol{u}\left(t_{i+1}\right)-\widetilde{\boldsymbol{u}}\left(t_{i+1}\right),\boldsymbol{u}\left(t_{i+1}\right),\phi\right)\right|+\left|c\left(\widetilde{\boldsymbol{u}}\left(t_{i+1}\right),\boldsymbol{u}\left(t_{i+1}\right)-\widetilde{\boldsymbol{u}}\left(t_{i+1}\right),\phi\right)\right| \\ &\quad\leq 8\sqrt{2}\tau^{\frac{3}{2}}\|\boldsymbol{u}_{tt}\|_{L^2(t_{i-1},t_{i+1};L^2)}\|\boldsymbol{u}\left(t\right)\|_{L^\infty(0,T;W^{1,\infty})}\|\phi\|_1,\end{aligned} \tag{96}$$

where the integration by parts is applied on $c\left(\boldsymbol{u}\left(t_{i+1}\right)-\widetilde{\boldsymbol{u}}\left(t_{i+1}\right),\boldsymbol{u}\left(t_{i+1}\right),\phi\right)$. For the second term on the right-hand side of (95), it holds

$$\begin{aligned}&c\left(\widetilde{\boldsymbol{u}}\left(t_{i+1}\right),\widetilde{\boldsymbol{u}}\left(t_{i+1}\right),\phi\right)-c\left(\widetilde{\boldsymbol{u}}_h^{i+1},\widetilde{\boldsymbol{u}}_h^{i+1},\phi\right) \\ &\quad=c\left(\widetilde{\boldsymbol{u}}\left(t_{i+1}\right)-\widetilde{\boldsymbol{u}}_h^{i+1},\widetilde{\boldsymbol{u}}\left(t_{i+1}\right),\phi\right)+c\left(\mathrm{P}_{st}\widetilde{\boldsymbol{u}}\left(t_{i+1}\right),\widetilde{\boldsymbol{u}}\left(t_{i+1}\right)-\widetilde{\boldsymbol{u}}_h^{i+1},\phi\right)+c\left(\tilde{e}_u^{i+1},\widetilde{\boldsymbol{u}}\left(t_{i+1}\right)-\widetilde{\boldsymbol{u}}_h^{i+1},\phi\right).\end{aligned}$$

With integration by parts, we have

$$\left|c\left(\widetilde{\boldsymbol{u}}\left(t_{i+1}\right)-\widetilde{\boldsymbol{u}}_h^{i+1},\widetilde{\boldsymbol{u}}\left(t_{i+1}\right),\phi\right)\right|\leq 18\|\boldsymbol{u}\left(t\right)\|_{L^\infty(0,T;W^{1,\infty})}\|\widetilde{\boldsymbol{u}}\left(t_{i+1}\right)-\widetilde{\boldsymbol{u}}_h^{i+1}\|_0\|\phi\|_1,$$

By Lemma 2.1, we have

$$c\left(\mathrm{P}_{st}\widetilde{\boldsymbol{u}}\left(t_{i+1}\right),\widetilde{\boldsymbol{u}}\left(t_{i+1}\right)-\widetilde{\boldsymbol{u}}_h^{i+1},\phi\right)\leq 3C_1\|\boldsymbol{u}\left(t\right)\|_{L^\infty(0,T;W^{1,\infty})}\|\widetilde{\boldsymbol{u}}\left(t_{i+1}\right)-\widetilde{\boldsymbol{u}}_h^{i+1}\|_0\|\phi\|_1. \tag{97}$$

By Sobolev embedding inequalities (8) and Lemma 4.1, it holds

$$\left|c\left(\tilde{e}_u^{i+1},\widetilde{\boldsymbol{u}}\left(t_{i+1}\right)-\widetilde{\boldsymbol{u}}_h^{i+1},\phi\right)\right|\leq 9(C_3)^2C_5h^{\frac{1}{4}}\|\widetilde{\boldsymbol{u}}\left(t_{i+1}\right)-\widetilde{\boldsymbol{u}}_h^{i+1}\|_0\|\phi\|_1. \tag{98}$$

Lastly, with integration by parts, we also have

$$\begin{aligned}&\left|e_Q^{i+1}\exp\left(\tfrac{t_{i+1}}{T}\right)c\left(\widetilde{\boldsymbol{u}}_h^{i+1},\widetilde{\boldsymbol{u}}_h^{i+1},\phi\right)\right| \\ &=\left|e_Q^{i+1}\exp\left(\tfrac{t_{i+1}}{T}\right)\left(\left(\widetilde{\boldsymbol{u}}_h^{i+1}\cdot\nabla\widetilde{\boldsymbol{u}}_h^{i+1},\phi\right)+\left((\nabla\widetilde{\boldsymbol{u}}_h^{i+1})^T\widetilde{\boldsymbol{u}}_h^{i+1},\phi\right)+\left(\nabla\cdot\widetilde{\boldsymbol{u}}_h^{i+1}\widetilde{\boldsymbol{u}}_h^{i+1},\phi\right)\right)\right|\leq 54(C_5C_7^{\{T\}})^2\left|e_Q^{i+1}\right|\|\phi\|_1.\end{aligned} \tag{99}$$

Thus we get from (95)-(99)

$$\begin{aligned}\widetilde{\mathbb{K}}_6\leq& 8\sqrt{2}\tau^{\frac{3}{2}}\|\boldsymbol{u}_{tt}\|_{L^2(t_{i-1},t_{i+1};L^2)}\|\boldsymbol{u}\left(t\right)\|_{L^\infty(0,T;W^{1,\infty})} \\ &+\left((18+3C_1)\|\boldsymbol{u}\left(t\right)\|_{L^\infty(0,T;W^{1,\infty})}+9(C_3)^2C_5\right)\|\widetilde{\boldsymbol{u}}\left(t_{i+1}\right)-\widetilde{\boldsymbol{u}}_h^{i+1}\|_0+54(C_5C_7^{\{T\}})^2\left|e_Q^{i+1}\right|.\end{aligned}$$

Now, we are turning to analyze the third term on the right-hand side of (93). According to [13], we have by (7)

$$\widetilde{\mathbb{K}}_3\leq C_4(C_3+1)\left\|A_h^{-\frac{1}{2}}\tfrac{3e_u^{i+1}-4e_u^i+e_u^{i-1}}{2\tau}\right\|_0,$$

and by (92)

$$\begin{aligned}\left\|A_h^{-\frac{1}{2}}\tfrac{3e_u^{i+1}-4e_u^i+e_u^{i-1}}{2\tau}\right\|_0\leq&\ \nu\|\nabla e_u^{i+1}\|_0+\left\|\mathcal{N}(\boldsymbol{u}(t_{i+1}),\boldsymbol{u}(t_{i+1}))-Q^{i+1}\exp\left(\tfrac{t_{i+1}}{T}\right)\mathcal{N}(\widetilde{\boldsymbol{u}}_h^{i+1},\widetilde{\boldsymbol{u}}_h^{i+1})\right\|_{-1} \\ &+C_0h^2\|P\left(t_{i+1}\right)\|_2+\left\|\boldsymbol{u}_t(t_{i+1})-\tfrac{3\boldsymbol{u}(t_{i+1})-4\boldsymbol{u}(t_i)+\boldsymbol{u}(t_{i-1})}{2\tau}\right\|_{-1}+\left\|\tfrac{4\eta^{i+1}-3\eta^i+\eta^{i-1}}{2\tau}\right\|_{-1}.\end{aligned}$$

Combination of all the above estimates gives us

$$
\begin{aligned}
&\gamma\|P\left(t_{i+1}\right)-P_h^{i+1}\|_0\\
&\quad\le\left(C_4(C_3+1)+1\right)\Big\{\nu\|\nabla e_u^{i+1}\|_0+C_0h^2\|P\left(t_{i+1}\right)\|_2+\tfrac{\tau^{\frac{3}{2}}C_4}{2}\|\boldsymbol{u}_{ttt}\|_{L^2(t_{i-1},t_{i+1};L^2)}\\
&\qquad+\tfrac{\sqrt{102}C_2C_4\tau^{\frac{1}{2}}h^3}{6}\|\boldsymbol{u}_t\|_{L^2(t_{i-1},t_{i+1};H^3)}+8\sqrt{2}\tau^{\frac{3}{2}}\|\boldsymbol{u}_{tt}\|_{L^2(t_{i-1},t_{i+1};L^2)}\|\boldsymbol{u}\left(t\right)\|_{L^\infty(0,T;W^{1,\infty})}\\
&\qquad+\left((18+3C_1)\|\boldsymbol{u}\left(t\right)\|_{L^\infty(0,T;W^{1,\infty})}+9(C_3)^2C_5\right)\|\widetilde{\boldsymbol{u}}\left(t_{i+1}\right)-\widetilde{\boldsymbol{u}}_h^{i+1}\|_0+54(C_5C_7^{\{T\}})^2\left|e_Q^{i+1}\right|\Big\}
\end{aligned}
$$

Taking square on the both sizes, multiplying by τ, summing up from $i=0$ to n, and applying the Cauchy-Schwarz inequality and Theorem 4.4, we finally obtain

$$
\begin{aligned}
&\tau\sum_{i=1}^{n}\|P\left(t_{i+1}\right)-P_h^{i+1}\|_0^2\\
&\le\tfrac{8(C_4(C_3+1)+1)^2}{\gamma^2}\Big(C_{10}^{\{T\}}\exp(TC_9^{\{T\}})\Big(5\widetilde{\mathcal{B}}(T,\mu)+2\widetilde{\mathcal{G}}(T,\mu)\Big)(\tau^4+h^4)\\
&\quad+\tfrac{(C_4)^2}{4}\tau^4\|\boldsymbol{u}_{ttt}\|^2_{L^2(t_0,T;L^2)}+\tfrac{102(C_2C_4)^2\tau h^6}{36}\|\boldsymbol{u}_t\|^2_{L^2(t_0,T;H^3)}+128\tau^4\|\boldsymbol{u}\|^2_{L^\infty(t_0,T;H^3)}\|\boldsymbol{u}_{tt}\|^2_{L^2(t_0,T;L^2)}\\
&\quad+\left((18+3C_1)\|\boldsymbol{u}\left(t\right)\|_{L^\infty(0,T;W^{1,\infty})}+9(C_3)^2C_5\right)^2Th^4\Big)\\
&\le\widetilde{\mathcal{K}}(T,\mu)(h^4+\tau^4),
\end{aligned}
$$

where $C_{10}^{\{T\}}=(C_0)^2+1+54^2(C_5C_7^{\{T\}})^4+\left((18+3C_1)\|\boldsymbol{u}\left(t\right)\|_{L^\infty(0,T;W^{1,\infty})}+9(C_3)^2C_5\right)^2T$ and

$$
\begin{aligned}
\widetilde{\mathcal{K}}(T,\mu)=&\tfrac{8(C_4(C_3+1)+1)^2}{\gamma^2}\Big(C_{10}^{\{T\}}\exp(TC_9^{\{T\}})\Big(5\widetilde{\mathcal{B}}(T,\mu)+2\widetilde{\mathcal{G}}(T,\mu)\Big)+\frac{(C_4)^2}{4}\|\boldsymbol{u}_{ttt}\|^2_{L^2(t_0,T;L^2)}\\
&+\tfrac{102(C_2C_4)^2}{36}\|\boldsymbol{u}_t\|^2_{L^2(t_0,T;H^3)}+128\|\boldsymbol{u}\|^2_{L^\infty(t_0,T;H^3)}\|\boldsymbol{u}_{tt}\|^2_{L^2(t_0,T;L^2)}\\
&+\left((18+3C_1)\|\boldsymbol{u}\left(t\right)\|_{L^\infty(0,T;W^{1,\infty})}+9(C_3)^2C_5\right)^2T\Big),
\end{aligned}
$$

which completes the proof. □

Remark 4.13. *Note that one could conduct similar robust error estimates on the convection and skew-symmetric forms of nonlinearity. Due to the introduced grad-div stabilization, the local mass conservation could be refined, so there is no much difference on the performance.*

5. Numerical experiments

In this section, we will numerically verify the optimality of the error estimates proved in Theorems 4.4, 4.6, 4.9 and 4.12 for the proposed sIMEX1-FEM (13) and sIMEX2-FEM (15) schemes. Furthermore, we will investigate the stabilization effect brought by the grad-div and ESAV approaches and demonstrate the effectiveness of the proposed schemes for simulations of problems with large Reynolds numbers. The finite element software package FreeFEM++[25] is used to implement all the numerical schemes and experiments.

5.1. **Test of convergence orders: the lattice-vortex problem.** We take the lattice-vortex problem [3, 5, 44] in two dimensions to test the convergence order of the proposed two schemes, whose exact solution is given by:

$$
\begin{aligned}
\boldsymbol{u}&=\begin{pmatrix}\sin(2\pi x)\sin(2\pi y)\\ \cos(2\pi x)\cos(2\pi y)\end{pmatrix}\exp(-8\nu\pi^2t),\\
p&=-\tfrac{1}{2}\left(\sin^2(2\pi x)+\cos^2(2\pi y)\right)\exp(-16\nu\pi^2t),
\end{aligned}
$$

so that the source function $\boldsymbol{f}=0$. We set the spatial domain $\Omega=(0,1)^2$ with the Dirichlet boundary condition and the terminal time $T=0.5$. For the sIMEX1-FEM scheme, since the errors are expected to be $\mathcal{O}(\tau+h^2)$, we repeatedly decrease the time step size τ by a factor of 4 and the spatial mesh size h by a factor of 2 to test the convergence. For the sIMEX2-FEM scheme, since the errors are expected to be $\mathcal{O}(\tau^2+h^2)$, we simultaneously decrease the time step and spatial mesh size by a factor of 2. We also fix the ESAV stabilizing parameter to be the standard choice $\theta=1$.

The viscosity is first chosen as $\nu = 10^{-1}$. We choose the grad-div stabilizing parameter $\mu = 0$ and 1, respectively. For this low Reynolds number case, the proposed two schemes are expected not sensitive to the grad-div stabilization term. Numerical results on the L^2 and H^1 errors of the simulated velocity and the L^2 errors of the simulated pressure at the terminal time $T = 0.5$ as well as their corresponding convergence rates are reported in Table 1 for the sIMEX1-FEM scheme and Table 2 for the sIMEX2-FEM scheme. We clearly observe the second-order convergence in all cases, which implies our derived error estimates are optimal for both schemes. It is also easy to see the sIMEX2-FEM scheme can be computationally much more efficient than the sIMEX1-FEM scheme in order to achieve similar level of accuracy.

TABLE 1. Numerical results on the errors of the simulated velocity and pressure at the terminal time $T = 0.5$ produced by the proposed sIMEX1-FEM scheme (13) for the lattice-vortex problem with the viscosity $\nu = 10^{-1}$. The ESAV stabilizing parameter $\theta = 1$.

sIMEX1-FEM		$\|\boldsymbol{u} - \boldsymbol{u}_h\|_0$	CR	$\|\boldsymbol{u} - \boldsymbol{u}_h\|_1$	CR	$\|P - P_h\|_0$	CR
h	τ	$\mu = 0$					
1/10	1/20	5.530e-3	-	5.463e-2	-	5.633e-3	-
1/20	1/80	1.247e-3	2.08	1.229e-2	2.09	1.254e-3	2.11
1/40	1/320	3.058e-4	2.03	3.009e-3	2.03	3.071e-4	2.03
1/80	1/1280	7.606e-5	2.01	7.480e-4	2.01	7.635e-5	2.01
h	τ	$\mu = 1$					
1/10	1/20	5.291e-3	-	5.245e-2	-	5.420e-3	-
1/20	1/80	1.247e-3	2.08	1.229e-2	2.09	1.254e-3	2.11
1/40	1/320	3.058e-4	2.03	3.009e-3	2.03	3.071e-4	2.03
1/80	1/1280	7.606e-5	2.01	7.480e-4	2.01	7.635e-5	2.01

TABLE 2. Numerical results on the errors of the simulated velocity and pressure at the terminal time $T = 0.5$ produced by the proposed sIMEX2-FEM scheme (15) for the lattice-vortex problem with the viscosity $\nu = 10^{-1}$. The ESAV stabilizing parameter $\theta = 1$.

sIMEX2-FEM		$\|\boldsymbol{u} - \boldsymbol{u}_h\|_0$	CR	$\|\boldsymbol{u} - \boldsymbol{u}_h\|_1$	CR	$\|P - P_h\|_0$	CR
h	τ	$\mu = 0$					
1/10	1/20	1.141e-3	-	1.215e-2	-	1.350e-3	-
1/20	1/40	2.305e-4	2.31	2.576e-3	2.24	2.787e-4	2.28
1/40	1/80	5.257e-5	2.13	6.020e-4	2.10	6.396e-5	2.12
1/80	1/160	1.261e-5	2.06	1.461e-4	2.04	1.537e-5	2.06
h	τ	$\mu = 1$					
1/10	1/20	1.341e-3	-	1.430e-2	-	1.562e-3	-
1/20	1/40	2.459e-4	2.45	2.770e-3	2.37	2.943e-4	2.41
1/40	1/80	5.358e-5	2.20	6.160e-4	2.17	6.498e-5	2.18
1/80	1/160	1.268e-5	2.08	1.474e-4	2.07	1.543e-5	2.07

Next, we test the performance of the proposed schemes for the problem with a small viscosity $\nu = 10^{-4}$, where the spatial mesh size is much larger compared to the viscosity. For this large Reynolds number case, it is expected that the grad-div stabilization term will have significant effect on the proposed schemes. For the grad-div stabilizing parameter we test three different values $\mu = 0$, 10^{-2} $(=\sqrt{\nu})$ and 1, respectively. Numerical errors and corresponding convergence rates are presented in Table 3 for the sIMEX1-FEM scheme and Table 4 for the sIMEX2-FEM scheme. The proposed schemes without grad-div stabilization produce downgraded convergence rates and sometimes even fails to converge. The grad-div stabilization seems essential for the pressure since the errors of pressure stay as a constant in all cases with $\mu = 0$. It is also easy to see that the schemes with grad-div stabilization still perform well and produce roughly optimal convergence rates with either $\mu = 10^{-2}$ or $\mu = 1$. Note that the time step sizes are much smaller compared to the mesh sizes in this test, thus the spatial errors could dominate, and consequently, the L^2 errors of the velocity show third order convergence, which is one order higher than its H^1 errors. Furthermore, we also

observe that both the sIMEX1-FEM and sIMEX2-FEM schemes with $\mu = 10^{-2}$ produces better results than with $\mu = 1$, especially in terms of velocity (up to 4 times smaller). Although it was analyzed in [26] that optimal grad-div stabilizing parameter μ is of $\mathcal{O}(1)$ for the Taylor-Hood element, our test results indicate that $\mu \approx \mathcal{O}(\sqrt{\nu})$ could be more suitable for the proposed EMAC-ESAV type finite element schemes.

TABLE 3. Numerical results on the errors of the simulated velocity and pressure at the terminal time $T = 0.5$ produced by the proposed sIMEX1-FEM scheme (13) for the lattice-vortex problem with the viscosity $\nu = 10^{-4}$. The ESAV stabilizing parameter $\theta = 1$.

sIMEX1-FEM		$\|\boldsymbol{u} - \boldsymbol{u}_h\|_0$	CR	$\|\boldsymbol{u} - \boldsymbol{u}_h\|_1$	CR	$\|P - P_h\|_0$	CR
h	τ	$\mu = 0$					
1/20	1/200	2.439e-1	-	3.265e1	-	2.773e-1	-
1/40	1/800	1.015e-1	1.26	1.200e1	1.44	2.776e-1	-0.00
1/80	1/3200	6.248e-2	0.70	6.562e0	0.87	2.775e-1	0.00
1/160	1/12800	2.301e-2	1.44	3.746e0	0.81	2.775e-1	-0.00
h	τ	$\mu = 10^{-2}$					
1/20	1/200	1.566e-2	-	1.760e0	-	7.479e-3	-
1/40	1/800	8.727e-4	4.17	2.545e-1	2.79	1.460e-3	2.36
1/80	1/3200	9.535e-5	3.19	5.516e-2	2.21	3.561e-4	2.04
1/160	1/12800	8.452e-6	3.50	8.955e-3	2.62	8.838e-5	2.01
h	τ	$\mu = 1$					
1/20	1/200	2.744e-2	-	1.651e0	-	1.505e-2	-
1/40	1/800	3.459e-3	2.99	4.272e-1	1.95	2.117e-3	2.83
1/80	1/3200	2.643e-4	3.71	1.196e-1	1.84	3.746e-4	2.50
1/160	1/12800	3.522e-5	2.91	3.283e-2	1.87	8.967e-5	2.06

TABLE 4. Numerical results on the errors of the simulated velocity and pressure at the terminal time $T = 0.5$ produced by the proposed sIMEX2-FEM scheme (15) for the lattice-vortex problem with the viscosity $\nu = 10^{-4}$. The ESAV stabilizing parameter $\theta = 1$.

sIMEX2-FEM		$\|\boldsymbol{u} - \boldsymbol{u}_h\|_0$	CR	$\|\boldsymbol{u} - \boldsymbol{u}_h\|_1$	CR	$\|P - P_h\|_0$	CR
h	τ	$\mu = 0$					
1/20	1/200	3.449e-1	-	4.301e1	-	2.475e-1	-
1/40	1/400	1.276e-1	1.43	1.211e1	1.83	2.541e-1	-0.04
1/80	1/800	8.287e-2	0.62	6.757e0	0.84	2.563e-1	-0.01
1/160	1/1600	1.478e-2	2.49	1.595e0	2.08	2.632e-1	-0.04
h	τ	$\mu = 10^{-2}$					
1/20	1/200	1.522e-2	-	9.218e-1	-	8.100e-2	-
1/40	1/400	8.560e-4	4.15	2.537e-1	1.86	1.423e-3	5.83
1/80	1/800	9.529e-5	3.17	5.515e-2	2.20	3.462e-4	2.04
1/160	1/1600	8.451e-6	3.50	8.954e-3	2.62	8.573e-5	2.01
h	τ	$\mu = 1$					
1/20	1/200	2.435e-2	-	1.283e0	-	1.575e-2	-
1/40	1/400	3.391e-3	2.84	4.158e-1	1.63	2.083e-3	2.92
1/80	1/800	2.643e-4	3.68	1.196e-1	1.80	3.632e-4	2.52
1/160	1/1600	3.522e-5	2.91	3.283e-2	1.87	8.673e-5	2.07

In the following experiments, we will only take the sIMEX2-FEM scheme (15) for testing due to its much better accuracy and efficiency.

5.2. **The Gresho problem.** We next consider the Gresho standing vortex problem [18]. The domain $\Omega = (-0.5, 0.5) \times (-0.5, 0.5)$. The initial condition is given by the solution of an steady Euler equation:

$$
\begin{aligned}
r \le 0.2 &: \begin{cases} \boldsymbol{u}_0 = \binom{-5y}{5x} \\ p_0 = 12.5r^2 + K_1 \end{cases}, \\
r > 0.4 &: \begin{cases} \boldsymbol{u}_0 = \binom{0}{0} \\ p_0 = 0 \end{cases}, \\
0.2 \le r \le 0.4 &: \begin{cases} \boldsymbol{u}_0 = \begin{pmatrix} \frac{-2y}{r} + 5y \\ \frac{2x}{r} - 5x \end{pmatrix} \\ p_0 = 12.5r^2 - 20r + 4\log(r) + K_2 \end{cases},
\end{aligned} \tag{100}
$$

where

$$
r = \sqrt{x^2 + y^2}, \quad K_2 = (-12.5)(0.4)^2 + 20(0.4)^2 - 4\log(0.4), \quad K_1 = C_2 - 20(0.2) + 4\log(0.2).
$$

The external force $\boldsymbol{f} = 0$, and the zero-Dirichlet boundary conditions are imposed. Slightly different from the original settings (for the Euler equation), we now have a viscous term with an extremely small viscosity number $\nu = 10^{-7}$ (i.e., an extremely large Reynolds number). The terminal time is chosen to be $T = 5$. In this problem, the initial solution configuration will be well maintained along the time, with almost neglectible diffusion caused by the tiny viscosity. Same to the spatial-temporal mesh settings used for the fully-implicit nonlinear schemes in [10, 11], we choose the spatial mesh size $h = 1/50$ and the time step size $\tau = 0.01$.

We will test the sIMEX2-FEM scheme and demonstrate the nice advantages brought by the ESAV and grad-div stabilization strategies under such relatively large time step size. That is, we will conduct some crossing contrast tests on the two stabilizing parameters $\theta = 1$ or 10^{-3} and $\mu = 0$ or $\mu = 10^{-3}$ (note that $10^{-3} \approx \mathcal{O}(\sqrt{\nu})$ since $\nu = 10^{-7}$). The plots of the simulated velocity magnitudes at times $t = 0$, 1 and 5 are shown in Figure 1, where $(\theta, \mu) = (1, 0)$, $(1, 10^{-3})$, $(10^{-3}, 0)$ and $(10^{-3}, 10^{-3})$ from top to bottom rows. It is observed that the numerical accuracy of the sIMEX2-FEM scheme is bad as shown on the first row when $\theta = 1$ and $\mu = 0$ (which corresponds to the standard implicit-explicit ESAV-BDF2 approach). If we add the grad-div stabilization with $\mu = 10^{-3}$, it can be seen from the second row that the simulation result gets significantly improved. The solution pattern is roughly preserved, but its peak magnitude becomes larger than 1 and there are lots of small oscillations. If we only change $\theta = 1$ to $\theta = 10^{-3}$, which means stronger stabilization from the ESAV dynamics, the simulation quality also gets much better along the time, as shown on the third row. However, it still suffers from the spurious oscillations with largest magnitude higher than 1. Finally, thanks to the combination of the grad-div stabilization with $\mu = 10^{-3}$ and the ESAV stabilization with $\theta = 10^{-3}$, we obtain very accurate and stable simulation results until the terminal time $T = 5$, as shown on the fourth row. The corresponding evolutions of the simulated kinetic energy ($\frac{1}{2}\|\boldsymbol{u}_n\|_0^2$), momentum ($\int_\Omega \boldsymbol{u}_n d\boldsymbol{x}$) and angular momentum ($\int_\Omega \boldsymbol{u}_n \times \boldsymbol{x}\, d\boldsymbol{x}$) of the numerical solutions are presented in Figure 2. We can see that the kinetic energy are very nicely preserved by the sIMEX2-FEM scheme with $\theta = 10^{-3}$ (with or without the grad-div stabilization) but not with $\theta = 1$. As for the momentum and the angular momentum, the sIMEX2-FEM scheme almost can conserve them perfectly along the time with either values of θ, except the sIMEX2-FEM scheme with $\theta = 1$ produces up to 0.05% deviations for the angular momentum.

For the purpose of comparison, we additionally test the widely used implicit-explicit BDF2 scheme with grad-div stabilization (using the same parameter $\mu = 10^{-3}$) , i.e., a numerical scheme consisting of the equation (15a) without $Q^{n+1}\exp(t_{n+1}/T)$ and the equation (15b). We find that the grad-div stabilized implicit-explicit BDF2 scheme unfortunately breaks down at $t = 0.18$ (i.e., 18 time steps), which implies that the introduction of the stabilized ESAV approach to the EMAC formulation does further improve the numerical stability of the system.

5.3. **The channel flow past a forward-backward facing step.** We finally test the problem of the channel flow passing a forward-backward facing step. The domain in two dimensions is a rectangle of $(0, 40) \times (0, 10)$ used to represent the channel, with a 1×1 'step' located at $(5, 6) \times (0, 1)$. Again no body force is imposed, i.e., $\boldsymbol{f} = 0$. In addition, the boundary condition is given by no-slip condition on the top and bottom walls and the step, no-flux condition of the outflow in the right side, and a constant-in-time parabolic inflow with

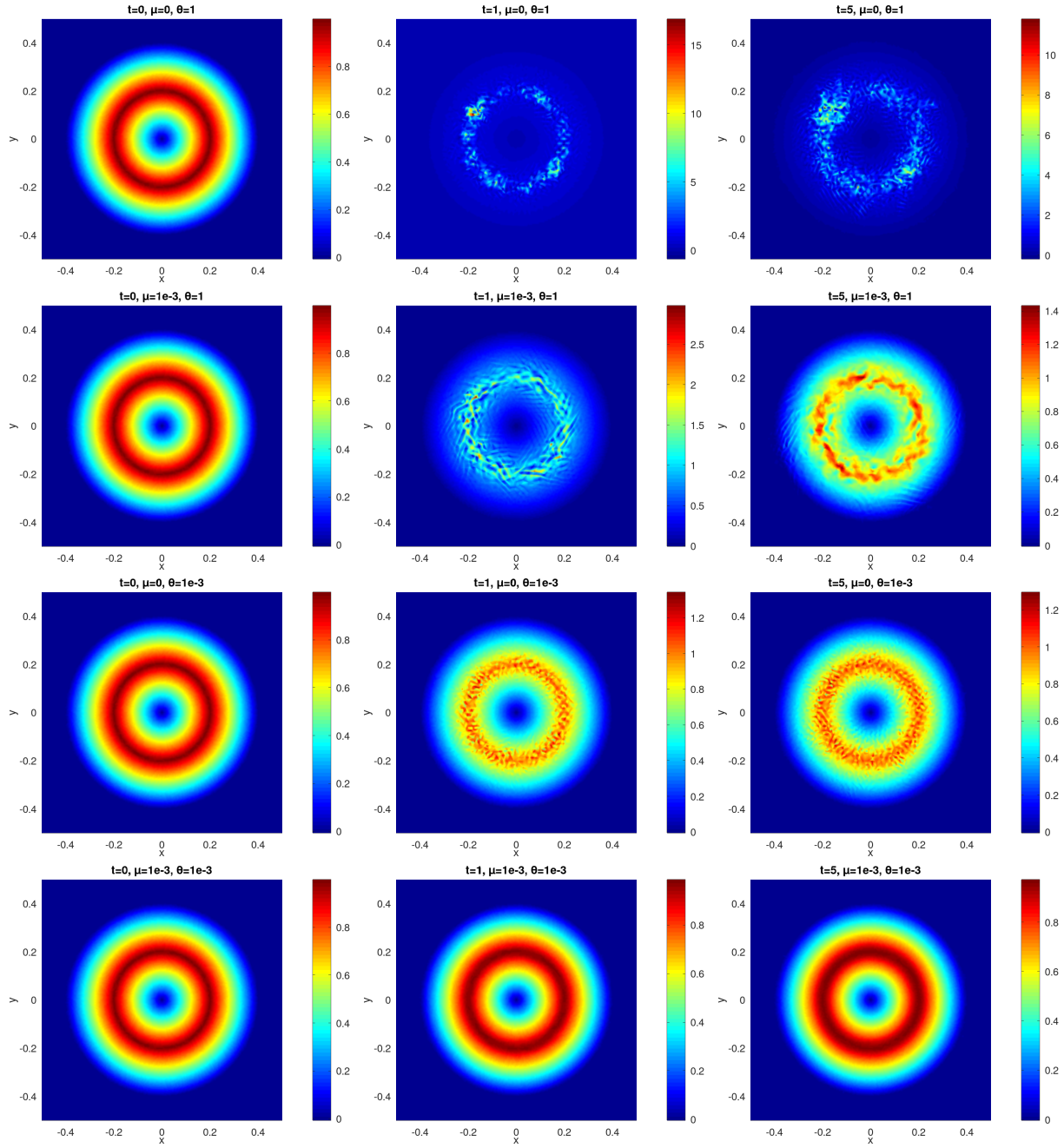

FIGURE 1. Plots of the magnitude of the simulated velocity at $t = 0$, 1 and 5 respectively generated by the proposed sIMEX2-FEM scheme (15) for the Gresho problem with the viscosity $\nu = 10^{-7}$. The spatial mesh size $h = 1/50$ and the time step size $\tau = 0.01$. For top to bottom rows: $(\theta = 1, \mu = 0)$, $(\theta = 1, \mu = 10^{-3})$, $(\theta = 10^{-3}, \mu = 0)$, and $(\theta = 10^{-3}, \mu = 10^{-3})$.

max inlet velocity of 1 in the left side, that is

$$\boldsymbol{u}(0, y, t) = (y(10 - y)/25, 0), \quad 0 \le y \le 10.$$

The initial velocity is set to be $\boldsymbol{u}_0 = 0$, the viscosity $\nu = 10^{-4}$, and the terminal time $T = 20$. We generate a spatial mesh with 8,310 vertices and 16,110 triangles for the domain, and choose a relatively large time step size $\tau = 0.005$.

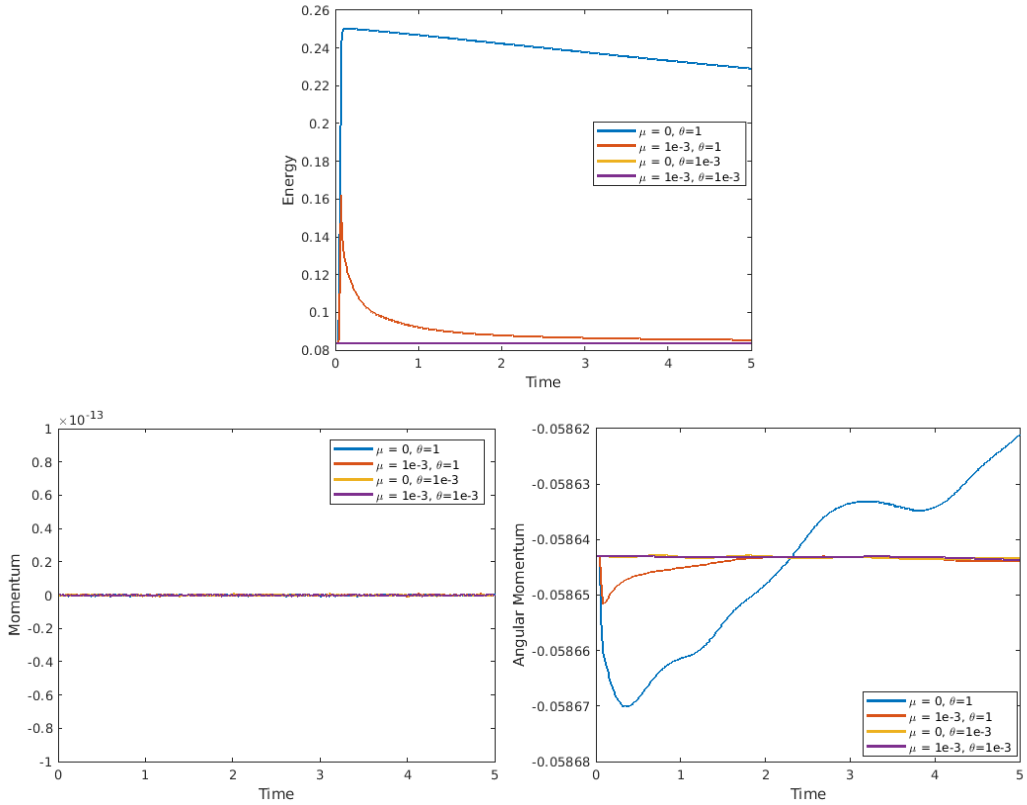

FIGURE 2. Evolutions of the simulated kinetic energy (top), momentum (bottom left) and angular momentum (bottom right) of the numerical solution generated by the proposed sIMEX2-FEM (15) for the Gresho problem with the viscosity $\nu = 10^{-7}$. The spatial mesh size $h = 1/50$ and the time step size $\tau = 0.01$.

For this challenging large Reynolds number problem, we take the sIMEX2-FEM scheme and set the stabilizing parameters $\mu = 10^{-2}$ and $\theta = 10^{-3}$ (approximately $\mathcal{O}(\sqrt{\nu})$ based in the numerical studies and findings obtained from the previous example). The plots of the magnitude of the simulated velocity at times $t = 5$, 10, 15 and 20 are shown in Figure 3, along with the corresponding zoom-in plots around the subregion $[4, 12] \times [0, 4]$ in Figure 4. It is well-known that the eddies will form behind the step, and gradually grow and detach from the step [37] in this problem. Such phenomenon can be clearly observed from the simulation results produced by the proposed IMEX2-sFEM scheme. On the other hand, we also remark that some small oscillations are still present in our simulations, for example, at time t =15 in the region $[6, 6.5] \times [0, 0.5]$. The main reason could be that some tiny eddies are generated around the right upper corner of the step. These tiny eddies carry the kinematic energy, but the currently used mesh is not fine enough to resolve them, therefore the unresolved energy is accumulated to incur the oscillations. To overcome such issue, some time-relaxation method [14] or time filters [21] could be further combined with our proposed schemes to filter out these unresolved tiny-scale eddies.

For the purpose of comparison, we also test the implicit-explicit BDF2 scheme and the fully-implicit BDF2 schemes with grad-div stabilization We use the same spatial-temporal mesh and the same stabilizing parameter $\mu = 10^{-2}$. Compared to the experiments done in [37], note that our viscosity ν is 16 times smaller than theirs, but our time step size is only about 2 times smaller. We observe that the grad-div stabilized implicit-explicit BDF2 scheme unfortunately breaks down at $t = 0.065$ (i.e., 13 time steps). As for the grad-div stabilized fully-implicit BDF2 scheme, we implement the Picard iteration for the nonlinear solve at each time step and set the stopping criteria as 10^{-8} (measured in terms of L^2 norm). The used number of nonlinear iterations at each time step is shown in Figure 5. As one can see, it requires at least 6 iterations per each time step. In addition, we run the grad-div stabilized fully-implicit BDF2 scheme with the larger

time step size $\tau = 0.025$ and find the numerical solution quickly diverges. All these comparisons imply that our proposed sIMEX2-FEM could be more efficient.

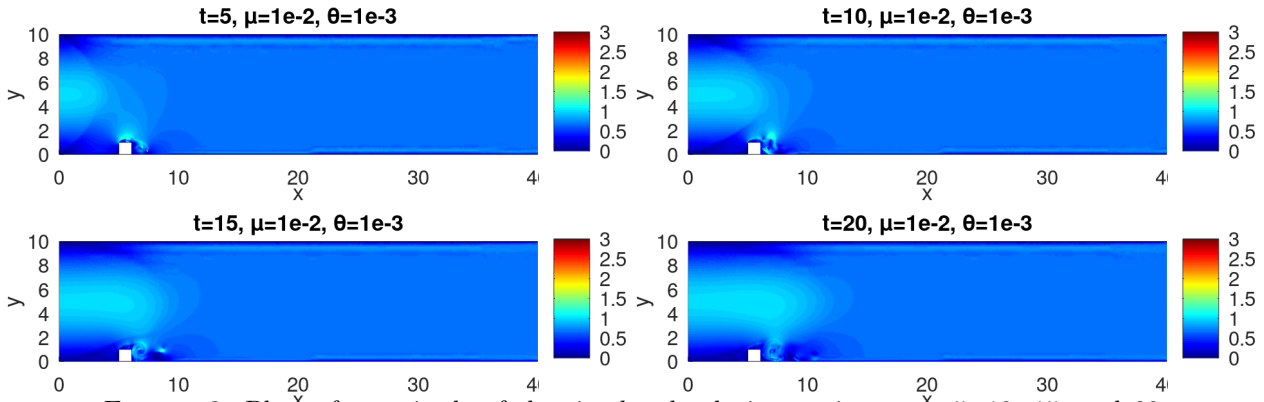

FIGURE 3. Plots of magnitude of the simulated velocity at times $t = 5$, 10, 15, and 20 generated by the proposed sIMEX2-FEM scheme (15) with $\mu = 10^{-2}$ and $\theta = 10^{-3}$ for the channel flow past a forward-backward facing step problem with the viscosity $\nu = 10^{-4}$.

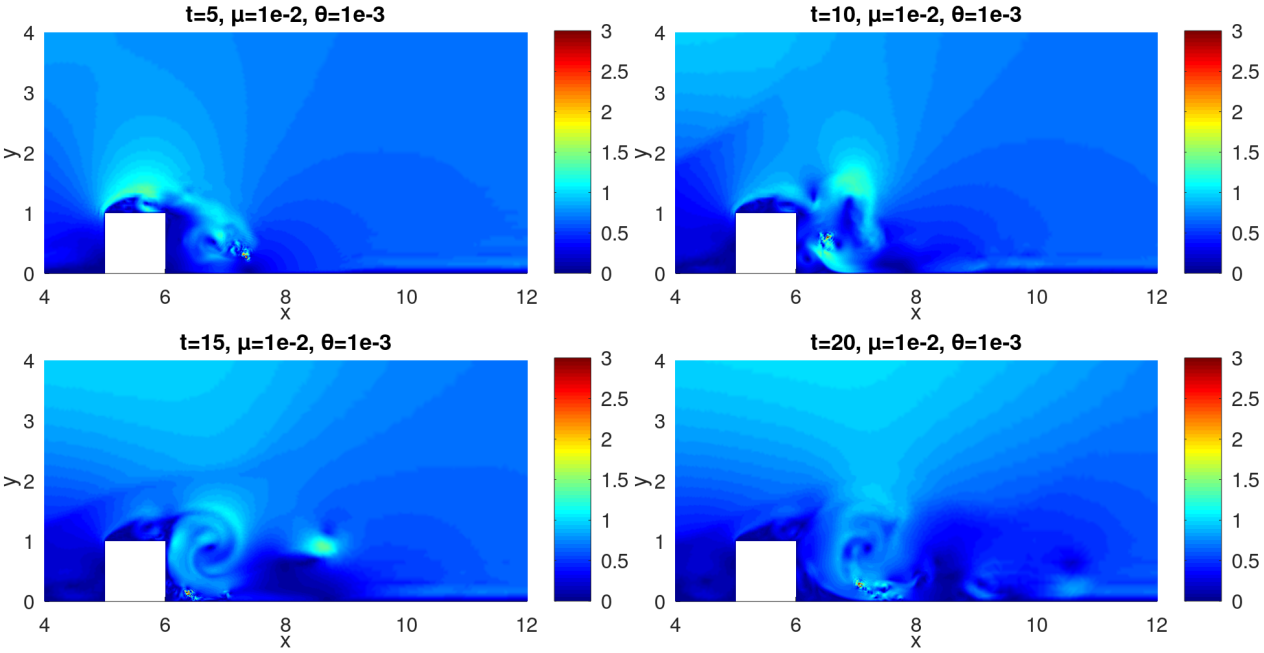

FIGURE 4. Zoom-in plots around the subregion $[4, 12] \times [0, 4]$ of magnitude of the simulated velocity at times $t = 5$, 10, 15, and 20 generated by the proposed sIMEX2-FEM scheme (15) with $\mu = 10^{-2}$ and $\theta = 10^{-3}$ for the channel flow past a forward-backward facing step problem with the viscosity $\nu = 10^{-4}$.

6. CONCLUSIONS

In this paper, we present and analyze first and second-order (in time) stabilized linear finite element schemes for the incompressible Navier-Stokes (NS) equations, which can effectively handle high Reynolds number problems. The proposed sIMEX1-FEM and sIMEX2-FEM schemes utilize the EMAC formulation and the Taylor-Hood element with grad-div stabilization in space, alongside the stabilized ESAV approach and the implicit-explicit BDF schemes in time. We also develop a novel decoupling strategy for efficiently

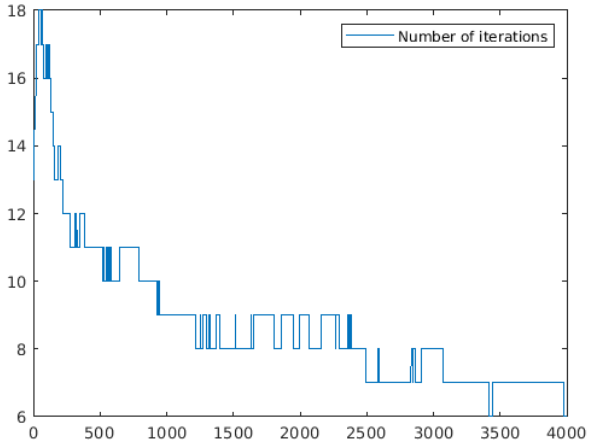

FIGURE 5. Evolution of the used number of Picard iterations at each time step used for the fully-implicit BDF2 scheme with grad-div stabilization.

solving the resulting fully-discrete systems, which only requires one linear Stokes solve at each time step. We prove optimal error estimates for the proposed schemes with viscosity-independent Gronwall constants, which essentially improve the existing convergence analysis results for SAV approach-based linear schemes for the incompressible NS equations. Moreover, we show that the grad-div stabilization term can greatly alleviate the viscosity-dependence of the mesh size constraint needed for error estimates of the schemes with grad-div stabilization. Three benchmark problems – the lattice vortex problem, Gresho standing vortex problem, and the channel flow past a forward-backward facing step – are tested to verify the theoretical results and demonstrate the performance of the proposed schemes for problems with large Reynolds numbers, along with illustrating the effect of the grad-div and ESAV stabilization strategies.

There are also some challenging questions that remain to be explored in the future. First, we will continue to more thoroughly investigate the effect and optimal choices of the two stabilizing parameters in the proposed sIMEX1-FEM and sIMEX2-FEM schemes, which will provide more precise guidance for the application of these schemes in practice. Second, we are interested in a unified analysis framework to directly analyze the case of the grad-div stabilization parameter $\mu \geq 0$ and show how critical constants behave and deteriorate as μ approaches zero. Third, to deal with the oscillations caused by accumulations of unresolved tiny eddies, we will combine some time relaxation methods to filter out these unresolved eddies to further improve the proposed schemes. Such an approach is also commonly used in classic nonlinear schemes that treat the nonlinear term implicitly and require the Picard or Newton iteration for solution. Fourth, the incompressible NS equations are an important component of multi-phase flow systems, and we will extend our proposed numerical schemes and analysis techniques to study these more complex and coupled models.

REFERENCES

1. Robert A Adams and John JF Fournier, *Sobolev spaces*, Elsevier, 2003.
2. Rong An, Huadong Gao, and Weiwei Sun, *Optimal error analysis of euler and Crank–Nicolson projection finite difference schemes for Landau–Lifshitz equation*, SIAM Journal on Numerical Analysis **59** (2021), no. 3, 1639–1662.
3. Andrea L. Bertozzi Andrew J. Majda, *Vorticity and incompressible flow*, Cambridge University Press, 2001.
4. Garth A. Baker, Vassilios A. Dougalis, and Ohannes A. Karakashian, *On a higher order accurate, fully discrete Galerkin approximation to the Navier-Stokes equations*, Mathematics of Computation **39** (1982), 339–375.
5. Jeffrey Belding, Monika Neda, and Rihui Lan, *An efficient discretization for a family of time relaxation models*, Computer Methods in Applied Mechanics and Engineering **391** (2022), 114510.
6. Richard Bellman, *The stability of solutions of linear differential equations*, Duke Math. J. **10** (1943), no. 1, 643–647.
7. Daniele Boffi, Franco Brezzi, Michel Fortin, et al., *Mixed finite element methods and applications*, vol. 44, Springer, 2013.
8. Susanne C. Brenner and L. Ridgway Scott, *The mathematical theory of finite element methods*, Springer-Verlag, 1994.
9. Michael A Case, Vincent J Ervin, Alexander Linke, and Leo G Rebholz, *A connection between Scott–Vogelius and grad-div stabilized Taylor–Hood FE approximations of the Navier–Stokes equations*, SIAM Journal on Numerical Analysis **49** (2011), no. 4, 1461–1481.
10. Sergey Charnyi, Timo Heister, Maxim A Olshanskii, and Leo G Rebholz, *On conservation laws of Navier–Stokes Galerkin discretizations*, Journal of Computational Physics **337** (2017), 289–308.

11. ———, *Efficient discretizations for the EMAC formulation of the incompressible Navier–Stokes equations*, Applied Numerical Mathematics **141** (2019), 220–233.
12. Alexandre Joel Chorin, *Numerical solution of the Navier-Stokes equations*, Mathematics of Computation **22** (1968), no. 104, 745–762.
13. Javier de Frutos, Bosco García-Archilla, Volker John, and Julia Novo, *Analysis of the grad-div stabilization for the time-dependent Navier–Stokes equations with inf-sup stable finite elements*, Advances in Computational Mathematics **44** (2018), 195–225.
14. Vincent J. Ervin, William J. Layton, and Monika Neda, *Numerical analysis of a higher order time relaxation model of fluids*, International Journal of Numerical Analysis and Modeling **4** (2007), 648–670.
15. Richard S Falk and Michael Neilan, *Stokes complexes and the construction of stable finite elements with pointwise mass conservation*, SIAM Journal on Numerical Analysis **51** (2013), no. 2, 1308–1326.
16. Bosco García-Archilla, Volker John, and Julia Novo, *On the convergence order of the finite element error in the kinetic energy for high Reynolds number incompressible flows*, Computer Methods in Applied Mechanics and Engineering **385** (2021), 114032.
17. Vivette Girault and Larkin Ridgway Scott, *A quasi-local interpolation operator preserving the discrete divergence*, Calcolo **40** (2003), no. 1, 1–19.
18. Philip M Gresho and Stevens T Chan, *On the theory of semi-implicit projection methods for viscous incompressible flow and its implementation via a finite element method that also introduces a nearly consistent mass matrix. Part 2: Implementation*, International Journal for Numerical Methods in Fluids **11** (1990), no. 5, 621–659.
19. Thomas Hakon Gronwall, *Note on the derivatives with respect to a parameter of the solutions of a system of differential equations*, Annals of Mathematics (1919), 292–296.
20. Jean-Luc Guermond, Peter Minev, and Jie Shen, *An overview of projection methods for incompressible flows*, Computer Methods in Applied Mechanics and Engineering **195** (2006), no. 44-47, 6011–6045.
21. Ahmet Guzel and William Layton, *Time filters increase accuracy of the fully implicit method*, BIT Numerical Mathematics **58** (2018), 301–315.
22. Johnny Guzmán and Michael Neilan, *Conforming and divergence-free Stokes elements on general triangular meshes*, Mathematics of Computation **83** (2014), no. 285, 15–36.
23. Wei-Wei Han, Yao-Lin Jiang, and Zhen Miao, *Numerical analysis of the SAV scheme for the EMAC formulation of the time-dependent Navier–Stokes equations*, Journal of Computational and Applied Mathematics **438** (2024), 115514.
24. Yongbin Han, Yanren Hou, and Min Zhang, *Analysis of divergence-free H^1 conforming fem with IMEX-SAV scheme for the Navier-Stokes equations at high Reynolds number*, Mathematics of Computation **92** (2023), no. 340, 557–582.
25. Frédéric Hecht, *New development in FreeFem++*, Journal of Numerical Mathematics **20** (2012), no. 3-4, 251–266.
26. Eleanor W Jenkins, Volker John, Alexander Linke, and Leo G Rebholz, *On the parameter choice in grad-div stabilization for the Stokes equations*, Advances in Computational Mathematics **40** (2014), 491–516.
27. Volker John, *Finite element methods for incompressible flow problems*, vol. 51, Springer, 2016.
28. Volker John, Alexander Linke, Christian Merdon, Michael Neilan, and Leo G Rebholz, *On the divergence constraint in mixed finite element methods for incompressible flows*, SIAM Review **59** (2017), no. 3, 492–544.
29. Andrei Kolmogorov, *The local structure of turbulence in incompressible viscous fluids for very large Reynolds numbers*, Doklady Akademii Nauk SSR **30** (1941), 9–13.
30. Alexandr Labovsky, William J Layton, Carolina C Manica, Monika Neda, and Leo G Rebholz, *The stabilized extrapolated trapezoidal finite-element method for the Navier–Stokes equations*, Computer Methods in Applied Mechanics and Engineering **198** (2009), no. 9-12, 958–974.
31. Buyang Li, Huadong Gao, and Weiwei Sun, *Unconditionally optimal error estimates of a Crank–Nicolson Galerkin method for the nonlinear thermistor equations*, SIAM Journal on Numerical Analysis **52** (2014), no. 2, 933–954.
32. Buyang Li and Weiwei Sun, *Unconditional convergence and optimal error estimates of a galerkin-mixed fem for incompressible miscible flow in porous media*, SIAM Journal on Numerical Analysis **51** (2013), no. 4, 1959–1977.
33. Xiaoli Li and Jie Shen, *Error analysis of the SAV-MAC scheme for the Navier–Stokes equations*, SIAM Journal on Numerical Analysis **58** (2020), no. 5, 2465–2491.
34. Xiaoli Li, Jie Shen, and Zhengguang Liu, *New SAV-pressure correction methods for the Navier-Stokes equations: stability and error analysis*, Mathematics of Computation **91** (2022), no. 333, 141–167.
35. Lianlei Lin, Zhiguo Yang, and Suchuan Dong, *Numerical approximation of incompressible Navier-Stokes equations based on an auxiliary energy variable*, Journal of Computational Physics **388** (2019), 1–22.
36. Zhengguang Liu and Xiaoli Li, *The exponential scalar auxiliary variable (E-SAV) approach for phase field models and its explicit computing*, SIAM Journal on Scientific Computing **42** (2020), no. 3, B630–B655.
37. Carolina C Manica, Monika Neda, Maxim Olshanskii, and Leo G Rebholz, *Enabling numerical accuracy of Navier-Stokes-α through deconvolution and enhanced stability*, ESAIM: Mathematical modelling and numerical analysis **45** (2011), no. 2, 277–307.
38. Maxim A Olshanskii, *A low order Galerkin finite element method for the Navier–Stokes equations of steady incompressible flow: a stabilization issue and iterative methods*, Computer Methods in Applied Mechanics and Engineering **191** (2002), no. 47-48, 5515–5536.
39. Maxim A Olshanskii and Leo G Rebholz, *Longer time accuracy for incompressible Navier–Stokes simulations with the EMAC formulation*, Computer Methods in Applied Mechanics and Engineering **372** (2020), 113369.
40. Alfio Quarteroni, Fausto Saleri, and Alessandro Veneziani, *Factorization methods for the numerical approximation of Navier–Stokes equations*, Computer methods in applied mechanics and engineering **188** (2000), no. 1-3, 505–526.

41. Leo G Rebholz, Alex Viguerie, and Mengying Xiao, *Efficient nonlinear iteration schemes based on algebraic splitting for the incompressible Navier-Stokes equations*, Mathematics of Computation **88** (2019), no. 318, 1533–1557.
42. Leo G Rebholz and Mengying Xiao, *Improved accuracy in algebraic splitting methods for Navier–Stokes equations*, SIAM Journal on Scientific Computing **39** (2017), no. 4, A1489–A1513.
43. Fausto Saleri and Alessandro Veneziani, *Pressure correction algebraic splitting methods for the incompressible Navier–Stokes equations*, SIAM journal on numerical analysis **43** (2005), no. 1, 174–194.
44. Philipp W. Schroeder and Gert Lube, *Pressure-robust analysis of divergence-free and conforming FEM for evolutionary incompressible Navier-Stokes flows*, J. Numer. Math. **25** (2017), 249–276.
45. L Ridgway Scott and Michael Vogelius, *Conforming finite element methods for incompressible and nearly incompressible continua*, Lectures in Applied Mathematics **22** (1985), no. 2, 221–244.
46. ———, *Norm estimates for a maximal right inverse of the divergence operator in spaces of piecewise polynomials*, ESAIM: Mathematical Modelling and Numerical Analysis **19** (1985), no. 1, 111–143.
47. Jie Shen, Jie Xu, and Jiang Yang, *The scalar auxiliary variable (SAV) approach for gradient flows*, Journal of Computational Physics **353** (2018), 407–416.
48. ———, *A new class of efficient and robust energy stable schemes for gradient flows*, SIAM Review **61** (2019), no. 3, 474–506.
49. Cedric Taylor and Paul Hood, *A numerical solution of the Navier-Stokes equations using the finite element technique*, Computers & Fluids **1** (1973), no. 1, 73–100.
50. Roger Temam, *Navier-Stokes equations: theory and numerical analysis*, vol. 343, American Mathematical Soc., 2001.
51. Ricardo H. Nochetto Vivette Girault and L. Ridgway Scott, *Max-norm estimates for Stokes and Navier-Stokes approximations in convex polyhedra*, Numerische Mathematik **131** (2015), 771–822.
52. Cheng Wang and Jian-Guo Liu, *Convergence of gauge method for incompressible flow*, Mathematics of Computation **69** (2000), no. 232, 1385–1407.
53. E Weinan and Jian-Guo Liu, *Gauge method for viscous incompressible flows*, Communications in Mathematical Sciences **1** (2003), no. 2, 317–332.
54. Tong Zhang and JinYun Yuan, *Unconditional stability and optimal error estimates of Euler Implicit/Explicit-SAV scheme for the Navier–Stokes equations*, Journal of Scientific Computing **90** (2022), 1–20.

School of Mathematical Sciences, Ocean University of China, Qingdao, Shandong 266100, China
Email address: lanrihui@ouc.edu.cn

School of Mathematical Sciences, Ocean University of China, Qingdao, Shandong 266100, China
Email address: lmy3039@stu.ouc.edu.cn

Department of Mathematics, University of South Carolina, Columbia, SC 29208, USA
Email address: ju@math.sc.edu